VAPOUR-LIQUID EQUILIBRIUM MEASUREMENTS USING A STATIC TOTAL PRESSURE APPARATUS

A. M. Megne Motchelaho

[BSc. (Hons)]

University of Natal

Submitted in fulfillment of the Academic Requirements for the degree of Master of Science in Engineering in the School of Chemical Engineering, University of KwaZulu-Natal

Durban 2006

ABSTRACT

A novel static total pressure apparatus was designed, built and commissioned for the measurement of VLE data at low to moderate pressures and temperatures. The apparatus of Fischer and Gmehling [1994] was used as a basis for the current design. The continuous-dilution technique (Gibbs and Van Ness [1972]) for sample introduction has been incorporated in our apparatus, so that the full composition range of a mixture can be covered in two runs. This procedure has the considerable advantage of speed. If the liquid is properly degassed, the main limitation of the method is the accuracy with which one can establish overall compositions from metered volumes. Accurate injection of the two components is accomplished with a patented dual-action piston-injector (Raal [1999]). In the micromode the pump can accurately dispense submicrolitre volumes and the apparatus is thus particularly suited for VLE measurement in the very dilute region, and thus for determining limiting activity coefficients. γ_i^{∞} calculated using the method proposed by Maher and Smith [1979] ranged from about 3.8 to 59. The estimated accuracy of the injected volumes is ± 0.002 cm^3; this was obtained from calibration with distilled water. The estimated accuracies of the equilibrium temperature and pressure are ± 0.2 °C and ± 0.01 kPa respectively. The pure liquids were degassed for at least 8 hours according to the procedure proposed by Van Ness and Abbott [1978]. The static assembly and experimental procedure have been tested via pure component vapour pressure and binary vapour-liquid equilibrium measurements for a range of test systems (Water (1) + 1-Propanol (2) at 313.17 K , Water (1) + 2-Butanol (2) at 323.18 K, n-Hexane (1) + 2-Butanol at 329.22 K). The test systems data compared well with literature data and a high degree of confidence was then placed on the equipment set-up and experimental procedure. New vapour-liquid equilibrium (VLE) data were measured for the following binary systems:

- 1-Propanol (1) + n-Dodecane at 342.83K and 352.68 K
- 2-Butanol (1) + n-Dodecane at 342.83 K and 352.68 K
- Water (1) + o-Cresol at 342.83 K

The VLE measurements of the new systems were very challenging because of the large boiling point differences between the systems' constituents.

An accurate new method for determining the net interior volume of the cell V_{cell}^{tot} was tested and gave excellent linear plots of cumulative volume of injected liquid, v_1^L against $\left(\frac{P_1 - P_0}{P_0}\right)$, with the slope representing V_{cell}^{tot}.

The VLE data for all the systems measured were modeled using the combined ($\gamma - \phi$) method. The Barker's method of data reduction was implemented to convert the number of moles of each component injected into the cell to mole fraction of the vapour and liquid phase (Uusi-Kyyny et al. [2002]). Different Gibbs excess models namely NRTL, T-K Wilson and Van Laar together with the virial equation of state for vapour phase non-idealities were used. The T-K Wilson and NRTL gave the best fit.

PREFACE

The work presented in this dissertation was performed at the University of KwaZulu-Natal from May 2004 to June 2006 and was supervised by Professor D. Ramjugernath and Professor J. D Raal.

This dissertation is submitted as a full requirement for the degree of Master of Science in Chemical Engineering. All the work presented in this dissertation is original, unless otherwise stated. It has not (in whole or part) been previously submitted in any tertiary institution as part of a degree.

A. M. M. Motchelaho

ACKNOWLEDGEMENTS

I would like to acknowledge the following people for their contribution to this work:

- Firstly, my supervisors, Professor D. Ramjugernath and Professor J.D. Raal, for their guidance, support and ideas during this research.

- The workshop staff especially Kelly Robertson for the construction and maintenance of the equipment.

- The Thermodynamics Research Unit and Professor Ramjugernath for financial assistance during this project.

- Many thanks go to Dr P. Naidoo, Mr. C. Mandri, Dudley, Preyo and Mr. A Khanyile for their assistance.

- My colleagues in the Chemical Engineering Department for their ideas and friendship, in particular Z. Mbolekwa, M. Ndlovu, T. Mcknight, P. Moodley, C. Narasigadu, P. Reddy, E. Wilson, J. Knock, S.L. Clifford, I. Habyalimana, A. Hwengwere, M. Soni.

- My Friends, J.M. Moualeu, P.M. Talla, G. Foding, A. Kamdem, T. Ngatched, Marc & Nadege Louzolo, N. Womsi, S. Wambo and M. Feugeu.

- On a personal note to my parents Mr. & Mrs. Motchelaho and Buh Tamtseu family for years of support and motivation.

- My Daughter S. Foka and husband C. Foka for their love and support.

- Thanks to God almighty for the strength and perseverance over the years.

TABLE OF CONTENTS

LIST OF FIGURES

LIST OF TABLES

LIST OF SYMBOLS

a'	Parameter in the Tsonopoulos [1974] correlation
B_o	Parameter in the Pitzer-Curl [1957] correlation
B_1	Parameter in the Pitzer-Curl [1957] correlation
B_{ii}	Second virial coefficient of pure component i [cm^3/mol]
B_{ij}	Second virial coefficient for the species i – species j interaction [cm^3/mol]
f	Fugacity [kPa]
F	Objective function
G^E	Molar Gibbs ExcessEnergy [J/mol]
G_{12}	Parameter in the NRTL equation
G_{21}	Parameter in the NRTL equation
$g_{ij} - g_{ii}$	Parameter representing energy interactions between species in the NRTL equation
k	mixing rule parameter
$n_{i,k}^L$	Moles of component i of point k in the liquid phase
$n_{i,k}^{tot}$	Moles of component i in equilibrium cell in point k
$n_{i,k}^V$	Moles of component i of point k in the vapour phase
$n_{V,k}$	Total number of moles in the vapour phase of point k
NC	Number of components
NP	Number of data points
P	Pressure [kPa]
$P_{calc,k}$	Calculated pressure of point k
$P_{exp,k}$	Experimental pressure of point k
P_i^{sat}	Saturated pressure of component i
P_k	Total pressure at pont k
R	Universal gas constant [J/mol K]
T	Temperature [°C or K]
V	Molar or specific volume [cm^3/mol]
$v_{i,k}^L$	Liquid molar volume of component i at point k
v_k^L	Liquid molar volume at point k
v_k^V	Vapour molar volume at point k
$x_{i,k}$	Liquid phase mole fraction of component i at point k
$y_{i,k}$	Vapour phase mole fraction of component i at point k

$z_{i,k}$	Total composition in the equilibrium cell, mole fraction of component i at point k
Z	Compressibility factor

Greek letters

a_{12}	NRTL model parameter
t_{ij}	NRTL model binary interaction parameter [J/mol]
d	Denotes a residual
d_{ij}	Term relating the second virial coefficients
F	Ratio of fugacity coefficients with the Poynting correction factor
γ	Activity coefficient
γ^{∞}	Infinite dilution activity coefficient
ϕ	Fugacity coefficient
Λ_{ij}	Parameter in Wilson equation
$\lambda_{ij} - \lambda_{ii}$	Parameter representing molar interactions between species in the Wilson equations
μ	Dipole moment [Debye] and Chemical potential
ω	Acentric factor

Subscripts

1	Denotes component 1
2	Denotes component 2
c	Denotes a critical property
calc	Denotes a calculated value
exp	Denotes an experimental value
i	Denotes component i

Superscripts

E	Denotes excess property
id	Denotes ideal solution
L	Denotes liquid phase
Sat	Denote saturation

tot	Total
V	Denotes vapour

Abbreviations

EOS	Equation of State
VLE	Vapour-Liquid Equilibrium

CHAPTER ONE

INTRODUCTION

The separation of components in a chemical stream constitutes a major portion of many processes in the chemical and petroleum industries (Gess et al. [1991]). Separation processes are costly and constitute the majority of equipment expenditure in Chemical plants (Seader and Henley [1998]). Vapour-liquid equilibrium (VLE) data are of particular importance for the design and computation of phase separation processes. A reliable VLE data bank is essential because it provides values for thermodynamic functions which can be used directly in the design and operation of industrial plants.

Static methods for measurement of vapour-liquid equilibria have become increasingly important in recent years. The work of Gibbs and Van Ness [1972] and Fischer and Gmehling [1994] may be cited as examples. The method requires thorough degassing of the substances which constitute the mixture investigated, and unless this is accomplished properly, the measured pressures will be incorrect.

This project formed part of an ongoing study of VLE thermodynamics, in the Thermodynamic Research Unit at the University of Kwa-Zulu Natal. The main objective of this study was to design, construct and commission a relatively simple, versatile and reliable static synthetic total pressure apparatus capable of producing low to moderate pressure and temperature VLE data very accurately. The aim of the design was to build an apparatus which would complement the existing apparatus present in the Thermodynamic Research Unit, University of Kwa-Zulu Natal

The major components of the static apparatus that was used in this project (discussed in more detail in Chapter 3) are: a degassing assembly, a 190 cm^3 equilibrium cell, piston- injector assembly made of a mini- and macro-piston selectable by solenoid operation, an isothermal environment provided by a 14 litre constant temperature bath, and finally pressure and temperature measuring devices.

At present, there is general interest in vapour-liquid equilibrium (VLE) data for mixtures containing oxygenated compounds (alcohols) and hydrocarbons, because the former act as anti-knock agents in unleaded gasolines and provide pollution reduction through the use of catalysts in automobiles. VLE of such mixtures are used in the refining industry (Lorenzo et al. [1997]).

The apparatus developed in this project was used to obtain isothermal vapour-liquid equilibrium data for Water (1) + 1-Propanol (2) at 313.17K , Water (1) + 2-Butanol (2) at 323.18 K, n-Hexane (1) + 2-Butanol at 329.22 K, and 1-Propanol (1) + n-Dodecane (2) at 342.83 K and 352.68 K, 2-Butanol (1) + n-Dodecane (2) at 342.83 K and 352.68 K, and Water (1) + o-Cresol at 342.82 K. After intensive trial runs on test systems, an operating procedure was adopted and new systems were measured.

An accurate new method to find the net cell interior volume was tested. The P-z_i data obtained for all the systems were converted to P-x_i data using iterative procedures and regressed using Barker's method. The NRTL, T-K Wilson and Van Laar activity coefficient models were used to account for the non-ideality of the liquid phase. The non-ideal behaviour of the vapour phase was accounted for using the Pitzer and Curl [1957] correlation and the Prausnitz mixing rule [1986].

CHAPTER TWO

LITERATURE REVIEW

The tendency of a substance to enter the vapour phase by sublimation (solid-gas) or evaporation (liquid-gas) is defined by its vapour pressure. Knowledge of this property is crucially important for a wide variety of materials. Vapour pressure is one of the most important of the basic thermodynamic properties affecting liquids and vapours. Although there are a number of literature compilations of vapour pressure data, for many materials, such information is not available and the researcher either has to resort to measurement or prediction methods. An alternative description of the behaviour when two phases are present is that, at equilibrium conditions, the pressure exerted by the vapour above a pure liquid is dependent upon temperature only and is independent of the fraction of the liquid which has vaporized. If however, the sample consists of more than one component, the pressure is not independent of the fraction vaporized since the more volatile components evaporate more readily than the less volatile components and the compositions of the vapour and liquid differ. Vapor-liquid equilibrium (VLE) data are essential for the development and design of separation processes such as distillation, absorption, solvent extraction, and their experimental measurements have long been actively pursued.

2.1 Review of Vapour Liquid Equilibrium Equipment

There are several reviews of experimental procedures and equipment in the literature for low-pressure vapour-liquid equilibrium measurement, such as those of Hala et al. [1967], Malanowski

[1982], Abbott [1986] and Raal and Ramjugernath [2005]. Direct methods for low-pressure VLE measurement are classified according to Hala et al. [1967] into the following groups:

1. Distillation Methods
2. Dynamic Methods (Circulation)
3. Static Methods
4. Flow Methods
5. Dew and Bubble Point Methods

Since it would not be possible to discuss all the above-mentioned methods, for more detailed reviews, the reader is referred to Robinson and Gilliland [1950], Hala et al. [1967] and most recently Raal and Mühlbauer [1998] and Raal and Ramjugernath [2005]. Today, the most commonly used methods are the dynamic and static methods. These methods will now be discussed using examples from the literature.

2.1.1 The Dynamic Method

Dynamics stills account for a large portion of VLE data that have been published (Raal and Mühlbauer [1998]). Circulation methods have been known to produce results of high accuracy in a rapid and simple manner (Joseph [2001]). In all the circulation stills, which can be operated under isobaric or isothermal conditions, a liquid mixture is charged to a distilling flask and brought to boil. Evolved vapours are condensed (except in methods where there is direct circulation of the vapour phase) into a receiver; the vapour condensate returns to the distilling flask, where it mixes with the boiling liquid. Compositions of the boiling liquid and vapour condensate change with time until steady values are obtained. These are, in a properly functioning still, the true equilibrium liquid and vapour compositions, Abbott [1986]. Pressure is controlled and temperature is measured or vice versa. The liquid and vapour phases may be sampled and analyzed to obtain the composition of the respective phases. However, sample handling in wide-boiling systems has proved difficult and can result in substantial errors in composition when analyzing the fluids, (Hartwick et al. [1995]). Hala et al. [1967] review still designs through 1965 and Malanowski [1982a] presents a survey of circulation methods, stressing principles of operation and the relative strengths and weaknesses of various designs.

There are two types of dynamic apparatus, depending on the phases that are circulated or passed through the equilibrium cell (Hala et al. [1967]):

- Circulation of the vapour phase only, and
- Circulation of both the vapour and the liquid phases

An excellent review on the development of the circulation method and the various types of apparatus used in this method is provided by Joseph [2001]. An example of an up-to-date dynamic still is presented below.

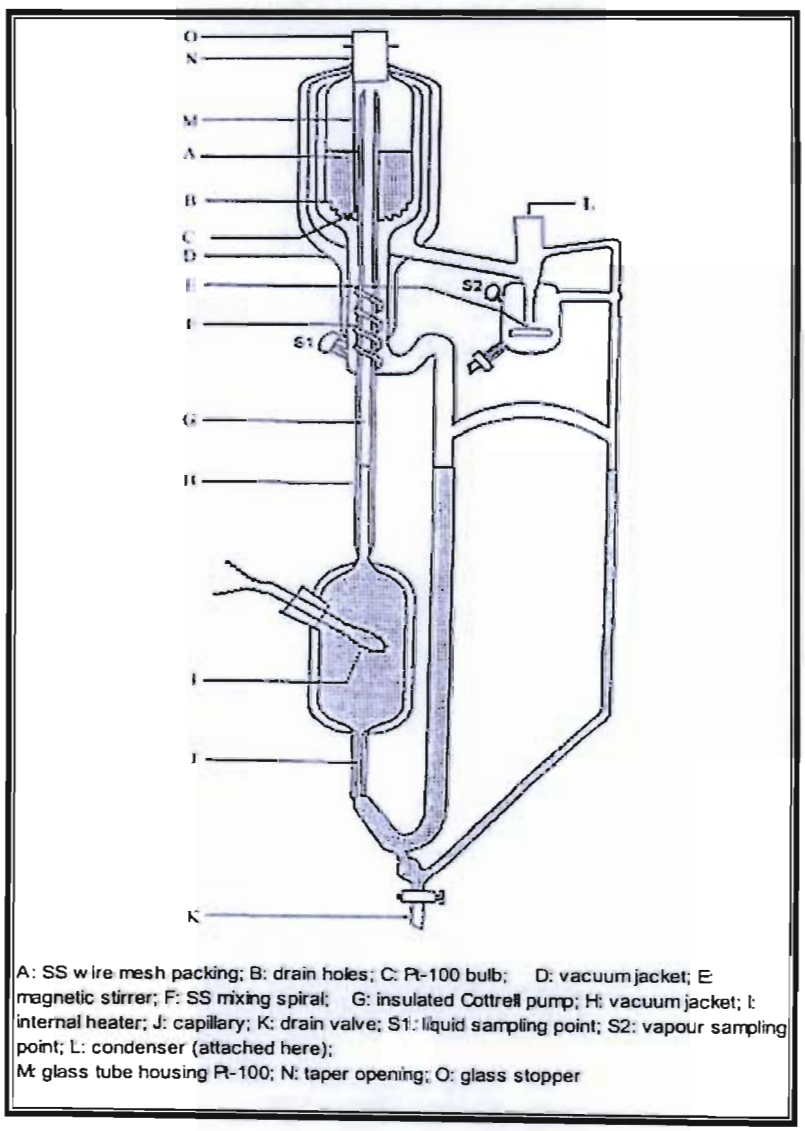

A: SS wire mesh packing; B: drain holes; C: Pt-100 bulb; D: vacuum jacket; E: magnetic stirrer; F: SS mixing spiral; G: insulated Cottrell pump; H: vacuum jacket; I: internal heater; J: capillary; K: drain valve; S1: liquid sampling point; S2: vapour sampling point; L: condenser (attached here);
M: glass tube housing Pt-100; N: taper opening; O: glass stopper

Figure 2-1: Schematic diagram of the VLE still (Raal and Mühlbauer [1998]).

The low pressure dynamic vapour liquid equilibrium still has been developed and improved over several years by Raal (Raal and Mühlbauer [1998]). A central feature of the design is the packed equilibrium chamber, which is concentric around a vacuum-insulated Cottrell tube. The isolated vapour and liquid phases are easily sampled before they are returned to the reboiler. Mechanical stirring is incorporated in both the condensate receiver and the reboiler. The still can be operated either isobarically or isothermally.

2.1.2 The Static Method

Static methods for the measurement of vapour-liquid equilibria have become increasingly important in recent years (Kolbe and Gmehling [1985]). An important step in this direction was made by Gibbs and Van Ness [1972]. A number of sets of apparatus were described. These include apparatus by Ronc and Ratcliff [1976], Tomlins and Marsh [1976], Aim [1978], Maher and Smith [1979], Tamir et al [1981], Mentzer et al. [1982] and more recently, Gmehling and Rarey [1993], and Fisher and Gmheling [1994] in which the principle of the static method was experimentally realized in various ways.

In static methods, a liquid mixture is charged into an evacuated equilibrium cell immersed in a constant temperature bath. The contents of the cell are then agitated mechanically until equilibrium is established between the liquid and its vapour. Temperature control is provided by the bath, and pressure is measured, hence the method is isothermal. The major difficulty of the static method is that, not only must the cell be thoroughly evacuated before the introduction of the liquids, but the liquids themselves must be degassed. The degassing cannot be ignored as its omission will result in inaccurate measured pressures. Degassing can be done by vacuum sublimation (Bell et al. [1968]) or by distillation (Van Ness and Abbott [1978]). Degassing can be either in-situ or external to the equilibrium cell.

Some of the most common and important features of static apparatus are:

- An agitated equilibrium cell. Agitation can be by stirring or shaking. Accurate temperature and pressure measurements are made in the cell.

- Isothermal bath. This provides an environment that controls the temperature of the equilibrium cell. Environmental control can be provided by an air, water or oil bath. It is vital to control and monitor the bath temperature accurately.
- Vacuum system. The equilibrium cell must be thoroughly evacuated before measurement can begin.
- Injection pumps. The components to be investigated are introduced into the equilibrium cell via injection pumps.
- Phase sampling. Only if a static analytical type of apparatus is used.

The static method can be subdivided into static analytical methods, in which one or both the vapour and liquid phases are sampled and analyzed, and the static synthetic method, for which no sampling of the phases is required.

2.1.2.1 The Static Analytical Method

Various researchers adopted this type of experimental apparatus, e.g.: Rigas et al.[1958], Karla et al. [1978], Ng and Robinson [1978], Figuiere et al. [1980], Guillevic et al. [1983], Zimmerman and Keller [1989], and Mühlbauer and Raal [1991]. The main differences between these studies were:

- Equilibrium cell designs and methods of sampling the liquid and vapour phases
- Methods of vaporizing and homogenizing the samples
- Methods of in-situ analysis of the liquid and vapour phases
- Methods of creating uniform equilibrium cell temperature
- Methods of agitating the equilibrium cell contents

This method presents great difficulties when sampling the vapour phase. At low pressures, the amount of vapour required for analysis is of the same order as the total amount of the vapour phase in the equilibrium cell (Hala et al. [1958]), so that removal of a sample upsets the equilibrium. Inoue et al. [1975] tried to address the problem of vapour phase sampling but according to Abbott [1986], their ideas were not popular with the majority of experimentalists who only measured the liquid composition. The vapour composition was then computed from the measured pressure and liquid composition values.

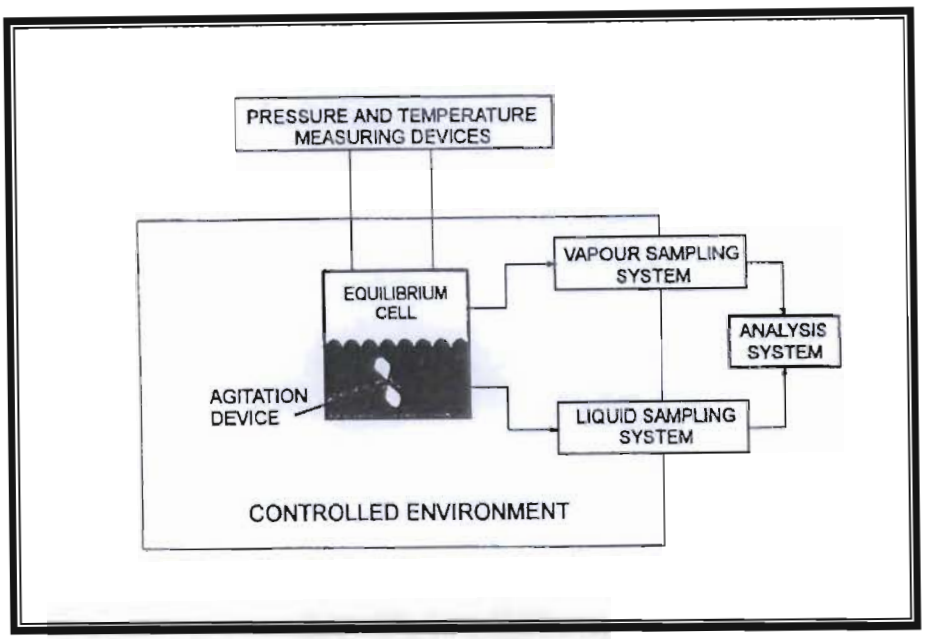

Figure 2-2: Schematic illustration of the static analytical method (Raal and Mühlbauer, [1994]).

2.1.2.2 The Static Synthetic Method

The equipment used for this study was of the synthetic type. Therefore, this section focuses on this type of equipment and follows the progression in this field of study. The static synthetic equipment measures the overall composition and the total pressure (z_i-P). This data can then be used to calculate the liquid equilibrium composition, x_i and the system pressure, P using mass balances and equilibrium relationships. Static synthetic equipment has all the features mentioned above with additional features:

- As the cell volume is required in calculating the phase compositions, it is important that it be known accurately.
- There are no sampling facilities.
- The injected liquid volumes must be known accurately.

The advantages of the static synthetic method are:

- No sampling of the phases is necessary, and therefore no complicated or expensive sampling and analytical devices are required.

- The experimental method is simple.
- Critical state investigations and measurements can be carried out on this type of experimental apparatus.
- An entire isopleth can be obtained from one filling of the equilibrium cell.

The main disadvantages of the static synthetic method are:

- For mixtures with more than two components, the information that can be obtained is very limited.
- Thermodynamic consistency cannot be tested.

Researchers that have adopted this type of experimental apparatus include, Gibbs and Van Ness [1972], Karel Aim [1978], Maher and Smith [1979], Kolbe and Gmehling [1985], Rarey and Gmehling [1993], and Fischer and Gmehling [1994]. The main differences between their studies were:

- Equilibrium cell designs.
- Methods of degassing the sample.
- Methods of agitating the equilibrium cell contents.

In order to explain the development of the static synthetic equipment, it is necessary to start reviewing the equipment of Gibbs and Van Ness [1972] since much work being done in this field is based on the work of Gibbs and Van Ness and operates according to the principles explained in that work.

Experimental apparatus of Gibbs and Van Ness [1972]

Gibbs and Van Ness [1972] developed a new apparatus for vapour liquid equilibria from total pressure measurements. The new apparatus was an improvement of the apparatus of Ljunglin and Van Ness [1962] and Van Ness et al. [1967a, b]. Although the previous experimental technique gave sufficiently accurate data, Gibbs and Van Ness felt that data collection was very slow. Pure degassed liquids were distilled directly into the equilibrium cell, which then had to be emptied and evacuated after each measurement and therefore a separate experiment was required for each measured vapour pressure.

In the new apparatus, pure degassed liquids are first transferred into evacuated piston-and cylinder devices, where they are stored for subsequent injection into the equilibrium cell. Operation of the apparatus commences with the introduction of the pure liquids into the two degassing units, where dissolved gases are removed by refluxing, cooling and evacuating in a special flask over a period of time. After the system has been completely evacuated, the degassed liquids are transferred to the piston injectors where they are stored under positive pressure. The glass equilibrium cell, $100cm^3$ capacity, which is submerged in a constant temperature bath, is half-filled by metering in one of the pure liquids. After equilibrium is reached, the vapour pressure is recorded and compared with literature values. Addition of a further quantity of the same liquid and remeasurement of vapour pressure is a test for complete degassing. A small amount of the second component is then added to the cell. The vapour pressure of this dilute solution is then recorded. The contents of the cell are thoroughly mixed by means of a magnetic stirrer. If the liquids are properly degassed, the main limitation of the method is the accuracy with which one can establish overall compositions from metered liquids volumes. A complete binary VLE experiment covering the entire liquid-composition range requires two runs, which can be done in one or two days (Abbott [1986]). The method is easily adapted to ternary systems (one merely adds a third piston injector), and can also be applied to systems which form two liquids phases (Loehe et al., [1983]). According to Raal and Mühlbauer [1998], this apparatus was found to give accurate results.

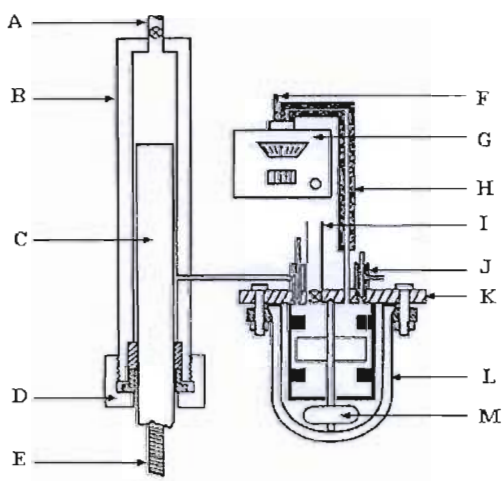

Figure X: Piston-injector and test cell: A, line to degassing vessel; B, piston-injector body; C, Piston; D, Packing nut; E, Lead screw; F, Line to reference vacuum; G, Texas Instruments pressure gauge; H, Heated line; I, Port to vacuum system; J, needle valves; K, cell cover; L Glass cup; M, Teflon coated magnet.

Figure 2-3: Piston injector and equilibrium cell of Gibbs and Van Ness [1972].

Experimental apparatus of Maher and Smith [1979]

The apparatus by Maher and Smith [1979] is an example of a modern static device, specially designed to produce large quantities of binary data in a short time. It consists of fifteen small cells (approximately 25 cm^3 each) which are charged with the two pure components and with thirteen mixtures. Overall compositions are established gravimetrically. After loading, the cells are connected via vacuum fittings to 15 bellows valves mounted in a ring and connected to a manifold. The contents of the cells are degassed in-situ by lengthy freezing-evacuating-thawing cycles. After degassing is complete, the manifold with the attached cells is placed in a constant-temperature bath and connected to a pressure transducer. The P-x isotherm is obtained by sequentially opening each cell to the transducer. Other isotherms are obtained by repeating the cell pressure measurements at other bath temperatures. The Maher and Smith apparatus produces in a week three or four complete isotherms for a single binary system. No provision was made for agitation of the equilibrium cell contents, and this may explain the long times required for equilibration. Data production is much faster with this equipment compared to that of Gibbs and Van Ness [1972] because the former has fifteen equilibrium cells whereas the latter has only one equilibrium cell.

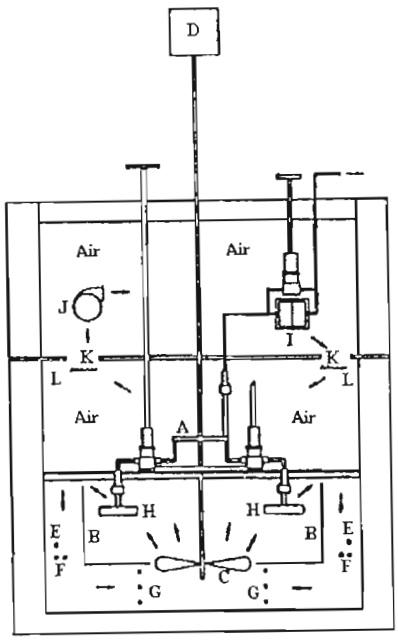

Figure: Schematic sketch of the PTx apparatus showing the liquid and air baths: A = manifold assembly; B = Baffle tank; C= impeller; D = impeller motor; E = auxiliary heater; F = auxiliary cooling coil; G = control heater; H = Cells; I = nulling transducer; J = air bath blower; K = openings for air flow; L = air bath heaters.

Figure 2-4: Experimental apparatus of Maher and Smith [1979].

Experimental apparatus of Kolbe and Gmehling [1985]

This apparatus operates according to the principles developed by Gibbs and Van Ness [1972]. The apparatus was designed to measure the total pressure as a function of the overall composition, and allowed measurement of VLE at temperatures up to 150°C and pressures between 100 mbar and 10 bars. The pure degassed liquids are stored in glass flasks and are closed by a Teflon valve. Exactly known volumes of the substances under study are introduced into the equilibrium cell using the dosage equipment as with the equipment of Gibbs and Van Ness [1972]. The dosage equipment (piston injectors) of 100 cm^3 capacity, was manufactured by Ruska Inc., Texas and consists of hand-driven pistons. The magnetically stirred equilibrium cell is then immersed in a thermostatted bath. The stirrer is driven via a magnetic coupling by an electric motor outside the cell. The temperature in the equilibrium cell is measured with a Hewlett-Packard 2801A quartz thermometer and the pressure with a Desgranges and Hout pressure balance. A differential pressure indicator is used to

separate the pressure balance from the equilibrium cell to avoid direct contact between the vapour and pressure balance and to keep the vapour volume as small as possible. Figure 2-5 is a schematic diagram of the equipment.

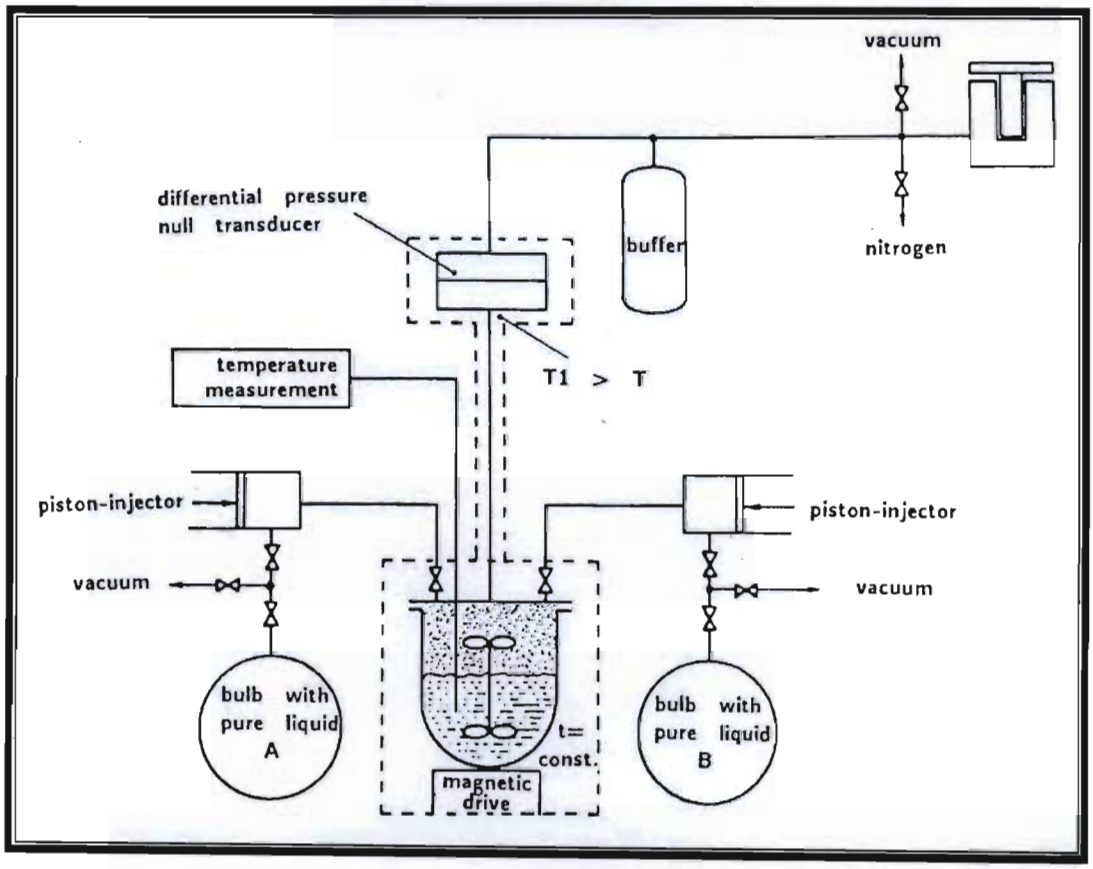

Figure 2-5: Schematic diagram of the apparatus of Kolbe and Gmehling [1985]

The cell and its lid are shown in Figure 2-6.The cell is made of a thick-walled (ca. 5mm) glass and has a volume of ca. 180 cm^3. The lid, including the valves for introducing the pure liquid, was made of Stainless steel (316 grade). The lid is sealed onto the equilibrium cell with a Teflon gasket.

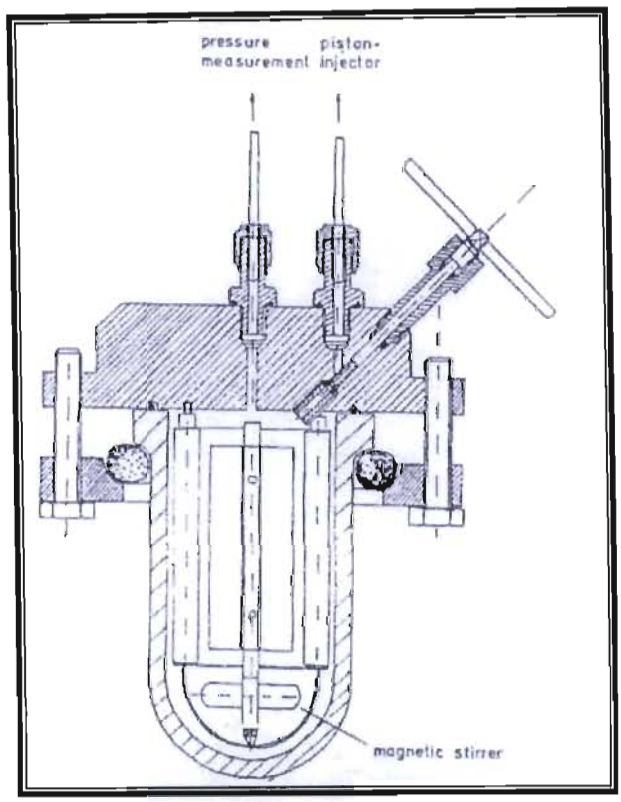

Figure 2-6: Section through the equilibrium cell, Kolbe and Gmehling [1985].

Experimental apparatus of Rarey and Gmehling [1993]

This static synthetic apparatus was developed by Rarey [1991] and fully described by Rarey and Gmehling [1993]. It is computer-operated and is based on the principles of the apparatus of Gibbs and Van Ness [1972]. Rarey and Gmehling [1993]'s equipment was set up to examine if an automatic procedure would be reliable and safe enough for liquid equilibrium by a static method. The apparatus can be used for the measurement of binary and ternary VLE data, activity coefficient at infinite dilution, gas solubilities, pure-component vapour pressure data and isothermal compressibilities of liquids in the temperature range from below 0 to 100 °C and up to 75 bar absolute pressure. Exactly known volumes of pure and degassed liquids are introduced into the equilibrium cell, submerged in a stirred high precision water bath, using an automated high precision piston pump. The precision of the injected volumes is $\pm 1 \times 10^{-6}$ dm^3. The content of the cell is stirred and once equilibrium is reached, the pressure is recorded and the composition is changed. Both injection of components and the measurement of equilibrium pressure and temperature are fully automated. Figure 2-7 is a schematic diagram of the equipment. The temperature of the bath is measured outside the cell with a HART Scientific 1506 thermometer pre-

calibrated by NIST and the pressure is measured using a DIGIQUARTZ-differential pressure sensor model 5012-D-002.

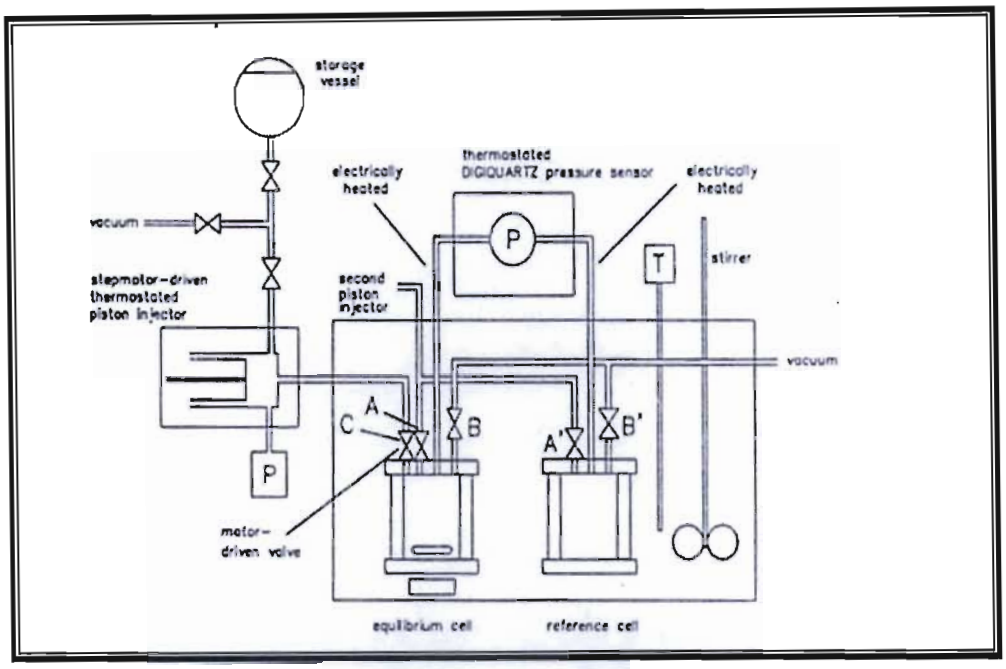

Figure 2-7: Schematic diagram of the apparatus of Rarey and Gmehling [1993].

The full automation of this apparatus is what makes its originality. The high precision injection pump was constructed following a design by Gaube [1988]. The piston is moved by a stepping motor with a resolution of 1000 steps/rotation. Figure 2-8 is a schematic diagram of the high precision injection pump. The maximum injectable volume of the piston injector is ca. 32 cm^3 and the minimum injectable volume is ca. 0.03 cm^3.

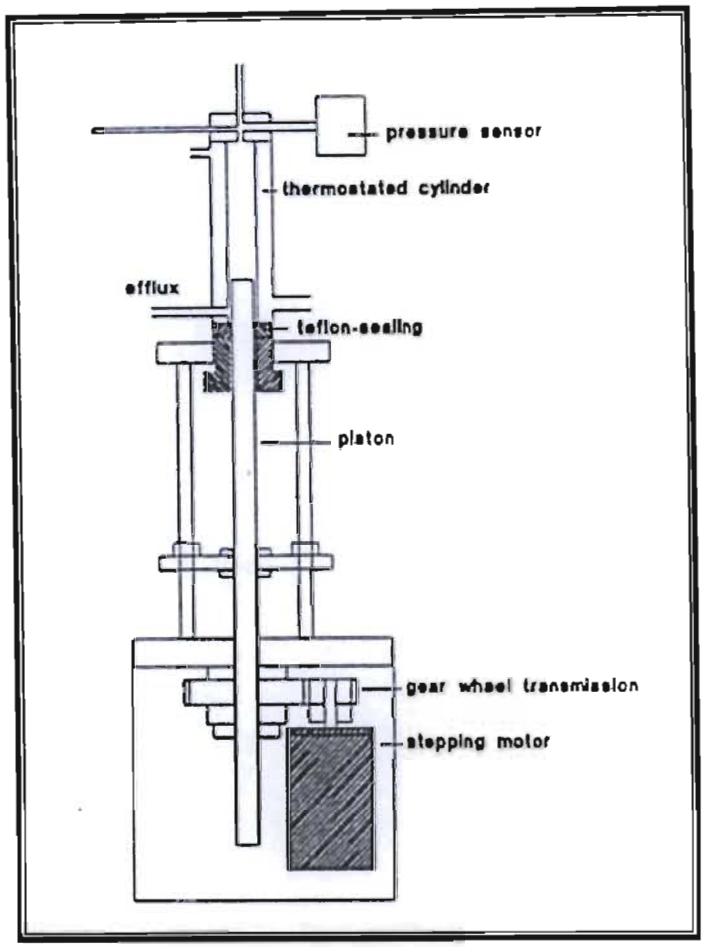

Figure 2-8: Schematic diagram of high precision injection pump of Gaube [1988].

Experimental apparatus of Fisher and Gmehling [1994]

The design and operation of this apparatus is similar to that of Kolbe and Gmehling [1985]. The equilibrium cell is thermostatted using a constant-temperature bath. The feed composition can be determined by reading liquid volume changes in the piston injectors. The system equilibrium pressure is compensated using a differential pressure null indicator, which is superheated to prevent condensation. There are however several improvements from the previous design: The liquids in the piston are kept at constant temperature ±0.1 K (by using a water jacket around the piston barrel) and pressure ±0.01bar. The maximum pressure of the equipment was extended to 120 bar by replacing the glass equilibrium cell with a steel one. The internal electric motor magnetically connected with the stirrer in the equilibrium cell was replaced with a rotating magnetic field induced by four solenoids.

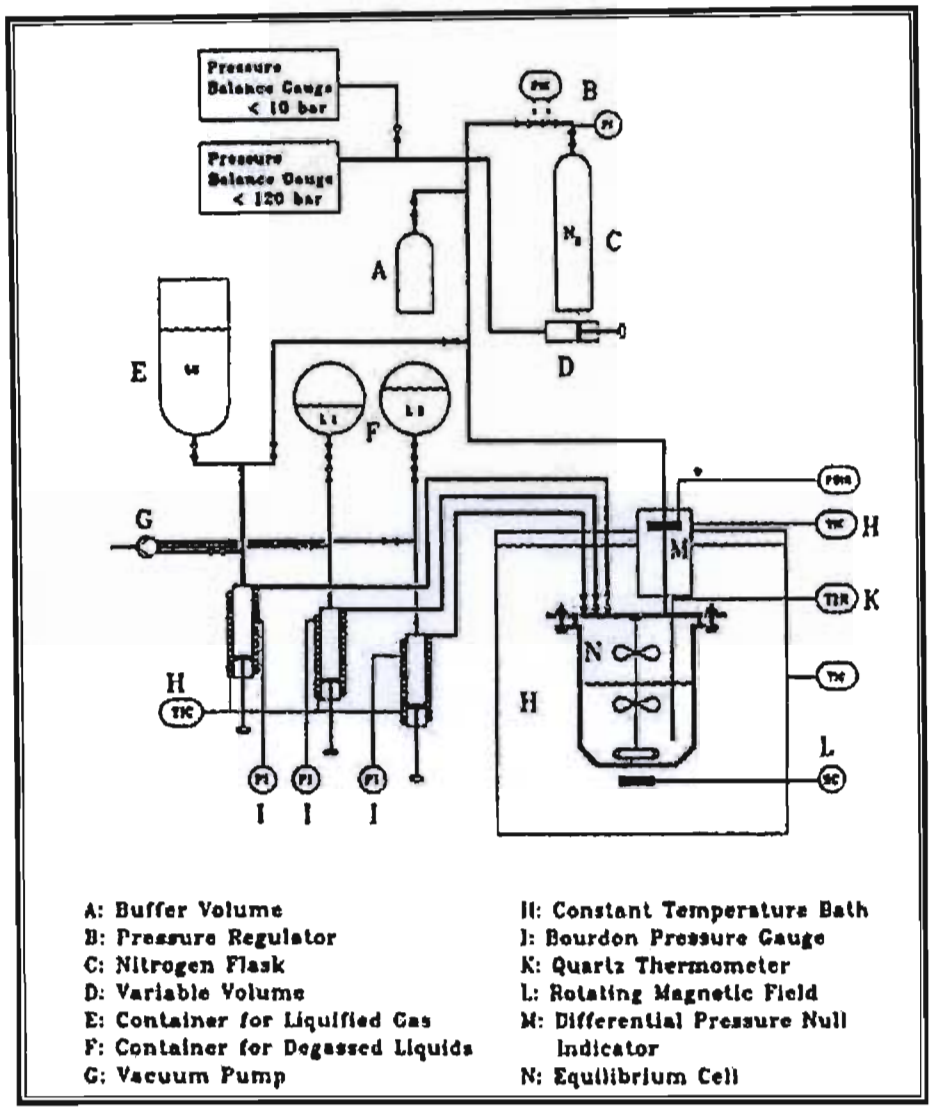

Figure 2-9: Schematic diagram of the apparatus of Fischer and Gmehling [1994].

The above review gives a description of some of the most widely used VLE apparatus and follows the development of the static synthetic equipment over the years. There are many other designs used with great success not mentioned here. The static total pressure apparatus used in this work is of the synthetic type. Its main parts are: The equilibrium cell with a total interior volume of 190 cm^3, two dual mode piston-injectors this is what makes the difference between the current design from other designs mentioned above, two simple degassing apparatus and a constant temperature bath to provide isothermal environment. More details on this design are given in the next Chapter.

2.2 Computation of Low Pressure Vapour Liquid Equilibrium

The separation of components in a chemical process stream constitutes a major portion of all processes in the chemical and petroleum industries Gess et al. [1991]. Experimental VLE data are often measured for binary systems and if such data are available for the desired components they may not be at the required operating conditions of temperature and pressure. It is therefore necessary to be able to use a limited number of experimental data points to interpolate or extrapolate to other conditions and to compute multi-component properties from binary data.

Experimental VLE measurements contain some combination of the measurable variables-temperature, pressure and liquid and/or vapour compositions. Static equilibrium cells, for example, may produce either P-T-x-y data or P-T-z_i data (z_i is the total charged composition of component i in the equilibrium cell). Since not all the important variables such as the liquid and /or the vapour phase composition could be measured, one should use a computational method to find the unmeasured variables. In recirculating equilibrium stills, all four variables may be measured. However, in some cases one of the measured variables may be considered unreliable and could be excluded in favour of computation. This section deals with the thermodynamic treatment of experimental VLE data.

2.2.1 Criterion for phase equilibria

The criterion for phase equilibrium as stated by Smith and Van Ness [1987] is: "Multiple phases at the same temperature and pressure are in equilibrium when the fugacity or chemical potential of each species is uniform throughout the system". Consider a closed system consisting of two phases, α and β, in equilibrium. Within this closed system, each of the individual phases is an open system, free to transfer mass to the other. Assuming that at equilibrium, the temperature and pressure are uniform throughout the entire system, the following equations can be written for each of the phases α and β:

$$d\left(nG\right)^{\alpha} = \left(nV\right)^{\alpha} dP - \left(nS\right)^{\alpha} dT + \sum \mu_i^{\alpha} dn_i^{\alpha} \qquad (2\text{-}1)$$

$$d(nG)^{\beta} = (nV)^{\beta} dP - (nS)^{\beta} dT + \sum \mu_i^{\beta} dn_i^{\beta} \tag{2-2}$$

Where μ_i is the chemical potential and it is defined in terms of the Gibbs energy as:

$$\mu_i = \left[\frac{\partial (nG)}{\partial n_i} \right]_{T,P,n_j} \tag{2-3}$$

Equations (2-1) and (2-2) may be added to give the total changes for the system:

$$d(nG) = (nV) dP - (nS) dT + \sum \mu_i^{\alpha} dn_i^{\alpha} + \sum \mu_i^{\beta} dn_i^{\beta} \tag{2-4}$$

In equation (2-4), the total system properties were obtained using the following relation:

$$nM = (nM)^{\alpha} + (nM)^{\beta} \tag{2-5}$$

Since the two-phase system is closed, the following equation is valid:

$$d(nG) = (nV) dP - (nS) dT \tag{2-6}$$

Comparison of equation (2-4) and equation (2-6) shows that at equilibrium:

$$\sum \mu_i^{\alpha} dn_i^{\alpha} + \sum \mu_i^{\beta} dn_i^{\beta} = 0 \tag{2-7}$$

Since the conservation of mass (for systems without chemical reaction) requires that $dn_i^{\alpha} = -dn_i^{\beta}$, equation (2-7) reduces to:

$$\sum (\mu_i^{\alpha} - \mu_i^{\beta}) dn_i^{\alpha} = 0 \tag{2-8}$$

Equation (2-8) can only be satisfied if the term in the parenthesis is separately zero since the quantities dn_i are independent and arbitrary. Hence

$$\mu_i^{\alpha} = \mu_i^{\beta} \tag{2-9}$$

This result may be generalized to more than two phases by considering the phases by pairs. The general result for π phases with N chemical species is:

$$\mu_i^{\alpha} = \mu_i^{\beta} = ... = \mu_i^{\pi} \quad (i = 1, 2, ..., N) \tag{2-10}$$

An alternative and equally general criterion for equilibrium can be derived from the following equation:

$$d\bar{G}_i = RTd \ln f_i \text{ (Constant T)} \tag{2-11}$$

f_i is the fugacity of species i in solution, it has the dimension of pressure and is more readily related to measurable quantities such as temperature and pressure than μ_i. $\bar{G}_i$ is the partial molar Gibbs energy and it is given by

$$\bar{G}_i = \left[\frac{\partial(nG)}{\partial n_i}\right]_{T,P,n_j} \tag{2-12}$$

Comparison of equation (2-12) and (2-3) implies that $\mu_i = \bar{G}_i$. Thus equation (2-11) becomes:

$$d\mu_i = RTd \ln f_i \text{ (Constant T)} \tag{2-13}$$

Integration of equation (2-13) at constant temperature gives:

$$\mu_i = RT \ln f_i + \theta_i(T) \tag{2-14}$$

Since θ_i is dependent on the temperature only and since all the phases are at the same temperature, substitution of equation (2-14) in (2-10) yields:

$$f_i^{\alpha} = f_i^{\beta} = ... = f_i^{\pi} \quad (i = 1,2,...,N) \tag{2-15}$$

According to equation (2-15), the condition for phase equilibrium between a liquid (L) and its vapour (V) phase at the same temperature and pressure is:

$$f_i^{L} = f_i^{V} \tag{2-16}$$

For an ideal system, the compositions of the vapour and liquid phase can be related as follows:

$$y_i P = x_i P_i^{sat} \tag{2-17}$$

This ideal situation is commonly known as the Raoult's Law.

2.2.2 Fugacity Coefficient

The fugacity coefficient ϕ_i is a measure of non-ideality and its departure from unity is the measure of the extent to which a molecule i interacts with its neighbours. Fugacity and fugacity coefficients have been successfully applied for both the vapour and liquid phases through equations of state. Only the fugacity coefficient for the vapour phase non-ideality is considered. The fugacity $\hat{f}_i^V$ of a component i in the vapour phase is related to its mole fraction y_i in the vapour phase and to the total pressure p by the fugacity coefficient:

$$\phi_i = \frac{\hat{f}_i^V}{y_i p} \tag{2-18}$$

The fugacity coefficient is a function of temperature, total pressure, and composition of the vapour phase; it can be calculated from volumetric data for the vapour mixture. The fugacity coefficient can be found by using an equation of state in the rigorous thermodynamic relation Beattie [1949]:

$$\ln \phi = \frac{1}{RT} \int_V^\infty \left[\left(\frac{\partial P}{\partial n_i} \right)_{T,V,n_{j \neq i}} - \frac{RT}{V} \right] dV - \ln z \tag{2-19}$$

Where n_i stands for the number of moles of component i, V is the total volume of the vapour mixture, and z is the compressibility factor of the vapour mixture,

$$z = \frac{PV}{(n_1 + n_2 + ...)RT} \tag{2-20}$$

At low pressures, less than one atmosphere, it may be a good assumption to set $\phi = 1$, but even at moderately low pressures, say in the vicinity of 1 to 10 atm, ϕ is often significantly different from

unity, especially if i is a polar component (Prausnitz et al.[1967]). For this project vapour phase fugacity coefficients were evaluated using the virial equation of state truncated after the second term.

2.2.3 Activity Coefficient and Excess Gibbs Free Energy Models

Knowledge of activity coefficient values is necessary for use of the $\gamma - \phi$ approach for modeling Phase Equilibria. The activity coefficient, γ, is a useful concept to describe the non-ideality of a condensed phase. It is used to account for the departure from ideal solution behaviour and is defined by the equation:

$$\gamma_i = \frac{f_i}{f_i^{id}} = \frac{f_i}{x_i f_i^0} \tag{2-21}$$

The standard-state fugacity f_i^0 is usually taken as the fugacity of component i at the same temperature as that of the mixture but at some fixed composition and some specified pressure.
Activity a of a compound i is:

$$a_i = x_i \gamma_i \tag{2-22}$$

For an ideal solution the activity equals the mole fraction, that is $a_i = x_i$. Thus for an ideal solution the activity coefficient is unity.
There is no explicit thermodynamic relation for the activity coefficient in terms of experimental quantities, but it may be related to them indirectly with the use of the following form of the Gibbs-Duhem equation (Gibbs, [1928])

$$\sum_i x_i \left(\frac{\partial \ln \gamma_i}{\partial x_i} \right)_{T,P} = 0 \tag{2-23}$$

In practice, the Gibbs-Duhem equation is most valuable when used with the concept of the excess Gibbs free energy, which is defined by

$$\frac{G^E}{RT} = \sum_i x_i \ln \gamma_i \tag{2-24}$$

This equation gives G^E as a function of the activity coefficients of all species in a mixture. By applying the Gibbs-Duhem equation, we can relate the individual activity coefficients to G^E by differentiation

$$\ln \gamma_i = \left[\frac{\partial \left(nG^E / RT \right)}{\partial n_i} \right]_{P,T,n_j} \tag{2-25}$$

In order to use these equations, a mathematical relation for G^E as a function of composition is needed. For this purpose, many different excess Gibbs models (G^E models) have been developed and examples are:

1. Margules
2. Van Laar
3. Wilson
4. T-K Wislon
5. NRTL
6. UNIQUAC

These models are discussed in more detail by Walas [1985], Gess et al. [1991], Malanowski and Anderko [1992], Sandler [1994] and Raal and Mühlbauer [1998]. A brief discussion of the first five models is provided.

2.2.3.1 The Margules Equation

This equation was developed by Margules [1895] and is only applicable to binary systems. Despite having been developed long ago, it is still in common use today and gives accurate results for some systems. It has also, frequently, been found to be superior to other equations (Walas [1985]. It is convenient to write an expression for G^E in terms of the multiplier of the term $x_1 x_2$ since it will then satisfy the requirement that G^E should be zero at $x_1 = 0$ and $x_2 = 0$. This formed the basis of the formulation of the expression:

$$\frac{G^E}{RT} = x_1 x_2 \left[A_{21} x_1 + A_{12} x_2 \right] \tag{2-26}$$

From the above equation, the well-known Margules 3 suffix equations can be derived

$$\ln \gamma_1 = x_2^2 \left[A_{12} + 2\left(A_{21} - A_{12} \right) x_1 \right] \tag{2-27}$$

$$\ln \gamma_2 = x_1^2 \left[A_{21} + 2\left(A_{12} - A_{21} \right) x_2 \right] \tag{2-28}$$

The parameters A_{12} and A_{21} are nominally temperature independent constants (Raal and Mühlbauer [1998]).

.

2.2.3.2 The Van Laar Equation

This equation was developed by Van Laar [1910], originally using the Van Der Waals equation of state as a basis, but since the fit of activity coefficient data with Van Der Waals parameters is poor, the Van Laar equation is now regarded as purely empirical. It has been formulated by expanding $\frac{x_1 x_2}{\left(G^E / RT \right)}$ as a polynomial in $\left(x_1 - x_2 \right)$ to get

$$\frac{x_1 x_2}{\left(G^E / RT \right)} = B + C\left(x_1 - x_2 \right) \tag{2-29}$$

Which is equivalent to

$$\frac{G^E}{RT x_1 x_2} = \frac{A_{12}' A_{21}'}{A_{12}' x_1 + A_{21}' x_2} \tag{2-30}$$

The activity coefficient expressions derived from the equation above are:

$$\ln \gamma_2 = A_{21}' \left[1 + \frac{A_{21}' x_2}{A_{12}' x_1} \right]^{-2} \tag{2-31}$$

$$\ln \gamma_1 = A_{12}' \left[1 + \frac{A_{12}' x_1}{A_{21}' x_2} \right]^{-2} \tag{2-32}$$

The Van Laar Equation takes into account the size difference between molecules. For highly non-ideal systems, this equation is not a good choice. Although Walas [1985] found that this equation is capable of representing the activity coefficients of some complex mixtures, Prausnitz et al [1986] recommend the use of the Van Laar Equation for relatively simple non-polar solutions.

The Margules and Van Laar equations have been formulated empirically and have no sound theoretical basis. They are not readily extended to multi-component mixtures (Raal and Mühlbauer [1998]). The main advantages of these equations are that they are mathematically simple and provide flexibility in fitting VLE data for simple binary systems.

2.2.3.3 The Wilson Equation

This expression for G^E was developed by G.M. Wilson in 1964. He considered local compositions rather that the overall liquid composition in the formulation of his model by taking into account the effects of differences in the size and intermolecular forces of components. The expression that he gives is

$$\frac{G^E}{RT} = -x_1 \ln\left[x_1 + x_2\Lambda_{12}\right] - x_2 \ln\left[x_2 + x_1\Lambda_{21}\right] \tag{2-33}$$

This yields the following expressions for the activity coefficients:

$$\ln\gamma_1 = -\ln\left[x_1 + x_2\Lambda_{12}\right] + x_2\left[\frac{\Lambda_{12}}{x_1 + x_2\Lambda_{12}} - \frac{\Lambda_{21}}{x_2 + x_1\Lambda_{21}}\right] \tag{2-34}$$

$$\ln\gamma_2 = -\ln\left[x_2 + x_1\Lambda_{21}\right] + x_1\left[\frac{\Lambda_{12}}{x_1 + x_2\Lambda_{12}} - \frac{\Lambda_{21}}{x_2 + x_1\Lambda_{21}}\right] \tag{2-35}$$

The parameters Λ_{12} and Λ_{21} are related to the pure component liquid molar volumes (obtainable from the Rackett [1970] equation) by:

$$\Lambda_{12} = \frac{V_2}{V_1}\exp\left[-\frac{\lambda_{12} - \lambda_{11}}{RT}\right] \tag{2-36}$$

$$\Lambda_{21} = \frac{V_1}{V_2} \exp\left[-\frac{\lambda_{21} - \lambda_{22}}{RT} \right] \tag{2-37}$$

The parameters $(\lambda_{12} - \lambda_{11})$ and $(\lambda_{21} - \lambda_{22})$ represent the molecular interactions of the components. This equation is found to be superior to the Margules and Van Laar equations, and is applicable to highly non-ideal systems, including systems which contain polar and associating compounds. This equation is easily generalized to any number of components; only binary parameters are required for representing multi-component mixtures. However, it is unable to describe systems in which partial liquid miscibility occurs and this equation cannot also be used for systems exhibiting a maximum or minimum in the activity coefficient.

2.2.3.4 The T-K Wilson Equation

A modified version of the Wilson [1964] equation was proposed by Tsuboka and Katayama [1975]. This equation allows systems of partial liquid miscibility to be modeled satisfactorily. The excess Gibbs energy function of the T-K Wilson is:

$$\frac{G^E}{RT} = x_1 \ln\left[\frac{x_1 + V_{12} x_2}{x_1 + \Lambda_{12} x_2} \right] + x_2 \ln\left[\frac{x_2 + V_{21} x_1}{x_2 + \Lambda_{21} x_1} \right] \tag{2-38}$$

The corresponding activity coefficient equations are:

$$\ln \gamma_1 = \ln\left[\frac{x_1 + V_{12} x_2}{x_1 + \Lambda_{12} x_2} \right] + \left[\beta - \beta_v \right] x_2 \tag{2-39}$$

$$\ln \gamma_2 = \ln\left[\frac{x_2 + V_{21} x_1}{x_2 + \Lambda_{21} x_1} \right] - \left[\beta - \beta_v \right] x_1 \tag{2-40}$$

Where

$$\beta = \frac{\Lambda_{12}}{x_1 + \Lambda_{12} x_2} - \frac{\Lambda_{21}}{x_2 + \Lambda_{21} x_1} \tag{2-41}$$

$$\beta_v = \frac{V_{12}}{x_1 + V_{12} x_2} - \frac{V_{21}}{x_2 + V_{21} x_1} \tag{2-42}$$

$$V_{12} = \frac{V_2}{V_1} \tag{2-43}$$

$$V_{21} = \frac{V_1}{V_2} \tag{2-44}$$

V_{12} and V_{21} are the ratios of the molar volumes. The parameters Λ_{12} and Λ_{21} are as in the Wilson equation.

2.2.3.5 The NRTL (Non-random Two Liquid) Equation

The non-random two-liquid (NRTL) equation was developed by Renon and Prausnitz [1968] to address the deficiencies of the Wilson equation. This local composition model is able to correlate data for systems that contain partial liquid miscibility, while still being able to handle systems for which the Wilson equation is applicable. The NRTL equation for the excess Gibbs energy is:

$$\frac{G^E}{RT} = x_1 x_2 \left[\frac{\tau_{21} G_{21}}{x_1 + x_2 G_{21}} + \frac{\tau_{12} G_{12}}{x_2 + x_1 G_{12}} \right] \tag{2-45}$$

With the following expression for the activity coefficients

$$\ln \gamma_1 = x_2^2 \left[\tau_{21} \left(\frac{G_{21}}{x_1 + x_2 G_{21}} \right)^2 + \left(\frac{\tau_{12} G_{12}}{\left(x_2 + x_1 G_{12} \right)^2} \right) \right] \tag{2-46}$$

$$\ln \gamma_2 = x_1^2 \left[\tau_{12} \left(\frac{G_{12}}{x_2 + x_1 G_{12}} \right)^2 + \left(\frac{\tau_{21} G_{21}}{\left(x_1 + x_2 G_{21} \right)^2} \right) \right] \tag{2-47}$$

Where

$$\tau_{ji} = \frac{g_{ji} - g_{ii}}{RT} \tag{2-48}$$

$$G_{ji} = \exp\left[-\alpha_{ji} \tau_{ji} \right] \tag{2-49}$$

g_{ji} is a parameter for interaction between components j and i

$\alpha_{ij} = \alpha_{ji}$ is a non randomness parameter and,

$(g_{ji} - g_{ii})$ are the adjustable parameters.

The NRTL equation usually represents binary-equilibrium data quite well with its three parameters. It is superior to the Margules and Van Laar equations in that it is applicable to multi-component mixtures. The NRTL equation has, like the Wilson equation, the advantage of limited parameter temperature dependence although this does not apply to the third parameter α_{ij}. This is not a serious issue as the values of the activity coefficients are generally insensitive to values of α_{ij} in the range -1 to 0.5 (Walas [1985]). Walas [1985] proposed a value of α_{ij} = 0.3 for non-aqueous systems and α_{ij} = 0.4 for those containing water. However according to Raal and Mühlbauer [1998] a suitable value of α_{ij} should be found from the experimental data through reduction rather than using a fixed value. This equation has become one of the most useful and widely used equations in phase equilibrium studies (Raal and Mühlbauer [1998]).

2.2.4 Activity coefficient at infinite dilution

Much chemical processing occurs at conditions of high dilution for one or more of the species present. Hence there are special needs for activity coefficients at infinite dilution γ_i^{∞}. These quantities may of course be obtained from conventional VLE experiments by extrapolation of activity coefficients, or as limiting features of the correlated excess Gibbs energies (Abbott [1986]). Direct measurement of γ_i^{∞} is preferable to the extrapolated ones because the latter often lead to large errors.

Infinite dilution activity coefficients can be determined experimentally in fives ways:

1- Gas chromatographic methods
2- Differential static methods
3- Inert gas stripping
4- Ebulliometry
5- Raleigh distillation

Excellent reviews of these experimental methods are available in the book by Raal and Mühlbauer [1998] and will not be discussed here. Maher and Smith [1979] also described a method for finding γ_i^{∞} from experimental P-x_i data obtained in the dilute region. The evaluation of γ_i^{∞} is presented in Appendix A.

2.3 Approaches for VLE Data Reduction

Data reduction is the process of fitting various thermodynamic models to VLE data, determining the optimum parameters for these models and finally ascertaining which model best describes the data. The nature of a data-reduction procedure is conditioned by the type of VLE data being treated (isothermal vs. isobaric), by whether the data set is complete or partial, and by the level of statistical sophistication deemed necessary Abbott [1986]. There are mainly two different approaches to model phase equilibria Malanowski et al. [1992]. The two approaches are based on the fact that at thermodynamic equilibrium, fugacity values are equal in both vapour and liquid phases, at isothermal conditions. Only the case of isothermal data is considered here since isothermal data were measured in this project. The two approaches for regressing low pressure VLE data are:

1- The combined method ($\gamma - \phi$ approach)
2- The direct method ($\phi - \phi$ approach)

Wichterle [1978a, b] and Raal and Mühlbauer [1998] give excellent reviews on the two theoretical approaches mentioned above.

2.3.1 The combined method ($\gamma - \phi$ approach)

This approach is based on the activity coefficient model for the liquid phase non-ideality and an equation of state for the vapour phase non-ideality. (For this work, the Virial equation of state was used to account for the vapour phase non-ideality). The equilibrium equation (2-16) can be written:

$$x_i \gamma_i f_i = y_i \phi_i^V P \qquad (2\text{-}50)$$

Where the pure component fugacity f_i is:

$$f_i^L = \phi_i^{sat} P_i^{sat} \exp\left[\frac{V_i^L\left(P - P_i^{sat}\right)}{RT}\right] \tag{2-51}$$

The term $\exp\left[\frac{V_i^L\left(P - P_i^{sat}\right)}{RT}\right]$ is referred to as the Pointing factor and describes the effect of P on the liquid phase fugacity. V_i^L is the liquid molar volume and is evaluated using the Rackett [1970] equation:

$$V_i^L = V_{ci} Z_{ci}^{(1-T_r)^{0.2857}} \tag{2-52}$$

The critical molar volume, V_{ci} and compressibility factor, Z_{ci} are given in Reid et al [1988] for a large number of components and the reduced temperature T_r is calculated from T/T_c .

Data reduction using the combined method was pioneered by Barker [1953] and was the method used in this work. This method involves the following steps:

1. A suitable expression for G^E as a function of composition is assumed. Barker [1953] used the Scatchard [1949] polynomial (also known as the Redlich-Kister expansion)

$$\frac{G^E}{RT} = x_1 x_2 \left[a + b(x_1 - x_2) - c(x_1 - x_2)^2\right] \tag{2-53}$$

2. The system total pressure is given by

$$P = \frac{x_1 \gamma_1 P_1^{sat}}{\Phi_1} + \frac{x_2 \gamma_2 P_2^{sat}}{\Phi_2} \tag{2-54}$$

3. Activity coefficients γ_i are calculated by using the relation

$$\ln \gamma_i = \left[\frac{\partial\left(G^E/RT\right)}{\partial n_i}\right]_{P,T,n_j} \tag{2-55}$$

Expressions for γ_1 and γ_2, consistent with equation (2-53) for G^E are substituted into equation (2-54).

4. Combination of equation (2-54) and (2-55) gives an expression that does not involve vapour composition (y) except in the Φ_i, which are initially neglected, and the only unknowns are the fitting constants in equation (2-53) for G^E (or $\ln \gamma_i$). An optimal fitting procedure is used to find these unknowns producing the best fit for the experimental *P-x* data for the whole composition range. The correction factors Φ_i, assumed = 1 in the first iteration, are recalculated when the vapour compositions have been found (step 5).

5. Once suitable values for the fitting constants have been found, the problem is solved and either activity coefficients or vapour compositions can be calculated from equation (2-55) and (2-56).

$$y_i = \frac{x_i \gamma_i P_i^{sat}}{P \Phi_i} \tag{2-56}$$

The correction factors Φ_i are computed assuming that the vapour phase can be described by the truncated virial EOS. (This will be discussed later).

$$\Phi_i = \exp\left[\frac{\left(B_{ii} - V_i^L\right)\left(P - P_i^{sat}\right) + P y_i^2 \delta_{ij}}{RT}\right] \tag{2-57}$$

where $\delta_{ij} \equiv 2B_{ij} - B_{ii} - B_{jj}$

Barker [1953] minimized the pressure residual in her pioneering work. According to Van Ness et al. [1978] different objective functions will give different parameters for a given model except when the data are perfect. For a detailed review of different objective functions the reader is referred to an excellent compilation by Gess et al. [1991].

The choice of a correlating equation for the excess Gibbs free energy is an important decision in data reduction, and systems with complex behaviour may require the testing of several equations before a suitable fit is found. The search for an appropriate equation is complicated if there is much scatter in the data or if the data set is thermodynamically inconsistent.

2.3.2 The direct method ($\phi - \phi$ approach)

This method offers an alternative to the combined method in modeling low pressure vapour liquid equilibrium (Perry [1997]). The main feature of the direct method (Wichterle [1978]) is that the liquid and the vapour phase non-idealities of each component i, in an equilibrium mixture are described through their fugacity coefficients,

$$\hat{f}_i^L = x_i \phi_i^L = \hat{f}_i^V = y_i \phi_i^V \tag{2-58}$$

which are calculated using the exact thermodynamic relationships,

$$\ln \phi_i^L = \left(\frac{1}{RT}\right) \int_{V^l}^{\infty} \left[\left(\frac{\partial P}{\partial n_i} \right)_{T,V,n_j} - \frac{RT}{V^L} \right] dV - \ln \left[\frac{PV^L}{n_T RT} \right] \tag{2-59}$$

$$\ln \phi_i^V = \left(\frac{1}{RT}\right) \int_{V^l}^{\infty} \left[\left(\frac{\partial P}{\partial n_i} \right)_{T,V,n_j} - \frac{RT}{V^V} \right] dV - \ln \left[\frac{PV^V}{n_T RT} \right] \tag{2-60}$$

The principle challenges associated with the application of the direct method are:

- Selection of the most appropriate EOS to describe both the liquid and vapour phase non-idealities. Literally hundreds of EOS are described in the literature. The main criterion in the selection of an EOS is that it must be flexible enough to fully describe a pure substance's P,V,T behavior for both phases in the temperature and pressure ranges under study

- Selection of appropriate mixing rules, which are required to extend the pure-component form of the EOS to mixtures. Most mixing rules, although derived using theoretical assumptions, are somewhat empirical and tend to be system specific.

- Location of the appropriate roots for liquid and vapour molar densities when higher than cubic equations of state are used (Raal et al., [1980]).

The direct method was not used in this work therefore no further discussion is deemed necessary. For both the Combined and Direct methods, the use of an equation of state is necessary. Equations of state can be classified in several categories: empirical equations, cubic equations, and equations based on statistical mechanics.

2.4 The Virial Equation of State

The virial equation is the only equation of state with a firm theoretical basis (Prausnitz et al. [1967]). This equation is used to accurately represent experimental properties of pure compounds. The extension from pure compounds to fluid mixtures is problematic, as in theory a mixing rule is needed for each parameter. Gases and vapours at low pressures have been successfully correlated using the virial equation of state. The preferred truncated form of the virial equation of state is:

$$z = \frac{PV}{RT} = 1 + \frac{BP}{RT} \tag{2-61}$$

where z is the compressibility factor and it is unity for an ideal gas. B is the second virial coefficient, and it is a function of temperature only for pure components; for a mixture it is also function of composition as given by the relationship

$$B_{mixture} = \sum_{i}^{N} \sum_{j}^{N} y_i y_j B_{ij} \tag{2-62}$$

where y_i and y_j are the mole fraction of component i and j in the vapour phase mixture respectively. $B_{ij} = B_{ji}$ and is called the cross coefficient. The second virial coefficient for a binary mixture may thus be written as:

$$B_{mixture} = y_1 B_{11} + y_2 B_{22} + y_1 y_2 \delta_{12} \tag{2-63}$$

where $\delta_{12} \equiv 2B_{12} - B_{11} - B_{22}$

Accurate values of the second virial coefficients for pure components (B_{ii} and B_{jj}) are obtained from accurate volumetric data for pure gas i and for pure gas j; for accurate values of B_{ij} it is necessary to have accurate volumetric data for gaseous mixtures of i and j (Prausnitz et al. [1967]).

However, such data are usually not available, and it is necessary to estimate the desired second virial coefficients from correlations. There are several correlations that have been proposed for estimating the second virial coefficient and some of the most often used ones are the Pitzer and Curl [1957] correlation, the Tsonopoulos [1974] correlation and the Hayden and O'Connel [1975] correlation. These correlations vary greatly in their accuracy.

2.4.1 The Pitzer-Curl Correlation

The Pitzer and Curl correlation was developed to account for the vapour phase non-ideality. It is a relatively simple correlation that can be used for binary systems at low pressure. Pitzer and curl [1957] proposed a relation in which the second virial coefficient, B, is a function of reduced temperature, T_r:

$$\frac{BP_c}{RT_c} = B^0 + \omega B^1 \tag{2-64}$$

The values of B^0 and B^1 are functions of the reduced temperatures only and can be calculated by:

$$B^0 = 0.083 - \frac{0.422}{T_r^{1.6}} \tag{2-65}$$

$$B^1 = 0.139 - \frac{0.172}{T_r^{1.4}} \tag{2-66}$$

where $T_r = T/T_c$.

The term ω in Equation (2-64) is the accentric factor, which accounts for the nonsphericity of a molecule. The second virial coefficient for a mixture is calculated using the following relation:

$$B_{ij} = \frac{RT_{cij}}{P_{cij}}\left(B^0 + \omega_{ij} B^1\right) \tag{2-67}$$

The cross coefficient parameters are calculated using the mixing rule proposed by Prausnitz et al. [1986].

$$T_{cij} = \sqrt{T_{ci} T_{cj}}\left(1 - k_{ij}\right) \tag{2-68}$$

$$\omega_{ij} = \frac{\omega_i + \omega_j}{2} \tag{2-69}$$

$$P_{cij} = \frac{Z_{cij} R T_{cij}}{V_{cij}} \tag{2-70}$$

$$V_{cij} = \left(\frac{V_{ci}^{1/3} + V_{cj}^{1/3}}{2} \right)^3 \tag{2-71}$$

$$Z_{cij} = \frac{Z_{ci} + Z_{cj}}{2} \tag{2-72}$$

k_{ij} in equation (2-68) is the binary interaction parameter.

2.4.2 The Tsonopoulos Correlation

The Tsonopoulos [1974] correlation can be used to estimate the virial coefficients for polar and non-polar compounds. It is an extension of the Pitzer-Curl [1957] correlation. The Tsonopoulos correlation for non-polar gases is as follows:

$$\frac{BP_c}{RT_c} = f^{(o)}(T_r) + \omega f^{(1)}(T_r) \tag{2-73}$$

And

$$f^{(o)}(T_r) = 0.1445 - \frac{0.330}{T_r} - \frac{0.1385}{T_r^2} - \frac{0.0121}{T_r^3} - \frac{0.000607}{T_r^8} \tag{2-74}$$

$$f^{(1)}(T_r) = 0.0637 - \frac{0.331}{T_r^2} - \frac{0.423}{T_r^3} - \frac{0.008}{T_r^8} \tag{2-75}$$

For polar compounds, those with a nonzero dipole moment, the above equation for non-polar gases has an additional term that takes into account the polar effects:

$$\frac{BP_c}{RT_c} = f^{(o)}(T_r) + \omega f^{(1)}(T_r) + f^{(2)}(T_r) \tag{2-76}$$

where

$$f^{(2)}(T_r) = \frac{a}{T_r^6} \tag{2-77}$$

2.4.3 The Hayden and O'Connell Correlation

The Hayden and O'Connell [1975] correlation is more complex, containing its own terms for cross second virial coefficients, and is used for estimating pure and cross second virial coefficients for a large variety of compounds. It can be used for both polar and non-polar chemicals. The correlation requires the critical temperature (T_c) and pressure (P_c) of the components, mean radius of gyration (Rd), the parachor (P'), dipole moment (μ) and chemical association parameter (η) if necessary. The contribution to the second virial coefficient is considered to be the sum of three interactions.

$$B_{total} = B_{free} + B_{metastable} + B_{bound} \tag{2-78}$$

Where B_{free} is the interaction from free pairs $B_{metastable}$ is the contribution from molecular interactions that are metastably bound, and B_{bound} is the contribution in strongly non-ideal systems that associate. For more details the readers is referred to the paper by Hayden and O'Connell [1975].

2.5 Thermodynamic Consistency testing

The purpose of a thermodynamic consistency test is to evaluate the quality of the experimental data that have been measured. Often, there is an over-representation of the data because more variables are measured that are needed to adequately describe the system. Hence the consistency test is used to check whether one of these variables is consistent with the prediction of its value from the other variables. Thermodynamic consistency tests are based on the Gibbs-Duhem equation.

$$\sum x_i d\ln\gamma_i = \frac{V^E}{RT}dP - \frac{H^E}{RT^2}dT \tag{2-79}$$

Many different types of consistency test have been proposed both for low and high pressure, and all are based on some form of the Gibbs-Duhem equation. The classical area test and the Van Ness consistency test are widely used in low pressure applications. For high pressure data, commonly used methods include those of Chueh et al. [1965], Won and Prausnitz [1973], Christiansen and Fredenslund [1975] and Mühlbauer [1991]. The consistency test is the only possible advantage to be gained from redundant measurements of y (Van Ness et al. [1973]. Van Ness et al. suggested that, unless a consistency test is considered essential, experimental effort is better spent on improvement of the accuracy of P-x measurements that on measurement of redundant data. For this project, thermodynamic consistency was not tested as the vapour composition was not measured but was computed using Barker's method. As a result of this, no further discussion on the thermodynamic consistency tests will be provided.

2.5 Conclusion

The static synthetic type of apparatus was selected as the most suitable for this project. The relative simplicity of the static total pressure apparatus was the main attraction. Static total pressure apparatus produces isothermal VLE data which are preferred to isobaric data. Isothermal data are easily reduced because liquid phase excess properties depend much more on temperature than on pressure. Although thermodynamic consistency can not be tested on VLE data obtained from a static synthetic apparatus, Van Ness et al.[1973] suggested that, "unless a consistency test is considered essential, experimental effort is better spent on improvement of the accuracy of P-x measurements that on measurement of redundant data".

CHAPTER THREE

DESIGN AND CONSTRUCTION OF THE STATIC SYNTHETIC APPARATUS

Static synthetic methods for measurement of vapour-liquid equilibria have become increasingly important in recent years, especially because there is no need for analytical determination of phase concentration. The Thermodynamic Research Unit (TRU) at the University of KwaZulu-Natal did not have a static synthetic apparatus for vapour-liquid equilibrium measurements at low to moderate pressures despite the availability of a broad variety of phase equilibria equipment that has been developed over the years. The main objective of this project was to develop a new static synthetic apparatus together with equipment operating procedures for measuring low to moderate pressure vapour-liquid equilibrium. In retrospect, however, the initial aim of the project was to develop a new static synthetic apparatus together with equipment operating procedures for measuring extremely low vapour pressures. This aim failed when it was realized that the new Pirani gauge, used to measure extremely low pressure, was faulty and could not be fixed in due time. In this chapter, the design and construction of the current equipment is discussed.

3.1 Design and Construction of the new apparatus

The equipment used in this work was designed, constructed and commissioned in the Thermodynamic Research Unit, University of KwaZulu-Natal. The equipment review in Chapter 2 provided the basis for the current design. The apparatus was designed to operate at pressures up to 15 bar and temperatures up to 150°C. Due to these operating conditions, stainless steel was chosen

as the suitable material of construction for the apparatus as opposed to glass which could not withstand such pressures. Additional factors that made stainless steel the preferred choice are:

- Its resistance to corrosion (it is very important as no contamination is vital for accurate VLE)
- Its strength
- Its amagnetic properties
- Its availability and cost compared to other strong alloys.

The discussion presented in this chapter is divided into the following sections:

1. The equilibrium cell
2. The Piston-injectors
3. The degassing assembly
4. The temperature and pressure measuring devices

3.1.1 The equilibrium cell

One of the most important parts of the static synthetic apparatus is the equilibrium cell into which the system to be investigated is charged and brought to thermodynamic equilibrium. The simple cylindrical cell and its lid (with dimensions shown on Figure 3-1) were machined from 316 stainless steel in a workshop at the School of Chemical Engineering, University of KwaZulu-Natal Durban.

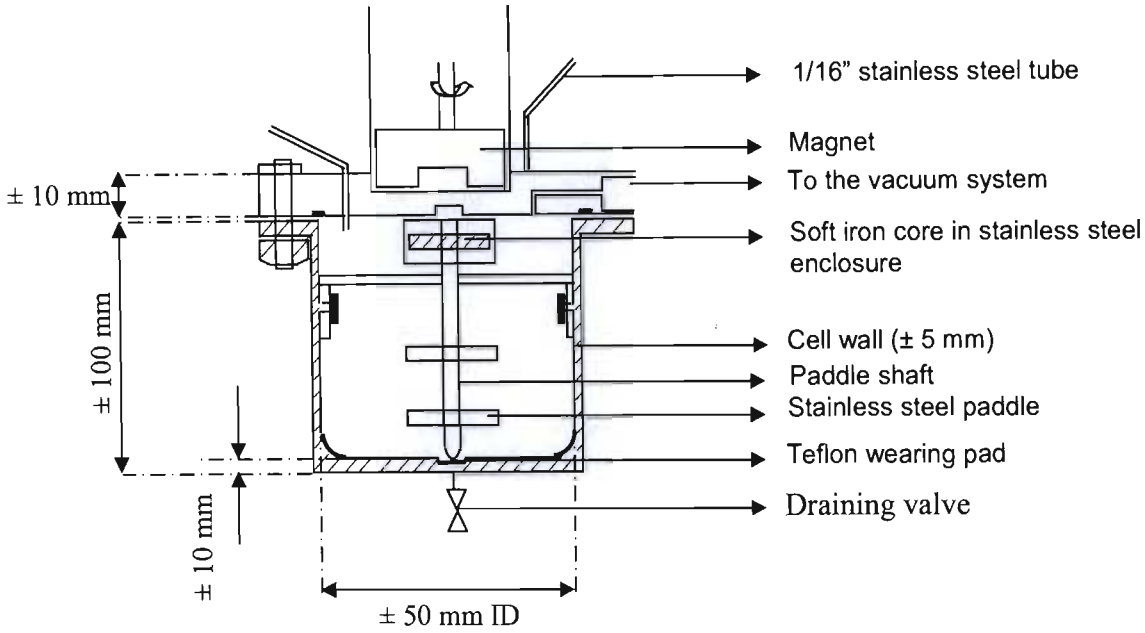

Figure 3-1: Drawing of the equilibrium cell showing some dimensions

The cell wall has a thickness of approximately 5 mm, this provides both an increased safety factor and a large thermal capacity. The thickness of the lid is approximately 15 mm towards the edges and ± 4 mm in the middle (this allows for easy communication of the magnet with the soft iron core and by doing so, makes the spinning of the paddle shaft easier). The lid has in its interior a groove that houses a viton O-ring which provides good sealing between the cell body and the lid.

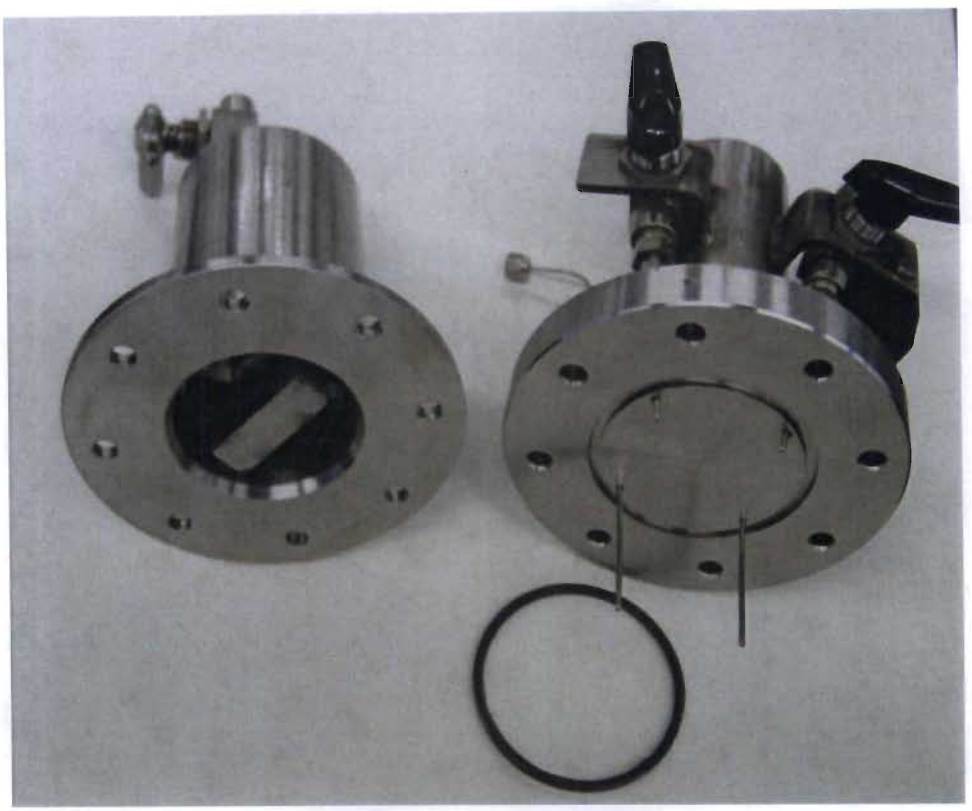

Figure 3-2: Photograph of the cell body, its lid and the O-ring

Figure 3-2 shows a photograph of the cell body, its lid and the O-ring. The lid is fastened to the cell body using 8 stainless steel bolts. It can also be noticed from the picture that there are 4 × 1/16" stainless steel tubes built into the lid, two of them are inlets for sample introduction, and the other two are outlets (one leads to the vacuum system and the other to the pressure measuring device). The valves are also built into the lid to keep the vapour volume as small as possible. In order to rapidly reach thermodynamic equilibrium inside the cell, a pair of stainless steel paddles (35mm × 5mm × 2mm) is used to mix the cell content. A variable speed stirrer unit (Heidolph RZR2040 model) is suspended from the cell lid and drives the stirrers via magnetic coupling. A 1/8" draining valve is situated at the bottom of the cell to facilitate cleaning and maintenance. The equilibrium cell has a total interior volume of 190 cm^3. This volume was chosen to keep the vapour space above the liquid mixture to a minimum. This volume was determined by injecting degassed water into the cell at 308.35 K. The calibration procedure is explained in Chapter 4. A novel feature of the cell was the rounding of the bottom contour to eliminate stagnant corners. Figure 3-3 shows the equilibrium cell when it is assembled.

Figure 3-3: Photograph of the assembled equilibrium cell

3.1.2 The Piston-injectors

Two pumps (one for each pure component) were also constructed in the workshop using 316 stainless steel. The main elements of the piston-injectors are: the mini piston, the macro piston, the solenoid windings, the removable water jacket and the pressure gauge. Figure 3-4 shows a drawing of the piston-injector with some important dimensions.

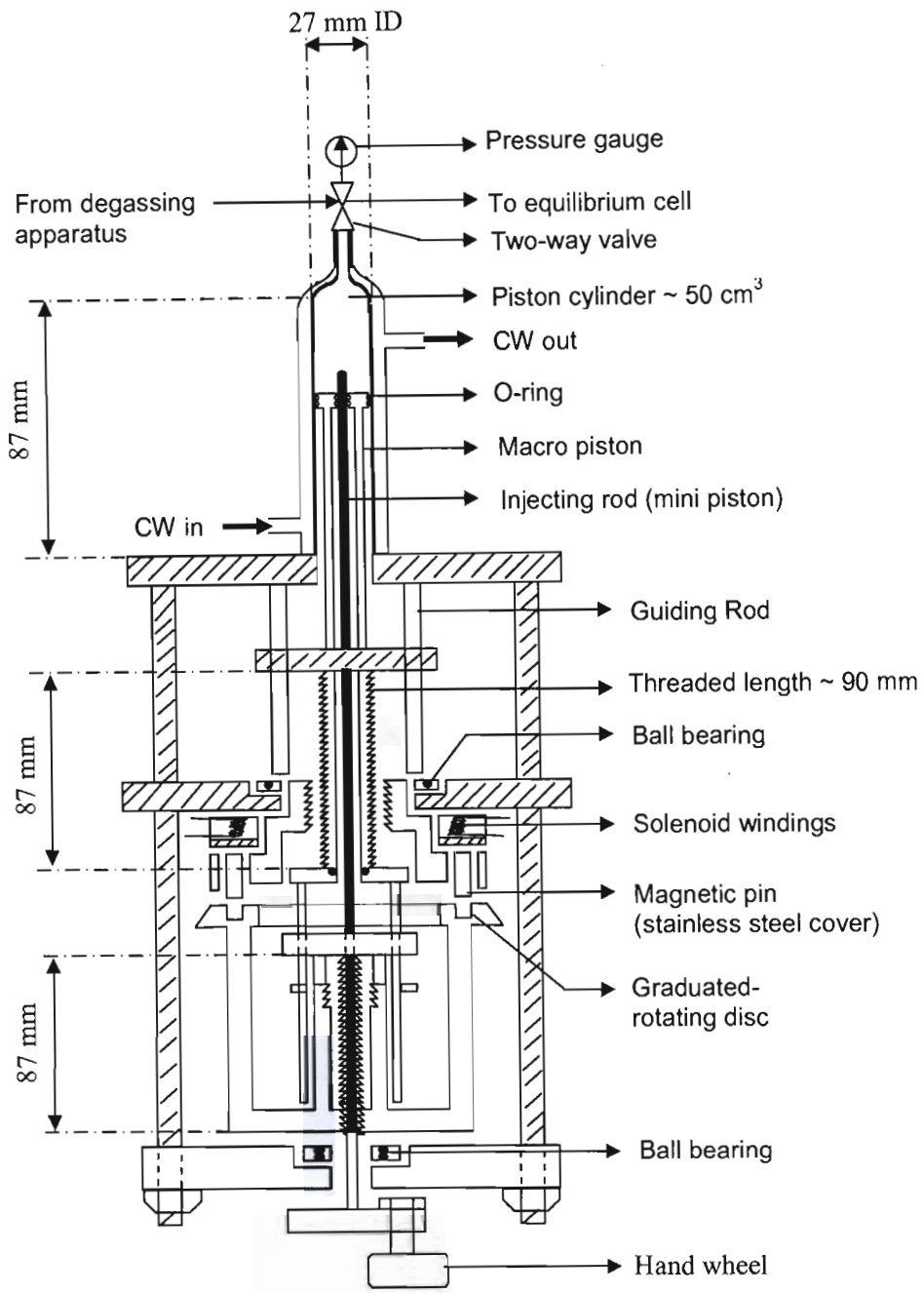

Figure 3-4: Drawing of the piston-injector (not to scale)

The mini-piston is a uniform and polished stainless steel rod with a length of 87 mm and a diameter of 8 mm. The rod is located in the center of the macro-piston and is fitted with guide pins to prevent

rotation. Pins slide in a Teflon sleeve. There are two viton O-rings (10 mm OD and 1.5 mm thickness) which provide a leak-tight seal between the macro and the mini piston. The top O-ring is situated at 3 mm from the piston's tip and the bottom one is 5 mm from the threaded part of the piston. The Parker seal O- ring handbook 5700 was consulted before deciding on a suitable type of O-ring and viton O-rings were found to be the most suitable type for our purpose. The mini-piston is used to dispense small amounts of liquid into the equilibrium cell therefore allowing data to be collected in the dilute region. The maximum injectable volume using the mini piston is 4.37 cm^3, this corresponds to 58 full turns or 87 mm travel of the piston (1 full turn corresponds to 1.5 mm travel of the pistons and a turn is further divided into 50 segments by a micrometer ring).

Figure 3-5: Photograph of the mini piston (stainless steel, uniform rod)

The macro piston is made of stainless steel and has a length of 87 mm and a diameter of 27 mm. There are two viton O-rings (26 mm OD and 3 mm thickness) which provide a leak-tight seal between the macro piston and the piston barrel. The O-rings are located in grooves 3 mm from the piston tip and 13 mm apart. The maximum injectable volume when the macro piston is in use is 49.81 cm^3, this also corresponds to 58 full turns or 87 mm travel of the piston.

Operation of the pistons pumps

The pistons are operated manually and the volume displaced is directly proportional to the distance moved by the piston. A solenoid operation is used to select either the macro or the mini mode. The concept that was used is as follows: Two magnetic pins enclosed in a stainless steel cover are embedded in the brass nut. Above the pins, a soft mild steel bobbin around which solenoid windings are wound is placed. Below the pins, a graduated, rotating, stainless steel disc is placed. The locating pins are attracted to the bobbin and remain there until a surge of power (6 Amperes and 27 Volts) is delivered to the solenoid to drive the locking pins down into the graduated rotating disc.

Once in the down position, the pins will remain there as the disc is slightly magnetic. When the pins are down (sticking to the graduated disc), both the mini and macro pistons are operating (The mini piston is embedded in the macro piston, as a result, both the mini and the macro pistons are used when the macro piston is needed). If the two pistons are no longer needed to operate together (ie only the mini piston is needed), a once off surge of power is delivered to the solenoid to drive the locking pins to the up position. To select between the two modes of operation, one just needs to select the up or the down position using a selector switch, then press the enabling button to deliver power to the solenoid windings. This safe- guards the solenoid from overheating and reduces the possibility of any malfunctions happening. On the safety side this operation eliminates injury to the operator since once the pins are in the needed position, no further power is required to keep them in place. Another safety point is that any power fluctuations would not affect the solenoid in any way. (The concept of solenoid operation was from the technician Mr Kelly Robertson who was involved with the construction of this apparatus). The dual mode of operation constitutes the originality of this piece of equipment (Raal [1999]).

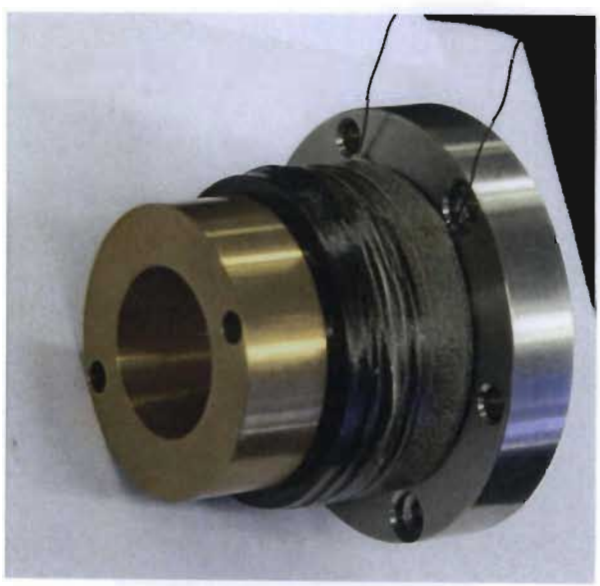

Figure 3-6: Photograph of the brass nut and solenoid windings

Removable water jacket and pressure gauge

To reduce the error in temperature and pressure-dependence of the liquid density (which must be known), the piston injectors are thermostatted using a stainless steel removable water jacket and kept at a constant pressure using SA pressure gauge. This also allows the measurements to be extended to substances with a normal melting point above ambient temperature.

The pistons were calibrated gravimetrically with distilled water prior to measurements. The calibration method is explained in Chapter 4. Figure 3-7 is a photograph of the assembled injector pump.

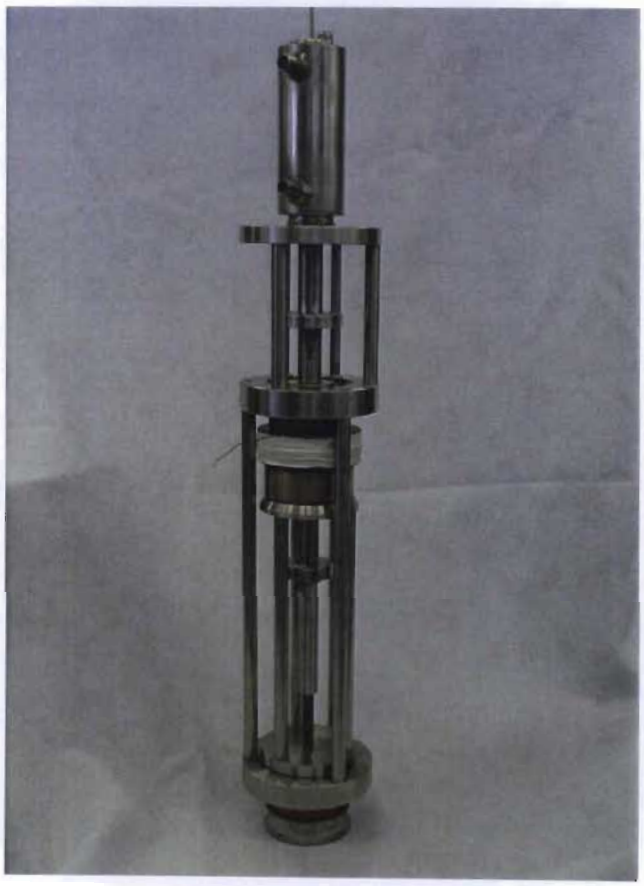

Figure 3-7: Photograph of the assembled piston-injector

The piston-injectors were used to accurately dispense a known quantity of degassed liquid into the equilibrium cell.

3.1.3 The degassing assembly

The all-glass, simple degassing apparatus presented in Figure 3-8 was made by Scitech - a glassware company based in Pietermaritzburg (two degassing apparatuses were used, one for each component). It consists of two main elements: a 250 ml flat bottomed three- neck flask, and a water-cooled condenser (20 cm high and 5 cm OD). The upper opening of the condenser leads to a

vacuum system through a fine capillary. A Platinum resistance thermometer (Pt-100 class B) is placed in one of the side-necks to measure the temperature of the degassing liquid and Teflon tubing is fitted into the other side neck to transfer the degassed liquid to the piston-injector. Two pairs of viton O-rings of suitable size were used for each of the side necks to provide good sealing. The liquid in the flask is stirred with a Teflon coated stirrer bar. The degassing apparatus is protected with a Perspex shield which protects the operator in the case of an explosion.

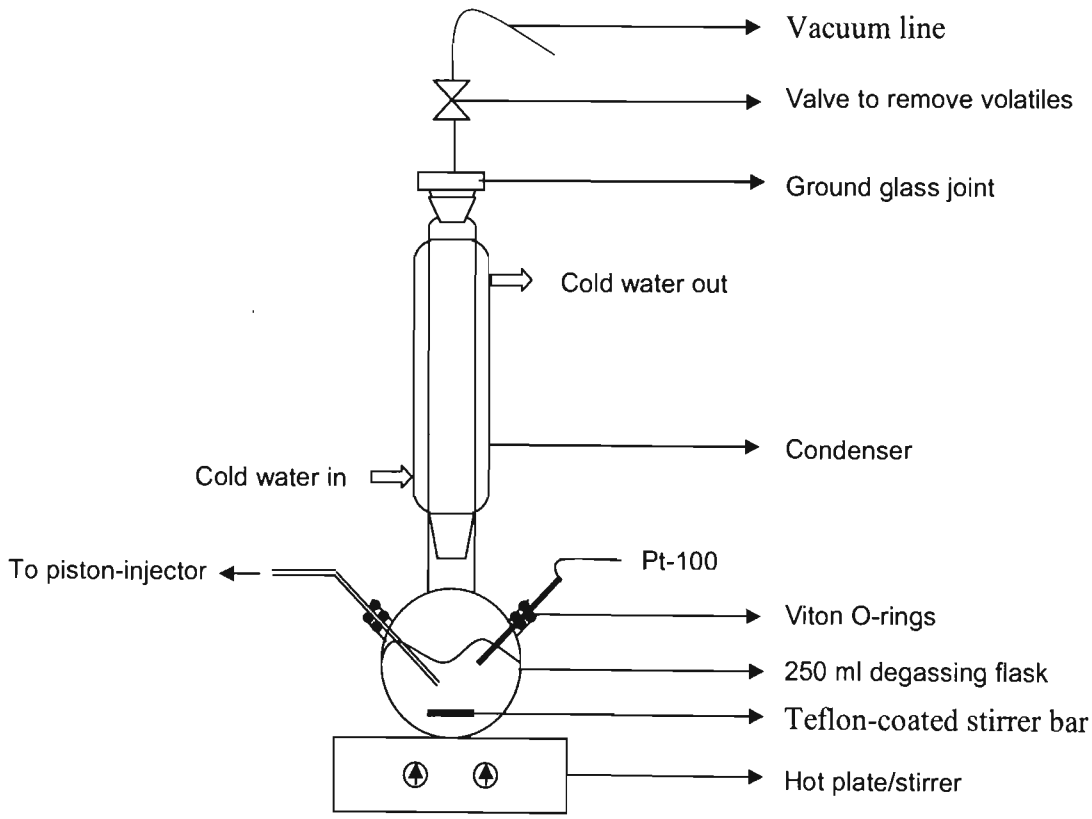

Figure 3-8: Drawing of the degassing apparatus

3.1.4 The temperature and pressure measuring devices

Temperature measurement is of critical importance to VLE measurement. Platinum resistance thermometers (Pt-100) were used to measure the temperature at several points during the operation of the static apparatus. These are:

- The equilibrium temperature, measured using a class A Pt -100 placed in an oil bath close to the equilibrium cell wall.
- The piston-injector barrel temperature, measured using a class A Pt-100.
- The degassing liquid temperature, measured using a class B Pt-100.
- The temperature of the connecting line to pressure transmitter and connecting valve, measured using a class B Pt-100.

All these temperature probes were connected to a single 4 ½ digit temperature display via a selector switch which has up to 12 positions. The probes had to be calibrated to give the actual reading. Calibration of the Pt-100s are discussed in Chapter 4.
Pressure measurement is the principal measurement. The pressure in the equilibrium cell is measured with a D-10-P, 0-1 bar WIKA absolute pressure transmitter. The output signal was relayed to a Pentium 4 computer via an RS 232 port.

3.2 The Static VLE apparatus

The main parts of the static synthetic apparatus were discussed above. Apart from the equilibrium cell, piston-injectors, degassing equipment, temperature and pressure measuring devices, the experimental equipment also has a two-stage Edwards vacuum pump, a refrigeration unit (Model CMS34FN3N, 220Volts Low temperature evaporator copper coil), two DC power supplies (6 amperes and 27 volts), two hot/stirrer plates, two Polychem constant temperature baths, one Grant 120 temperature controller (this was used to control the temperature of the bath). The temperature stability of the bath was estimated to be 0.2°C. The equipment comprised of the following axillaries; three AC voltage regulators (0-250Volts), one water pump (used to pump cold water in the condenser unit of the degassing apparatus), one selector switch with 12 positions (allowing up to 12 temperatures to be measured on a single display) and a 50 litre ballast tank. Figures 3-9 and 3-10 below, show a schematic diagram of the static assembly set-up and a photograph taken in the laboratory respectively. The whole apparatus was mounted on a stainless steel frame. The constant temperature bath was the movable part of the set-up. A car jack was used to raise the bath to submerge the equilibrium cell and to lower the bath to expose the cell. The next Chapter focuses on the specific techniques used in order to collect data from the static apparatus presented here.

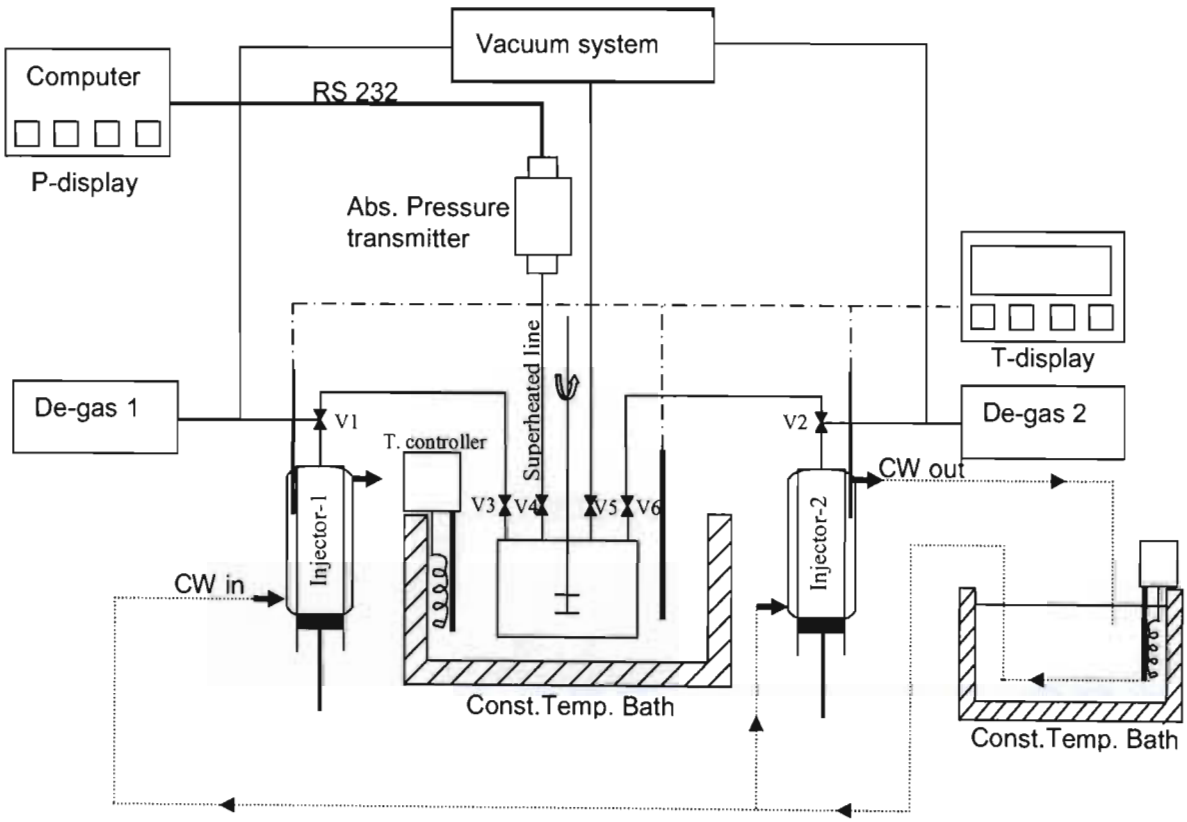

Figure 3-9: Schematic Diagram and layout of the static cell assembly

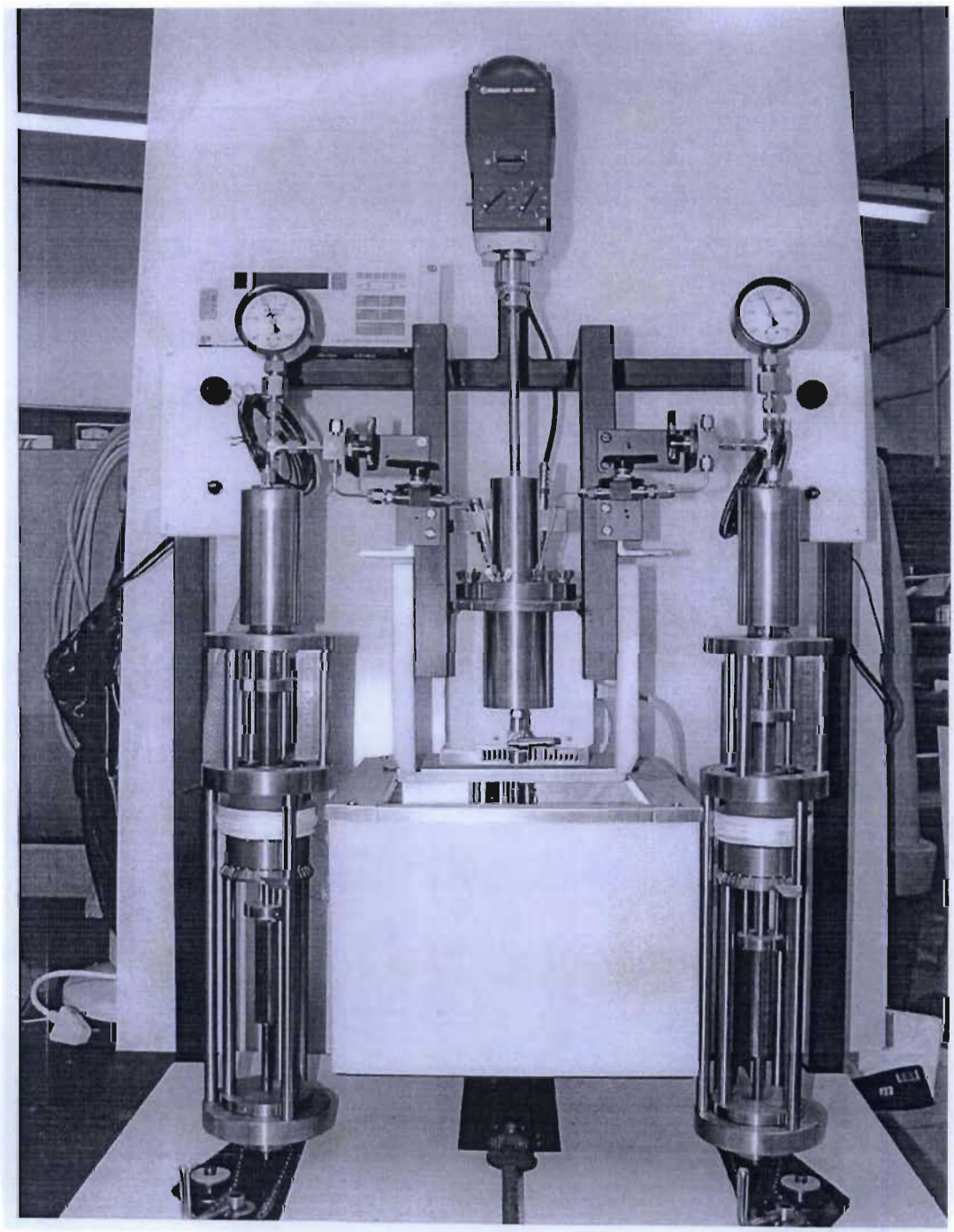

Figure 3-10: New static equilibrium apparatus with liquid dispensing pumps attached on either side. Note: Water jacket and temperature measurement for dispensed fluids.

CHAPTER FOUR

EXPERIMENTAL PROCEDURE

This Chapter details the specific techniques that were employed in collecting the VLE data for the systems measured using the equipment presented in Chapter 3. The operating procedure presented here is a result of several trial runs. These trial runs were done on systems previously measured by other authors. In order to check the reproducibility of the equipment, the whole set of VLE data for one of the test systems was repeated at the same temperature as that at which the original data were measured. In order to obtain meaningful VLE data, the equipment should be cleaned, be completely leak-tight and the measuring devices calibrated.

4.1 Cleaning of the static apparatus

Before each run, the whole static assembly is washed and flushed with n-Hexane. The pure n-Hexane is charged into the degassing apparatus then transferred via valves V1 and V2 into the piston-injectors (refer to Figure 3-9). From the piston-injectors, n-Hexane is dispensed into the equilibrium cell via valves V3 and V6 and stirred vigorously then emptied using the draining valve situated at the bottom of the cell. This step is repeated at least 2 times. n-Hexane was chosen over acetone because unlike acetone, it doesn't affect viton O-rings and is also volatile. Once the washing is complete the equilibrium cell is immersed in the oil bath. The cell and pumps are then evacuated by opening valve V5 to remove any traces of n-hexane. All residual n-hexane boils away at very low pressures.

4.2 Leak detection and elimination

Leaks in the system are usually detected by pressurising the equipment and then using a soapy solution, for which bubbles would be seen when a leak is present. This method could not be used in this case because all the pressures measured in this project were below atmospheric pressure. The determination of the presence of leaks in the apparatus was thus achieved through evacuating the system using a two stage Edwards vacuum pump followed by complete isolation of the vacuum pump using valve V5. The pressure reading on the display was then noted. Any leaks in the system were manifested in an increase in the pressure reading. As a way of detecting the individual leaks, a small paint brush was dipped into acetone and applied to all suspected joints. The presence of a leak was then seen by a fluctuation in the system pressure which occurs as a result of the acetone vaporizing causing a slight increase in pressure before stabilization occurs. The identified leaks were then eliminated by tightening the joints and by using vacuum grease on ground glass joints.

4.3 Calibration

Calibration is essential for accurate VLE measurements. The piston-injectors and the equilibrium temperature measuring devices had to be calibrated before being used in the VLE measuring process.

4.3.1 Calibration of the piston-injectors

The injection volumes of the piston-injectors were calibrated gravimetrically with distilled water. Each piston-injector was filled with distilled water and kept at constant temperature, 300.15K inside the pump. In the macro-mode (refer to Chapter 3), a known volume of water was dispensed inside a cleaned and pre-weighed 75 ml beaker (the volume was calculated from the knowledge of the distance traveled by the piston and the inside diameter of the macro piston). The beaker containing water was weighed using a four-decimal-place balance and the mass of water determined. From the mass of water and the density of water at 300.15 K, the actual volume of water was obtained. For best accuracy, the same procedure was repeated until the piston-injector was emptied. A plot of actual volume against volume obtained from piston travel gave the relationship which was then

used to compute actual volume from dispensed volume or actual volume from number of turns of the brass nut which propels the piston. The piston was again filled with distilled water and the procedure was repeated using the mini-piston.

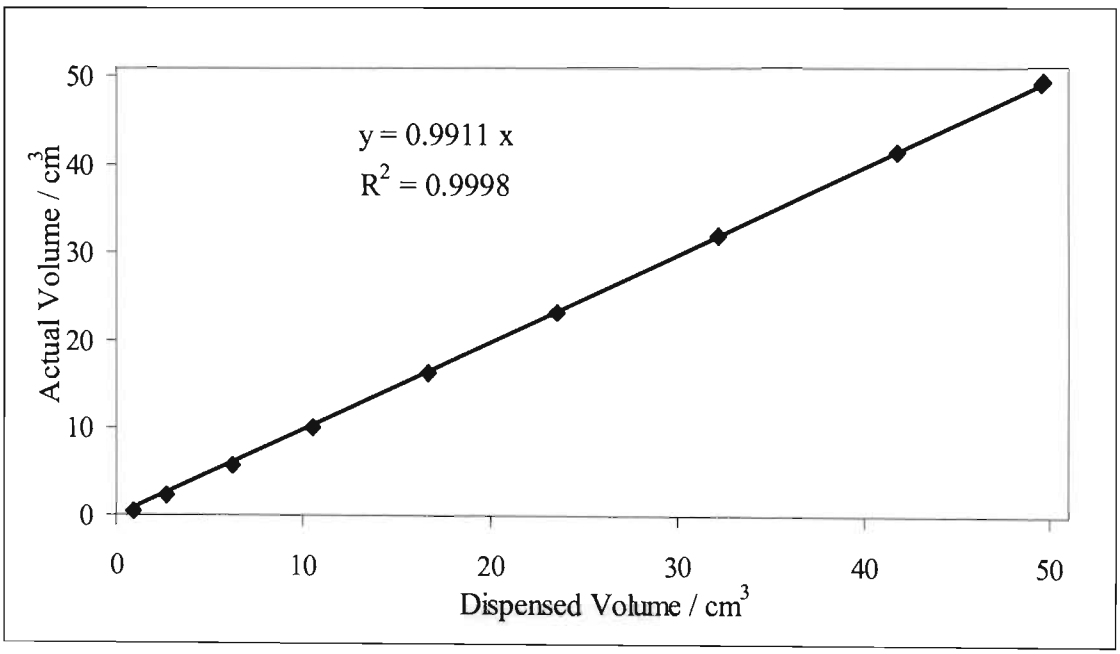

Figure 4-1: Calibration graph of the macro piston with distilled water at 300.15 K

Note: On the x-axis, the dispensed volume is the volume obtained from the displacement of the piston. And on the y-axis is the actual volume, this was computed from the knowledge of the mass and density of water.

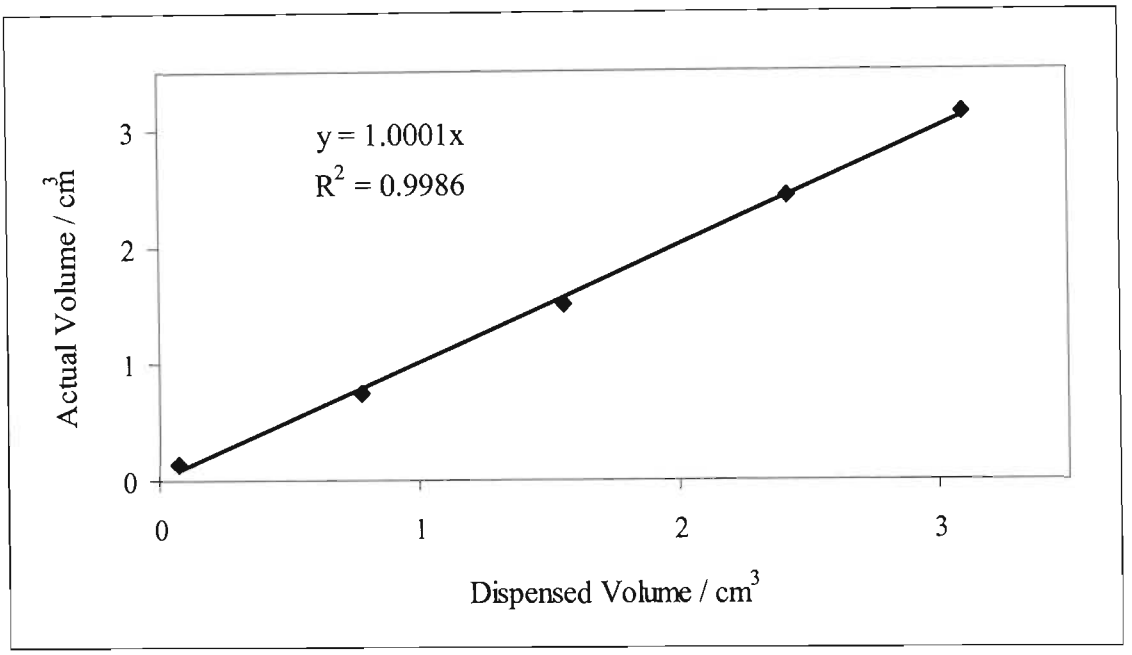

Figure 4-2: Calibration graph of the mini piston with distilled water at 300.15 K

4.3.2 Calibration of the temperature sensors

The platinum resistance thermometers (Pt-100) used in this work were calibrated against a reference four-wire resistance thermometer probe. The reference probe was calibrated by WIKA instruments (Pressure and Temperature Measurement division). The equilibrium cell temperature was measured by placing a Pt-100 in the oil bath close to the cell wall and therefore calibration of the Pt-100 was done by placing the Pt-100 and the standard probe in the oil bath very close to each other. A Grant temperature controller was used to set the oil temperature constant. When the set temperature was reached, the resistance of the standard probe was recorded and the temperature of the Pt-100 was recorded. The oil temperature was raised and the same procedure repeated until a set temperature of 100 °C was reached. The resistances of the standard probe were converted into actual temperatures using a chart obtained from WIKA. A plot of actual temperatures versus display temperatures gave a relationship which was then used to compute the actual temperatures from the measured temperatures. Figure 4-3 shows the calibration graph for the equilibrium cell temperature sensor.

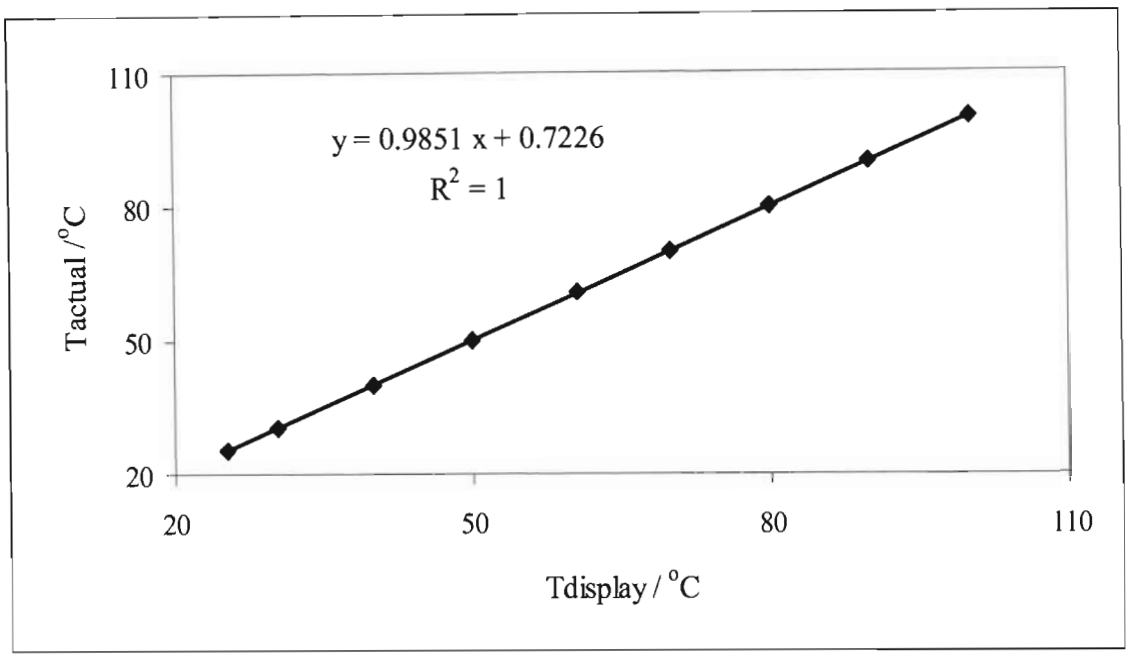

Figure 4-3: Calibration graph of the temperature sensor

4.4 Determination of the equilibrium cell total interior volume

In static synthetic methods where there is no phase analysis, the cell total interior volume is an important parameter in calculating phase compositions. It is therefore imperative to know the cell total interior volume very accurately. A very simple procedure for the determination of the cell interior volume was developed:

1- Evacuate the cell, piston-injector and all the connecting lines.
2- Fill the piston-injector with degassed distilled water and let it reach thermal equilibrium inside the pump
3- Fill the cell with dry air and submerge the cell in the oil bath at 308.35 K.
4- Let the dry air reach thermal equilibrium and record the temperature T_0 and the pressure P_0 inside the cell. Ideal gas law applies:

$$P_0V_0 = nRT_0 \quad V_0 \text{ and } n \text{ are unknown} \tag{4-1}$$

5- Add a known amount of degassed distilled water, v_1^L (this value is obtained from the number of turns or the piston displacement) into the cell, let it reach thermal equilibrium and record the pressure P_1. Now,

$$P_1 V_1 = nRT_1 \quad n \text{ is constant} \tag{4-2}$$

where n is the number of moles of gas and $V_1 = V_0 - v_1^L$. Substituting V_1 in Equation 4-2 gives:

$$P_1\left(V_0 - v_1^L\right) = nRT_1 \tag{4-3}$$

From Equation 4-1, n is obtained and substituted in Equation 4-3.The following relationship is obtained:

$$P_1\left(V_0 - v_1^L\right) = RT_1\left(\frac{P_0 V_0}{RT_0}\right) \tag{4-4}$$

T_1 and T_0 are equal because dry air and distilled water are at the same equilibrium temperature. Therefore T_1 and T_0 are cancelled from Equation 4-4 and we get:

$$P_1\left(V_0 - v_1^L\right) = P_0 V_0 \tag{4-5}$$

6- For best accuracy, Repeat step 5 by adding more distilled water in the cell and obtain a set of values (v_1^L , P_1). Rearranging Equation 4-5 gives:

$$v_1^L = V_0\left(\frac{P_1 - P_0}{P_0}\right) \tag{4-6}$$

7- Plot v_1^L against $\left(\frac{P_1 - P_0}{P_0}\right)$.This plot gives a straight line with slope V_0, which is the total net interior volume of the equilibrium cell. Figure 4-4 is the graph for the determination of the total interior volume. Note that the plots pass exactly through the origin as they must.

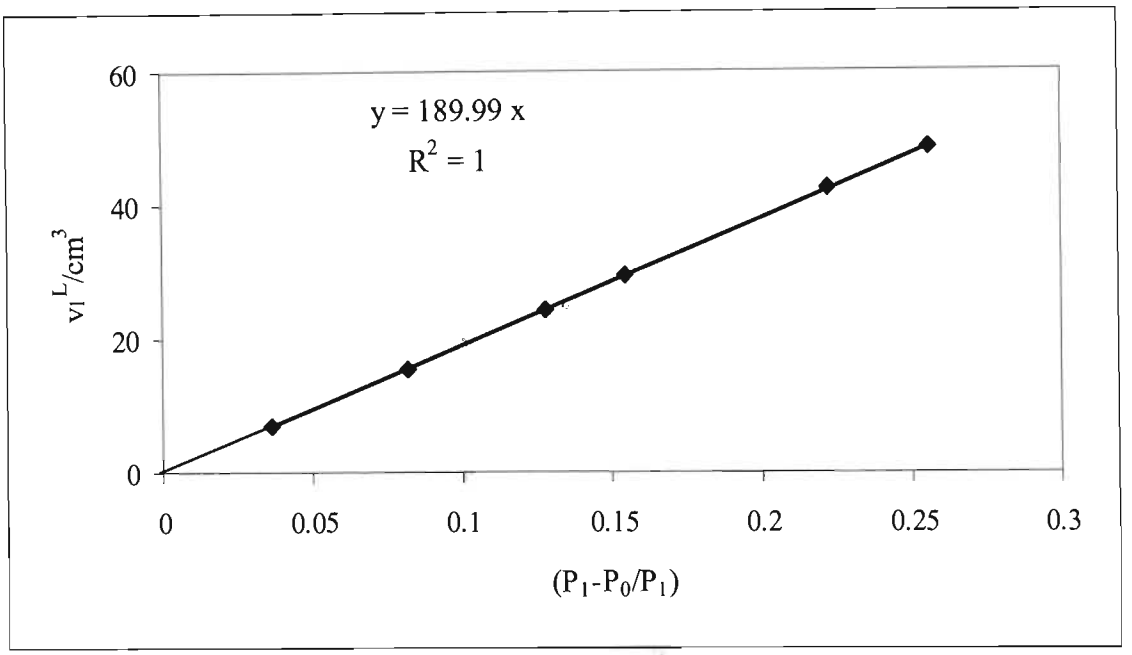

Figure 4-4: Graph for the determination of the cell total interior volume

4.5 Degassing of liquids

The components for which VLE were measured were degassed as suggested by Van Ness and Abbott [1978]. During vacuum distillation, the reboiler (flask) temperature was kept at approximately 30 °C and the liberated volatile gases were removed from the degassing flask through a fine capillary at the top of the column. The liquids were degassed for at least 8 hours. One of the disadvantages of this degassing method is that less volatile impurities if present, are enriched in the degassed liquid (Fischer and Gmehling [1994]). The degassed liquids were transferred from the degassing apparatus to the piston injector via 1/16" Teflon tubing. It was important to keep the temperature of the piston barrel below room temperature (~ 15 °C) to ease the flow of the liquids from the degassing flask to the piston-injectors. Success of the degassing procedure was examined by comparing measured vapour pressures with the values calculated from literature correlations.

4.6 VLE measurement

Before each measurement, components from the previous run were removed from the cell and the whole apparatus was cleaned with n-hexane and kept under vacuum for some time.

The degassed liquids were loaded into the piston-injector via thin Teflon tubing connecting the degassing flask to the piston and by placing valve V1 in the upright position. (Note that valves V1 and V2 are two-way valves). The liquid in each piston was then stored under positive pressure (approximately 3 barg) to avoid contamination with air. In order to compress the liquid inside the pumps, valve V1/V2 is turned in the down position and valve V3/V4 is closed.

An experimental plan was developed using an Excel spreadsheet giving the target injection volumes. The pressure effects on the liquid densities were ignored, but the temperature effect was taken into account by using the Rackett Equation to compute the liquid molar volume. In order to avoid condensation effects on the equilibrium pressure measurement, the tube (1/8" stainless steel) connecting the pressure transmitter to the equilibrium cell was kept at a temperature higher than that of the equilibrium cell. The loaded injection pumps were left to reach thermal equilibrium. Before starting measurements, valve V5 between the cell and the vacuum pump was closed and the pressure reading in the cell was ~0.03 kPa. While monitoring the internal pump pressure, valve V3 between the cell and the injector was manually opened. A significant pressure drop inside the pump indicated that the valve was open. The piston was then manually advanced to inject the first component into the cell. Then the valve (V3) was closed and the initial pressure inside the pumps rapidly restored to ensure that the discharge volume was exactly proportional to the piston travel. The injected volume (ΔV) was calculated from the difference in the piston travel or more accurately from the number of turns through which the hand wheel had turned (1 turn is 1.5 mm travel of the piston, further divided into 50 segments by a micrometer ring) minus the volume of liquid that remains in the line before the first drop reaches the cell. This volume was calculated to be 0.19 cm^3. A run consists of pure component and mixtures vapour pressures. Equation 4-7 shows how the number of moles of injected component are calculated from the injected volume.

$$n_i = \frac{\rho_{i(T)} \times \Delta V}{M_i} \tag{4-7}$$

Where $\rho_{i(T)}$ is the density of component i at temperature T inside the piston-injector. M_i is the molecular weigh of component i.

Once the first component (pure component 1) was introduced into the cell, the cell was stirred to accelerate achievement of thermal equilibrium. To check for complete degassing, a small amount of

component 1 was added to the cell and the equilibrium pressure was recorded. If the degassing was incomplete, the second value of the recorded pressure was higher. After measuring the vapour pressure of component 1, a predetermined amount of the second component (number of moles calculated as explained in equation 4-7) was added to the cell. The cell contents were mixed and allowed to equilibrate for 15 to 60 minutes depending on the system. The reading was taken when the pressure remained constant for about 5 min. The addition of component 2 continued until a mole fraction of 0.6 was reached. The equilibrium cell was emptied and evacuated after the last addition. The run continued with injection and checking of the vapour pressure of pure component 2. The number of moles of component 2 injected in the cell was calculated as explained in Equation 4-7. Predetermined amounts of component 1 were then added until this half of the isotherm coincided with the previous half. If both sides of the isotherm did not coincide, the reason could be leakage in the system. A number of data points of known temperature, pressure and overall composition (z_i) were obtained. The composition of the liquid phase (x_i) and the vapour phase (y_i) have to be calculated. An important feature of this equipment is its ability to accurately measure data in the dilute region. This is achieved by using the mini piston.

4.7 Shutting down the static equipment

At the end of the experiment, the equipment is shut down. Shutting down the equipment starts with the turning off of the heat to the bath and is followed by the lowering of the oil bath to expose the equilibrium cell. The equipment is allowed to cool down. Once the equipment is cool, the cell content is drained by opening valve V5 (to allow air in the cell and as a result forcing the liquid out) and the draining valve situated at the bottom of the equilibrium cell.

CHAPTER FIVE

EXPERIMENTAL RESULTS

Information about phase behaviour of fluid mixtures can be obtained in many ways. The direct measurement of phase equilibrium data remains an important source of information; even predictive models need a number of experimental points to adjust the interaction parameters and then obtain sufficiently accurate results. Therefore, experimental data are crucial for successfully developing and validating models capable of predicting the phase behaviour of binary systems over a wide temperature range. Before gathering new sets of data on the equipment presented in Chapter 3, measurements were carried out on test systems to develop the experimental procedure described in Chapter 4. The test systems measured were:

- Water (1) + 1-Propanol (2) at 313.17 K
- Water (1) + 2-Butanol (2) at 323.18 K
- n-Hexane (1) + 2-Butanol at 329.22 K

These three test systems were measured in order to check the reliability and the reproducibility of the new equipment presented in Chapter 3. The choice of the test systems was based on the availability of high purity chemicals in our laboratory, the presence of consistent data on the systems in the literature at the desired temperature and pressure and the compatibility of chemicals with viton O-rings. Once the test systems gave satisfactory results, therefore confirming the operating procedures of the new equipment, new systems were measured. These systems had no isothermal VLE data available in the open literature at the time the experiments were conducted. The systems are:

- 1-Propanol (1) + n-Dodecane at 342.83K and 352.68 K
- 2-Butanol (1) + n-Dodecane at 342.83 K and 352.68 K
- Water (1) + o-Cresol at 342.83 K

5.1 Chemicals used

The chemicals used, their purities and the suppliers are presented in Table 5-1. All the chemicals, except distilled water, were dried over molecular sieves for at least 24 hours before degassing. Triple distilled water was obtained from the Chemistry department at the same university where this work was performed.

Table 5-1: Chemicals and their purities

Reagent	Supplier	Min Purity specified by supplier (Mass %)	GC Analysis (Mass %)
n-Dodecane	Merck	= 99.0	99.99
n-Hexane	Fluka	= 99.5	99.71
2-Butanol	Fluka	> 99.7	99.87
1-Propanol	Riedel-deHaen	99.9	99.98
o-Cresol	Merck	99.5	99.50

5.2 Vapour pressures

Vapour pressures are highly sensitive to experimental conditions and the purity of chemicals used. Therefore measuring pure component vapour pressures also gives an indication of the chemicals' purity. Table 5-2 shows the measured pure components vapour pressures together with the calculated ones using literature correlations.

Table 5-2: Measured vapour pressures and values from literature correlations

Compounds	T	Vapour pressure (kPa)		
	(K)	This work	(Reid et al.[1986])	(DDB [1998])
1-Propanol				
	313.17	6.99	7.11	6.94
	342.83	31.45	32.76	32.18
	352.68	49.80	50.74	49.83
Water				
	313.17	7.36	7.49	7.37
	323.18	12.18	12.53	12.32
	342.83	30.65	31.16	30.66
n-Dodecane				
	342.83	0.55	-	0.41
	352.68	0.78	-	0.72
2-Butanol				
	323.18	14.55	15.00	15.18
	329.22	10.74	11.04	10.87
	342.83	28.31	29.35	29.46
	352.68	44.19	45.70	45.62
n-Hexane				
	329.22	65.63	66.86	66.85
o-Cresol				
	342.83	0.83	0.84	0.87

The main physical properties of components collected from literature (Dortmund Databank for Thermo Physical Properties (DDB)) are presented in Table 5-3.

Table 5-3: Physical properties of pure components; critical temperature T_C, critical pressure P_C, accentric factor ω, critical liquid molar volume v_c and the critical compressibility factor z_c [DDB-1998]

Compound	T_c (K)	P_c (atm)	ω	v_c (cm^3/mol)	Z_c
n-Dodecane	658.8	17.86	0.562	713.0	0.240
n-Hexane	507.4	29.30	0.296	370.0	0.260
2-Butanol	536.0	41.40	0.576	268.0	0.252
1-Propanol	536.7	51.00	0.624	218.5	0.253
o-Cresol	697.6	49.40	0.240	282.0	0.240
Water	647.3	217.60	0.344	56.0	0.229

5.3 Vapour-Liquid Equilibrium

5.3.1 Error Analysis

In science, it is not possible to measure quantities exactly. It is therefore important to be able to assess the accuracy of the measurements.

The uncertainty on the vapour and liquid mole fractions depends on many quantities like the uncertainties in the measurement of the cell temperature, pressure, and the overall composition of the mixture in the cell and the total volume of the cell. The uncertainty in the overall composition of the mixture in the cell depends on the uncertainty in the injected volumes. The uncertainty of injected volumes $\Delta V_1 = \pm 0.002$ cm^3 was obtained from the calibration experiments with distilled water. The estimated uncertainty on the total volume of equilibrium cell volume is ± 0.6 cm^3.The estimated inaccuracy of the equilibrium temperature and the temperature in the pumps is $\Delta T = \pm$ 0.2 °C.

The estimated uncertainty on densities is $\Delta\rho_i = \pm 0.02\,\rho_i$ and $d\rho_i/dT = \pm 0.001$ g cm^{-3}K^{-1}.

To estimate the uncertainty in the overall composition of the mixture in the cell, the theoretical maximum error for an injection is derived below. The pressure dependence of density was ignored.

$$n_1 = \frac{\rho_{1(T)} V_1}{M_1} \tag{5-1}$$

By differentiating the injected amount of moles n_1 we obtain

$$dn_1 = d\left(\frac{\rho_{1(T)} V_1}{M_1}\right) \tag{5-2}$$

The equation for the theoretical maximum error then results

$$\Delta n_1 = \frac{V_1}{M_1}\Delta\rho_1 + \frac{V_1}{M_1} \times \left|\frac{d\rho_1}{dT}\Delta T\right| + \frac{\rho_1}{M_1}\Delta V_1 \tag{5-3}$$

By taking the term $\rho_1 V_1 / M_1 = n_1$ as a multiplier

$$\Delta n_1 = n_1\left(\frac{\Delta\rho_1}{\rho_1} + \frac{1}{\rho_1}\left|\frac{d\rho_1}{dT}\right|\Delta T + \frac{\Delta V_1}{V_1}\right) \tag{5-4}$$

A corresponding equation is valid also for component 2.

$$\Delta n_2 = n_2\left(\frac{\Delta\rho_2}{\rho_2} + \frac{1}{\rho_2}\left|\frac{d\rho_2}{dT}\right|\Delta T + \frac{\Delta V_2}{V_2}\right) \tag{5-5}$$

Errors in overall mole fractions can be determined from

$$\Delta z_1 = \left|\frac{n_1}{n_1 + n_2} - \frac{(n_1 + \Delta n_1)}{(n_1 + \Delta n_1) + (n_2 - \Delta n_2)}\right| \tag{5-6}$$

5.3.2 Test Systems

The first step in VLE measurements is the calibration of the measuring devices. This topic was discussed in Chapter 4. Three highly non-ideal test systems were measured on the new apparatus.

The VLE data obtained are presented in Tables 5-4 to 5-6. The number of moles n_i of component i injected into the cell was calculated as explained in section 4-6.

Table 5-4: VLE data for the Water (1) + 1-Propanol (2) system at 313.17 K

n_1/ moles	n_2/ moles	z_1	P_{exp}/kPa
0.0000 ± 0.0000	0.4639 ± 0.0094	0.0000 ± 0.0000	6.99
0.0183 ± 0.0005	0.4639 ± 0.0094	0.0379 ± 0.0018	7.86
0.0430 ± 0.0010	0.4639 ± 0.0094	0.0848 ± 0.0034	8.65
0.0656 ± 0.0014	0.4639 ± 0.0094	0.1240 ± 0.0047	9.15
0.0756 ± 0.0016	0.4639 ± 0.0094	0.1402 ± 0.0052	9.35
0.1064 ± 0.0023	0.4639 ± 0.0094	0.1865 ± 0.0064	9.84
0.1404 ± 0.0030	0.4639 ± 0.0094	0.2323 ± 0.0075	10.28
0.1832 ± 0.0038	0.4639 ± 0.0094	0.2831 ± 0.0084	10.63
0.2241 ± 0.0046	0.4639 ± 0.0094	0.3257 ± 0.0091	10.83
0.2599 ± 0.0054	0.4639 ± 0.0094	0.3590 ± 0.0095	10.96
0.3662 ± 0.0075	0.4639 ± 0.0094	0.4411 ± 0.0101	11.21
0.4583 ± 0.0094	0.4639 ± 0.0094	0.4970 ± 0.0102	11.28
0.5220 ± 0.0107	0.4639 ± 0.0094	0.5295 ± 0.0101	11.20
1.0138 ± 0.0206	0.9688 ± 0.0196	0.5113 ± 0.0101	11.35
1.0138 ± 0.0206	0.6923 ± 0.0140	0.5942 ± 0.0097	11.38
1.0138 ± 0.0206	0.5716 ± 0.0116	0.6395 ± 0.0093	11.41
1.0138 ± 0.0206	0.4571 ± 0.0093	0.6892 ± 0.0086	11.30
1.0138 ± 0.0206	0.3430 ± 0.0070	0.7472 ± 0.0076	11.25
1.0138 ± 0.0206	0.2282 ± 0.0046	0.8163 ± 0.0060	11.35
1.0138 ± 0.0206	0.1703 ± 0.0035	0.8562 ± 0.0049	11.35
1.0138 ± 0.0206	0.1016 ± 0.0021	0.9089 ± 0.0033	11.17
1.0138 ± 0.0206	0.0443 ± 0.0009	0.9582 ± 0.0016	10.36
1.0138 ± 0.0206	0.0327 ± 0.0007	0.9687 ± 0.0012	9.83
1.0138 ± 0.0206	0.0274 ± 0.0006	0.9737 ± 0.0010	9.52
1.0138 ± 0.0206	0.0171 ± 0.0004	0.9834 ± 0.0007	8.85
1.0138 ± 0.0206	0.0093 ± 0.0002	0.9909 ± 0.0004	8.32
1.0138 ± 0.0206	0.0035 ± 0.0001	0.9965 ± 0.0002	7.82
1.0138 ± 0.0206	0.0006 ± 0.0000	0.9995 ± 0.0000	7.42
1.0138 ± 0.0206	0.0000 ± 0.0000	1.0000 ± 0.0000	7.36

n_1 and n_2 are the moles of components injected in the equilibrium cell; z_1 is the total mole fraction of component 1 and $z_1 = n_1/(n_1 + n_2)$; P_{exp} is the total pressure measured experimentally.

Table 5-5: VLE data for the Water (1) + 2-Butanol (2) system at 323.18 K

n_1/ moles	n_2/ moles	z_1	P_{exp}/kPa
0.0000 ± 0.0000	0.3933 ± 0.0080	0.0000 ± 0.0000	10.74
0.0169 ± 0.0005	0.3933 ± 0.0080	0.0412 ± 0.0262	11.54
0.0335 ± 0.0008	0.3933 ± 0.0080	0.0786 ± 0.0483	11.90
0.0779 ± 0.0017	0.3933 ± 0.0080	0.1653 ± 0.0933	13.27
0.1173 ± 0.0025	0.3933 ± 0.0080	0.2298 ± 0.1199	14.30
0.1506 ± 0.0032	0.3933 ± 0.0080	0.2769 ± 0.1346	15.11
0.1786 ± 0.0037	0.3933 ± 0.0080	0.3123 ± 0.1426	15.64
0.2060 ± 0.0043	0.3933 ± 0.0080	0.3437 ± 0.1471	16.27
0.2409 ± 0.0050	0.3933 ± 0.0080	0.3798 ± 0.1487	16.82
0.2771 ± 0.0057	0.3933 ± 0.0080	0.4133 ± 0.1462	17.31
0.3388 ± 0.0070	0.3933 ± 0.0080	0.4628 ± 0.1341	18.01
0.4038 ± 0.0083	0.3933 ± 0.0080	0.5066 ± 0.1130	18.50
0.4899 ± 0.0100	0.3933 ± 0.0080	0.5547 ± 0.0748	18.77
0.5582 ± 0.0114	0.3933 ± 0.0080	0.5866 ± 0.0383	18.77
1.1546 ± 0.0234	0.5556 ± 0.0113	0.6751 ± 0.0088	18.90
1.1546 ± 0.0234	0.4479 ± 0.0091	0.7205 ± 0.0081	19.01
1.1546 ± 0.0234	0.2989 ± 0.0061	0.7944 ± 0.0066	18.95
1.1546 ± 0.0234	0.1985 ± 0.0040	0.8533 ± 0.0050	19.02
1.1546 ± 0.0234	0.0989 ± 0.0020	0.9211 ± 0.0029	19.05
1.1546 ± 0.0234	0.0547 ± 0.0011	0.9547 ± 0.0017	19.02
1.1546 ± 0.0234	0.0306 ± 0.0006	0.9742 ± 0.0010	18.52
1.1546 ± 0.0234	0.0165 ± 0.0004	0.9859 ± 0.0006	16.10
1.1546 ± 0.0234	0.0149 ± 0.0031	0.9872 ± 0.0041	15.74
1.1546 ± 0.0234	0.0106 ± 0.0002	0.9909 ± 0.0004	15.42
1.1546 ± 0.0234	0.0078 ± 0.0002	0.9933 ± 0.0003	14.70
1.1546 ± 0.0234	0.0000 ± 0.0000	1.0000 ± 0.0000	12.18

Table 5-6: VLE data for the n-Hexane (1) + 2-Butanol (2) system at 329.22 K

n_1/ moles	n_2/ moles	z_1	P_{exp}/kPa
0.0000 ± 0.0000	0.3651 ± 0.0074	0.0000 ± 0.0000	14.55
0.0001 ± 0.0000	0.3651 ± 0.0074	0.0002 ± 0.0001	15.31
0.0004 ± 0.0000	0.3651 ± 0.0074	0.0011 ± 0.0001	15.52
0.0007 ± 0.0000	0.3651 ± 0.0074	0.0020 ± 0.0001	15.84
0.0011 ± 0.0000	0.3651 ± 0.0074	0.0031 ± 0.0002	16.16
0.0028 ± 0.0001	0.3651 ± 0.0074	0.0076 ± 0.0004	17.58
0.0046 ± 0.0001	0.3651 ± 0.0074	0.0123 ± 0.0005	18.67
0.0116 ± 0.0003	0.3651 ± 0.0074	0.0308 ± 0.0013	22.75
0.0194 ± 0.0004	0.3651 ± 0.0074	0.0505 ± 0.0020	26.08
0.0277 ± 0.0006	0.3651 ± 0.0074	0.0704 ± 0.0027	28.76
0.0450 ± 0.0009	0.3651 ± 0.0074	0.1098 ± 0.0041	34.81
0.0649 ± 0.0013	0.3651 ± 0.0074	0.1509 ± 0.0053	40.95
0.0965 ± 0.0020	0.3651 ± 0.0074	0.2090 ± 0.0068	47.17
0.1227 ± 0.0025	0.3651 ± 0.0074	0.2515 ± 0.0077	51.15
0.1639 ± 0.0033	0.3651 ± 0.0074	0.3098 ± 0.0088	55.03
0.2443 ± 0.0050	0.3651 ± 0.0074	0.4009 ± 0.0098	59.44
0.3706 ± 0.0075	0.3651 ± 0.0074	0.5037 ± 0.0102	62.96
0.5635 ± 0.0115	0.3651 ± 0.0074	0.6068 ± 0.0097	65.56
0.3308 ± 0.0067	0.2184 ± 0.0044	0.6023 ± 0.0097	66.12
0.3308 ± 0.0067	0.1323 ± 0.0027	0.7143 ± 0.0082	67.40
0.3308 ± 0.0067	0.0750 ± 0.0015	0.8153 ± 0.0061	68.40
0.3308 ± 0.0067	0.0366 ± 0.0008	0.9004 ± 0.0036	68.83
0.3308 ± 0.0067	0.0105 ± 0.0002	0.9691 ± 0.0013	67.96
0.3308 ± 0.0067	0.0068 ± 0.0002	0.9799 ± 0.0008	67.46
0.3308 ± 0.0067	0.0029 ± 0.0001	0.9915 ± 0.0004	66.58
0.3308 ± 0.0067	0.0016 ± 0.0001	0.9951 ± 0.0003	66.10
0.3308 ± 0.0067	0.0005 ± 0.0000	0.9984 ± 0.0001	65.67
0.3308 ± 0.0067	0.0000 ± 0.0000	1.0000 ± 0.0000	65.63

5.3.3 New Unmeasured Systems

Three new systems were measured using the new apparatus after intensive runs on test systems were performed to validate the experimental procedures. The experimental data for these systems are presented in Tables 5-7 to 5-11.

Table 5-7: VLE data for the 1-Propanol (1) + n-Dodecane (2) system at 342.83 K

n_1 / moles	n_2 / moles	z_1	P_{exp} /kPa
0.0000 ± 0.0000	0.0806 ± 0.0016	0.0000 ± 0.0000	0.57
0.0194 ± 0.0004	0.0806 ± 0.0016	0.1943 ± 0.0067	17.08
0.0377 ± 0.0008	0.0806 ± 0.0016	0.3187 ± 0.0090	23.88
0.0501 ± 0.0010	0.0806 ± 0.0016	0.3832 ± 0.0098	25.60
0.0666 ± 0.0014	0.0806 ± 0.0016	0.4526 ± 0.0102	26.86
0.0852 ± 0.0018	0.0806 ± 0.0016	0.5137 ± 0.0102	27.56
0.2319 ± 0.0047	0.2811 ± 0.0057	0.4521 ± 0.0100	27.03
0.2319 ± 0.0047	0.2242 ± 0.0045	0.5086 ± 0.0100	27.52
0.2319 ± 0.0047	0.1509 ± 0.0031	0.6059 ± 0.0096	28.27
0.2319 ± 0.0047	0.0993 ± 0.0020	0.7002 ± 0.0084	28.75
0.2319 ± 0.0047	0.0750 ± 0.0015	0.7557 ± 0.0074	28.98
0.2319 ± 0.0047	0.0550 ± 0.0011	0.8084 ± 0.0062	29.37
0.2319 ± 0.0047	0.0389 ± 0.0008	0.8563 ± 0.0049	29.72
0.2319 ± 0.0047	0.0233 ± 0.0005	0.9088 ± 0.0033	30.27
0.2319 ± 0.0047	0.0115 ± 0.0002	0.9526 ± 0.0018	30.74
0.2319 ± 0.0047	0.0015 ± 0.0000	0.9936 ± 0.0003	31.26
0.2319 ± 0.0047	0.0000 ± 0.0000	1.0000 ± 0.0000	31.45

Table 5-8: VLE data for the 1-Propanol (1) + n-Dodecane (2) system at 352.68 K

n_1 / moles	n_2 / moles	z_1	P_{exp} /kPa
0.0000 ± 0.0000	0.0831 ± 0.0017	0.0000 ± 0.0000	0.77
0.0074 ± 0.0002	0.0831 ± 0.0017	0.0818 ± 0.0034	13.24
0.0106 ± 0.0002	0.0831 ± 0.0017	0.1130 ± 0.0044	17.75
0.0170 ± 0.0004	0.0831 ± 0.0017	0.1700 ± 0.0060	22.01
0.0248 ± 0.0005	0.0831 ± 0.0017	0.2297 ± 0.0075	25.25
0.0358 ± 0.0008	0.0831 ± 0.0017	0.3014 ± 0.0088	30.67
0.0562 ± 0.0012	0.0831 ± 0.0017	0.4034 ± 0.0099	38.19
0.0839 ± 0.0017	0.0831 ± 0.0017	0.5024 ± 0.0102	42.01
0.1743 ± 0.0036	0.2102 ± 0.0043	0.4533 ± 0.0101	41.47
0.1743 ± 0.0036	0.1718 ± 0.0035	0.5036 ± 0.0102	42.20
0.1743 ± 0.0036	0.1341 ± 0.0027	0.5652 ± 0.0100	43.21
0.1743 ± 0.0036	0.0960 ± 0.0020	0.6449 ± 0.0093	44.09
0.1743 ± 0.0036	0.0693 ± 0.0014	0.7154 ± 0.0082	45.08
0.1743 ± 0.0036	0.0495 ± 0.0010	0.7789 ± 0.0070	45.99
0.1743 ± 0.0036	0.0281 ± 0.0006	0.8610 ± 0.0048	47.33
0.1743 ± 0.0036	0.0217 ± 0.0004	0.8891 ± 0.0040	47.63
0.1743 ± 0.0036	0.0141 ± 0.0003	0.9252 ± 0.0028	48.34
0.1743 ± 0.0036	0.0082 ± 0.0002	0.9549 ± 0.0018	48.99
0.1743 ± 0.0036	0.0044 ± 0.0001	0.9757 ± 0.0010	49.55
0.1743 ± 0.0036	0.0021 ± 0.0001	0.9883 ± 0.0005	49.67
0.1743 ± 0.0036	0.0004 ± 0.0000	0.9975 ± 0.0002	49.73
0.1743 ± 0.0036	0.0000 ± 0.0000	1.0000 ± 0.0000	49.80

Table 5-9: VLE data for the 2-Butanol (1) + n-Dodecane (2) system at 342.83 K

n_1 / moles	n_2 / moles	z_1	P_{exp} / kPa
0.0000 ± 0.0000	0.0998 ± 0.0020	0.0000 ± 0.0000	0.54
0.0096 ± 0.0002	0.0998 ± 0.0020	0.0875 ± 0.0035	5.96
0.0128 ± 0.0003	0.0998 ± 0.0020	0.1138 ± 0.0043	7.35
0.0183 ± 0.0004	0.0998 ± 0.0020	0.1549 ± 0.0055	9.34
0.0256 ± 0.0005	0.0998 ± 0.0020	0.2042 ± 0.0068	11.85
0.0436 ± 0.0009	0.0998 ± 0.0020	0.3040 ± 0.0088	16.45
0.0665 ± 0.0014	0.0998 ± 0.0020	0.4000 ± 0.0099	20.23
0.1030 ± 0.0021	0.0998 ± 0.0020	0.5080 ± 0.0102	23.15
0.1813 ± 0.0037	0.1795 ± 0.0036	0.5025 ± 0.0102	22.93
0.1813 ± 0.0037	0.1193 ± 0.0024	0.6031 ± 0.0097	24.17
0.1813 ± 0.0037	0.0773 ± 0.0016	0.7011 ± 0.0085	25.22
0.1813 ± 0.0037	0.0451 ± 0.0009	0.8009 ± 0.0064	26.30
0.1813 ± 0.0037	0.0322 ± 0.0007	0.8492 ± 0.0052	26.82
0.1813 ± 0.0037	0.0203 ± 0.0004	0.8993 ± 0.0037	27.36
0.1813 ± 0.0037	0.0097 ± 0.0002	0.9490 ± 0.0020	27.98
0.1813 ± 0.0037	0.0031 ± 0.0001	0.9833 ± 0.0007	28.15
0.1813 ± 0.0037	0.0003 ± 0.0000	0.9981 ± 0.0001	28.14
0.1813 ± 0.0037	0.0000 ± 0.0000	1.0000 ± 0.0000	28.31

Table 5-10: VLE data for the 2-Butanol (1) + n-Dodecane (2) system at 352.68 K

n_1/ moles	n_2/ moles	z_1	P_{exp}/ kPa
0.0000 ± 0.0000	0.0996 ± 0.0020	0.0000 ± 0.0000	0.79
0.0171 ± 0.0004	0.0996 ± 0.0020	0.1464 ± 0.0053	9.65
0.0357 ± 0.0007	0.0996 ± 0.0020	0.2639 ± 0.0081	17.75
0.0588 ± 0.0012	0.0996 ± 0.0020	0.3712 ± 0.0096	25.60
0.1880 ± 0.0038	0.2238 ± 0.0045	0.4565 ± 0.0101	33.53
0.1880 ± 0.0038	0.1515 ± 0.0031	0.5537 ± 0.0100	35.45
0.1880 ± 0.0038	0.0993 ± 0.0020	0.6543 ± 0.0091	37.33
0.1880 ± 0.0038	0.0614 ± 0.0013	0.7537 ± 0.0075	39.31
0.1880 ± 0.0038	0.0449 ± 0.0009	0.8071 ± 0.0063	40.22
0.1880 ± 0.0038	0.0320 ± 0.0007	0.8545 ± 0.0050	41.42
0.1880 ± 0.0038	0.0194 ± 0.0004	0.9064 ± 0.0034	42.41
0.1880 ± 0.0038	0.0104 ± 0.0002	0.9477 ± 0.0020	43.37
0.1880 ± 0.0038	0.0037 ± 0.0001	0.9806 ± 0.0008	43.92
0.1880 ± 0.0038	0.0000 ± 0.0000	1.0000 ± 0.0000	44.19

Table 5-11: VLE data for the Water (1) + o-Cresol system at 342.83 K

n_1/ moles	n_2/ moles	z_1	P_{exp}/ kPa
0.0000 ± 0.0000	0.2787 ± 0.0056	0.0000 ± 0.0000	0.83
0.0161 ± 0.0004	0.2787 ± 0.0056	0.0545 ± 0.0025	5.81
0.0221 ± 0.0006	0.2787 ± 0.0056	0.0735 ± 0.0032	7.11
0.0341 ± 0.0008	0.2787 ± 0.0056	0.1090 ± 0.0043	7.38
0.0518 ± 0.0012	0.2787 ± 0.0056	0.1568 ± 0.0057	9.12
0.0752 ± 0.0016	0.2787 ± 0.0056	0.2124 ± 0.0071	10.51
0.1229 ± 0.0026	0.2787 ± 0.0056	0.3060 ± 0.0089	12.41
0.1902 ± 0.0040	0.2787 ± 0.0056	0.4056 ± 0.0099	15.16
0.3342 ± 0.0069	0.2787 ± 0.0056	0.5453 ± 0.0101	17.50
0.4000 ± 0.0082	0.0000 ± 0.0000	1.0000 ± 0.0000	30.65

The reduction of these data is presented in the next Chapter. Three activity coefficient models (NRTL, T-K Wilson and Van Laar) were used to account for the liquid phase non-ideality and the

vapour phase non-ideality was accounted for by using the virial equation of state. The Pitzer-Curl correlation and the Prausnitz mixing rules were used to estimate the virial coefficients.

CHAPTER SIX

DISCUSSION

The knowledge of phase equilibrium data is the basis for the design and optimisation of many chemical processes, for example the design and analysis of separation processes like distillation can only proceed upon availability of such data. Experimental data are usually regressed using a model with adjustable parameters which allow for both interpolation and extrapolation of the measured properties. The theory of low-pressure VLE employed in the reduction of experimental data is reviewed in Chapter 2. Fitting thermodynamic models to raw data is extremely important for many reasons, some of which are:

- It allows large amounts of data to be summarized very compactly
- It can be used to develop VLE predictive methods. These methods are essential for the construction of future processes since experimental data will never be available for the enormous number of new binary and multicomponent mixtures.
- It allows one to extend binary data to predict multicomponent data. Most industrial separation processes deal with multicomponent streams but multicomponent VLE data are very time-consuming to measure and therefore only binary data are measured in most cases. Techniques are availabe for extending the constituent components' binary VLE data to multicomponent data. (Seader and Henley [1998])
- It allows accurate interpolation of the data as well as a limited amount of extrapolation.

This chapter deals with the regression of experimental data presented in Chapter 5 and the discussion of some of the results obtained from different models used.

6.1 Second Virial Coefficients and Liquid Molar Volumes

The second virial coefficients were estimated using the Pitzer and Curl [1957] correlation and the Rackett [1970] equation was used to calculate the liquid molar volumes. The virial coefficients and the liquid molar volumes for all the systems studied are listed in Table 6-1.

Table 6-1: Second virial coefficients and liquid molar volumes

Component	T (K)	V_i cm^3/mol	B_{ii} cm^3/mol	B_{12} cm^3/mol
n-Hexane (i=1)	329.22	136.26	-1466.80	-1548.80
2-Butanol (i=2)	329.22	93.79	-1620.40	
Water (i=1)	313.17	16.53	-602.10	-1087.30
1-Propanol (i=2)	313.17	74.94	-1606.90	
Water (i=1)	323.18	16.71	-548.10	-1091.90
2-Butanol (i=2)	323.18	92.98	-1715.80	
1-Propanol (i=1)	342.83	78.21	-1208.80	-3224.80
	352.68	79.41	-1107.40	-2949.60
n-Dodecane (i=2)	342.83	224.21	-7691.00	
	352.68	226.56	-7020.10	
2-Butanol (i=1)	342.83	95.70	-1430.90	-3434.00
	352.68	97.17	-1313.10	-1328.40
n-Dodecane (i=2)	342.83	224.21	-7691.00	
	352.68	226.56	-7020.10	
Water (i=1)	342.83	17.07	-461.30	-1328.40
o-Cresol (i=2)	342.83	86.96	-3101.10	

6.2 VLE Data Reduction

The importance of VLE data reduction is mentioned above. The combined method ($\gamma - \phi$ approach) of VLE data reduction was used for the modeling of experimental data. The Barker's method was implemented to convert the moles of each component injected into the cell to mole fractions of the vapour and liquid phase (Uusi-Kyyny et al. [2002]). Barker's method assumes that there is an activity coefficient model that can predict the bubble point pressure, P_{calc}, with higher accuracy than the experimental error of the measured total pressure. Barker's method is an iterative method which needs models for vapour and liquid phase non-idealities. Three activity coefficient models were used in the data reduction of the binary pairs namely, the Van Laar, T-K Wilson and NRTL equations. The second virial coefficients required to correct vapour phase non-idealities were calculated using the Pitzer-Curl [1957] correlation and the Prausnitz [1986] mixing rules. Although the Pitzer-Curl correlation produces second virial coefficients of moderate accuracy compared to the Tsonopoulos [1974] or the Hayden O'Connell [1975] correlations, Prausnitz et al. [1967] argued that vapour–liquid equilibrium at normal pressures (up to 5 or 10 atm) are not very sensitive to vapour phase fugacity coefficients and thus virial coefficients of limited accuracy introduce little error into the phase equilibrium calculations. The pressures measured in this work were low (below atmospheric pressure) and instead of assuming ideal gas phase behaviour, the Pitzer-Curl correlation, because of its mathematical simplicity, was used to estimate the second virial coefficient.

The regression programs were written in MATLAB. The built-in MATLAB optimization function *fminsearch* was utilized in the reduction of all experimental data presented in Chapter 5. The objective function in the regression programs was:

$$F = \left(\frac{P_{\exp} - P_{calc}}{P_{\exp}} \right)^2 \qquad (6\text{-}1)$$

There are many objective functions; however, the above-mentioned objective function is the best-suited for isothermal data (Harris [2004]).

The scheme for the data reduction adopted in this work is as follows:

Subscript i refers to the component and k refers to the data point. Initially assume the liquid composition $x_{i,k}$ equal to the total composition $z_{i,k}$

$$z_{i,k} = x_{i,k} = \frac{n_{i,k}^{tot}}{\sum_{i=1}^{NC} n_{i,k}^{tot}} \tag{6-1}$$

Assume the fugacity coefficient of each component in the vapour phase to be unity and calculate the molar volume of vapour from ideal gas equation

$$v_k^V = \frac{RT}{P_{\exp,k}} \tag{6-2}$$

Compute the bubble point pressure

$$P_{calc,k} = \frac{x_{1,k}\gamma_{1,k}P_1^{sat}}{\phi_{1,k}} + \frac{x_{2,k}\gamma_{2,k}P_2^{sat}}{\phi_{2,k}} \tag{6-3}$$

Minimizing the function F by varying the coefficients of the activity coefficient model

$$F = \sum_{allk}\left(\frac{P_{\exp} - P_{calc}}{P_{\exp}}\right)^2 \tag{6-4}$$

Solve for the number of moles in the vapour phase $n_{V,k}$ from

$$0 = V_{cell}^{tot} - \left[v_k^L\left(n_k^{tot} - n_{V,k}\right) + v_k^V \times n_{V,k}\right] \tag{6-5}$$

V_{cell}^{tot} was determined by the procedure given in section 4.4.

The liquid molar volume is

$$v_k^L = \sum_{i=1}^{NC} x_{i,k} v_{i,k}^L \tag{6-6}$$

Compute the vapour composition $y_{i,k}$ from

$$y_{i,k} = \frac{x_{i,k}\gamma_{i,k}P_i^{sat}}{\phi_{i,k}P_{calc,k}} \tag{6-7}$$

Calculate the number of moles of each component in the vapour phase

$$n_{i,k}^{V} = y_{i,k}n_{V,k} \tag{6-8}$$

And the liquid phase

$$n_{i,k}^{L} = n_{i,k}^{tot} - n_{i,k}^{V} \tag{6-9}$$

Update the liquid composition x_i

$$x_{i,k} = \frac{n_{i,k}^{L}}{\sum_{i=1}^{NC} n_{i,k}^{L}} \tag{6-10}$$

and compute the fugacity coefficient of each component in the vapour phase and the molar volume of the vapour from an equation of state. Return to Equation 6-3 repeat this scheme until the change of vapour phase moles and change of the liquid phase moles is below tolerance. For our measurements, the corrections to obtain the liquid mole fraction x_i from the total composition z_i are very small.

6.3 Test Systems

Three systems were measured to test the performance and the operating procedures of the new static total pressure apparatus set-up in this work. These systems were: Water (1) + 1-Propanol (2) at 313.17 K, Water (1) + 2-Butanol (2) at 323.18 K and n-Hexane (1) + 2-Butanol (2) at 329.22 K. All the experimental data can be found in Chapter 5.

VLE measurements started with the pure component vapour pressures and were followed by the binary mixtures vapour pressures as explained in Chapter 4. The raw data (z_i, P) were converted to (x_i, P) using an iterative calculation as outlined in Section 6.1.The data were regressed to obtained

parameters for the NRTL, T-K Wilson and Van Laar equations. The regressed data for Water (1) + 1-Propanol (2) at 313.17 K are shown in Tables 6.2 to 6-4 and Figure 6.1 shows a P-x-y diagram for Water (1) + 1-Propanol (2) at 313.17 K together with results measured earlier (Zielkiewicz et al. [1991]). It is clear from Figure 6-1 that the results obtained in this work are in good agreement with literature data. The regressed data for the other two test systems can be found in Appendix B. Figures 6-2 and 6-3 show the P-x-y diagram together with literature values for Water (1) + 2-Butanol (2) at 323.18 K and n-Hexane (1) + 2-Butanol (2) at 329.22 K respectively. The x_1-y_1 diagram for Water (1) + 2-Butanol (2) at 323.18 K is shown in Figure 6-4. The x_1-y_1 diagrams for the two other test systems can be found in Appendix C.

The three test systems showed a positive deviation from Raoult's Law and exhibit azeotropic behaviour and therefore cannot be separated by ordinary distillation. The Water (1) + 2-Butanol (2) system was the most difficult to measure of the three test systems measured. In the water rich region, Water and 2-Butanol are immiscible (two liquid phases are present) and as a result, the vapour pressure above the two liquids was unstable. For this reason few data points were measured in that region.

Table 6-2: Regressed data for Water (1) + 1-Propanol (2) at 313.17 K using the NRTL model

Experimental		NRTL				
x_1	P/kPa	P_{cal}/kPa	ΔP/kPa	y_1 cal	γ_1	γ_2
0.0000	6.99	6.99	0.00	0.0000	4.112	1.000
0.0378	7.86	7.80	0.06	0.1357	3.803	1.002
0.0847	8.65	8.62	0.03	0.2511	3.470	1.008
0.1238	9.15	9.17	-0.02	0.3206	3.227	1.016
0.1400	9.35	9.37	-0.02	0.3446	3.134	1.021
0.1863	9.84	9.87	-0.03	0.4017	2.890	1.037
0.2321	10.28	10.27	0.01	0.4458	2.678	1.058
0.2829	10.63	10.61	0.02	0.4847	2.468	1.088
0.3256	10.83	10.83	0.00	0.5113	2.310	1.120
0.3589	10.93	10.97	-0.04	0.5290	2.195	1.150
0.4411	11.21	11.21	0.00	0.5638	1.944	1.248
0.4969	11.28	11.29	-0.01	0.5816	1.794	1.340
0.5294	11.20	11.32	-0.12	0.5899	1.712	1.407
0.5129	11.35	11.31	0.04	0.5858	1.753	1.372
0.5957	11.38	11.34	0.04	0.6032	1.559	1.588
0.6409	11.41	11.34	0.07	0.6094	1.464	1.760
0.6906	11.31	11.33	-0.02	0.6135	1.366	2.019
0.7484	11.25	11.32	-0.07	0.6152	1.263	2.470
0.8173	11.35	11.33	0.02	0.6146	1.157	3.405
0.8571	11.35	11.31	0.04	0.6160	1.104	4.334
0.9096	11.17	11.14	0.03	0.6299	1.047	6.491
0.9586	10.36	10.25	0.11	0.6964	1.011	10.682
0.9694	9.83	9.84	-0.01	0.7304	1.006	12.176
0.9740	9.52	9.56	-0.04	0.7535	1.005	12.901
0.9836	8.85	8.95	-0.10	0.8109	1.002	14.647
0.9910	8.32	8.32	0.00	0.8772	1.001	16.229
0.9966	7.82	7.75	0.07	0.9461	1.000	17.587
0.9995	7.42	7.42	0.00	0.9914	1.000	18.354
1.0000	7.36	7.36	0.00	1.0000	1.000	18.504

Table 6-3: Regressed data for Water (1) + 1-Propanol (2) at 313.17 K using the T-K Wilson model

Experimental		T-K Wilson				
x_1	P/kPa	P_{cal}/kPa	ΔP/kPa	y_1 *cal*	γ_1	γ_2
0.0000	6.99	6.99	0.00	0.0000	3.831	1.000
0.0378	7.86	7.74	0.12	0.1301	3.620	1.001
0.0847	8.65	8.54	0.11	0.2461	3.373	1.006
0.1238	9.15	9.11	0.04	0.3182	3.181	1.013
0.1400	9.35	9.32	0.03	0.3433	3.104	1.016
0.1863	9.84	9.84	0.00	0.4035	2.894	1.030
0.2321	10.28	10.26	0.02	0.4499	2.701	1.049
0.2829	10.63	10.63	0.00	0.4905	2.501	1.078
0.3256	10.83	10.86	-0.03	0.5177	2.345	1.109
0.3589	10.93	11.01	-0.08	0.5355	2.230	1.138
0.4411	11.21	11.25	-0.04	0.5692	1.970	1.236
0.4969	11.28	11.33	-0.05	0.5855	1.812	1.332
0.5294	11.2	11.36	-0.16	0.5928	1.726	1.402
0.5957	11.38	11.38	0.00	0.6037	1.565	1.591
0.6409	11.41	11.37	0.04	0.6083	1.465	1.770
0.6906	11.31	11.37	-0.06	0.6110	1.365	2.039
0.7484	11.25	11.36	-0.11	0.6116	1.261	2.502
0.8173	11.35	11.37	-0.02	0.6113	1.154	3.449
0.8571	11.35	11.34	0.01	0.6136	1.102	4.376
0.9096	11.17	11.13	0.04	0.6298	1.046	6.502
0.9586	10.36	10.22	0.14	0.6985	1.011	10.617
0.9694	9.83	9.77	0.06	0.7350	1.006	12.090
0.9740	9.52	9.54	-0.02	0.7555	1.005	12.808
0.9836	8.85	8.92	-0.07	0.8132	1.002	14.543
0.9910	8.32	8.31	0.01	0.8781	1.001	16.124
0.9966	7.82	7.75	0.07	0.9460	1.000	17.489
0.9995	7.42	7.43	-0.01	0.9907	1.000	18.263
1.0000	7.36	7.36	0.00	1.0000	1.000	18.415

Table 6-4: Regressed data for Water (1) + 1-Propanol (2) at 313.17 K using the Van Laar model

Experimental		Van Laar				
x_1	P/kPa	P_{cal}/kPa	ΔP/kPa	y_1 *cal*	γ_1	γ_2
0.0000	6.99	6.99	0.00	0.0000	3.584	1.000
0.0378	7.86	7.69	0.17	0.0041	3.430	1.001
0.0847	8.65	8.46	0.19	0.0186	3.243	1.005
0.1238	9.15	9.01	0.14	0.0330	3.091	1.010
0.1400	9.35	9.22	0.13	0.0490	3.029	1.013
0.1863	9.84	9.76	0.08	0.1132	2.856	1.025
0.2321	10.28	10.20	0.08	0.1706	2.689	1.042
0.2829	10.63	10.59	0.04	0.3368	2.511	1.067
0.3255	10.83	10.85	-0.02	0.4502	2.367	1.095
0.3589	10.93	11.01	-0.08	0.5288	2.258	1.122
0.4410	11.21	11.27	-0.06	0.6278	2.004	1.215
0.4969	11.28	11.36	-0.08	0.6902	1.844	1.308
0.5294	11.20	11.39	-0.19	0.7440	1.756	1.378
0.5957	11.38	11.41	-0.03	0.7697	1.587	1.570
0.6409	11.41	11.41	0.00	0.7941	1.481	1.756
0.6906	11.31	11.41	-0.10	0.8179	1.374	2.039
0.7484	11.25	11.43	-0.18	0.8336	1.263	2.533
0.8173	11.35	11.48	-0.13	0.8439	1.151	3.548
0.8571	11.35	11.47	-0.12	0.8434	1.098	4.531
0.9096	11.17	11.24	-0.07	0.8544	1.043	6.710
0.9586	10.36	10.21	0.15	0.8719	1.010	10.611
0.9694	9.83	9.73	0.10	0.9041	1.006	11.916
0.9740	9.52	9.48	0.04	0.9588	1.004	12.536
0.9836	8.85	8.86	-0.01	0.9715	1.002	13.995
0.9910	8.32	8.26	0.06	0.9871	1.001	15.280
0.9966	7.82	7.73	0.09	0.9925	1.000	16.359
0.9995	7.42	7.42	0.00	0.9975	1.000	16.959
1.0000	7.36	7.36	0.00	1.0000	1.000	17.075

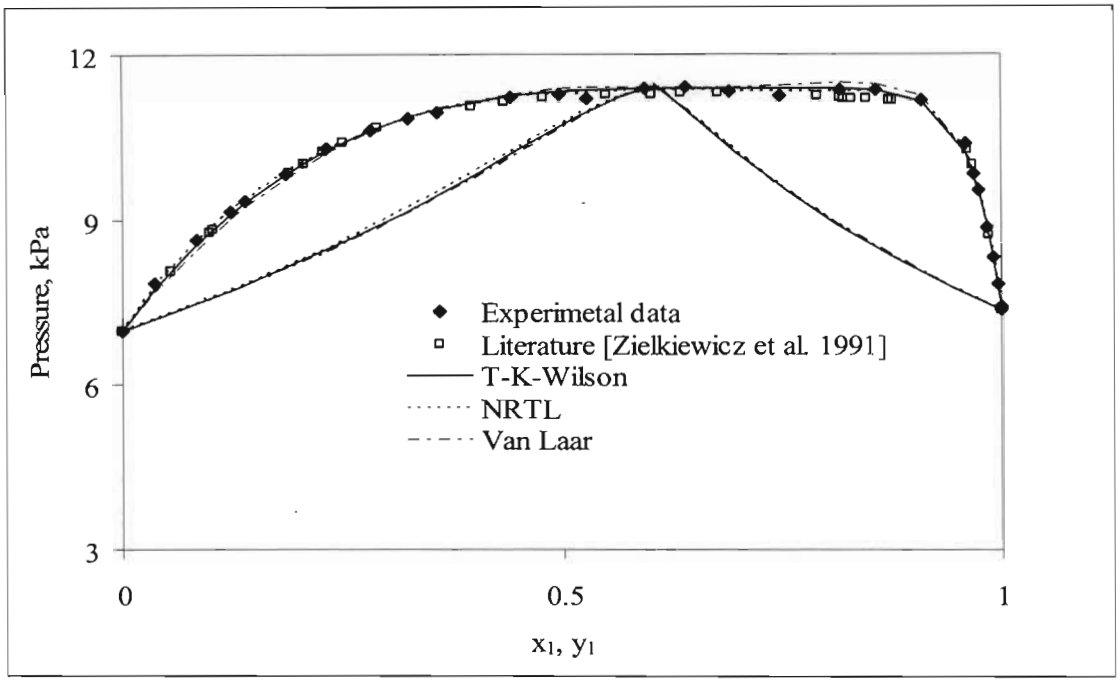

Figure 6-1: The P-x-y diagram for Water (1) + 1-Propanol (2) system at 313.17 K

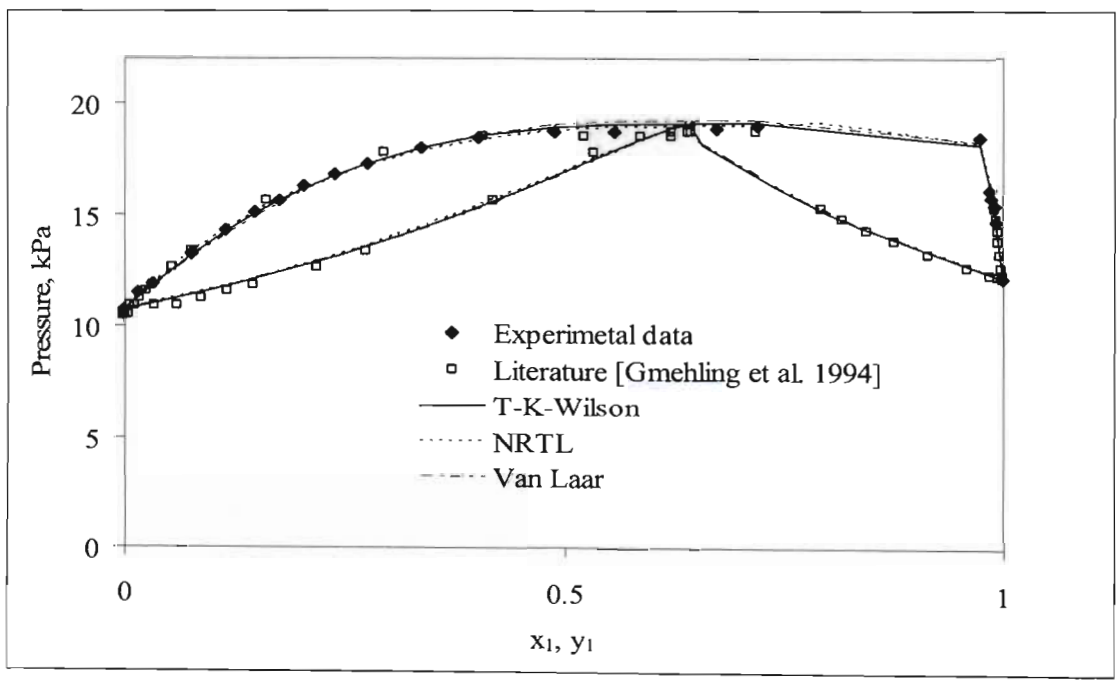

Figure 6-2: The P-x-y diagram for Water (1) + 2-Butanol (2) system at 323.18 K

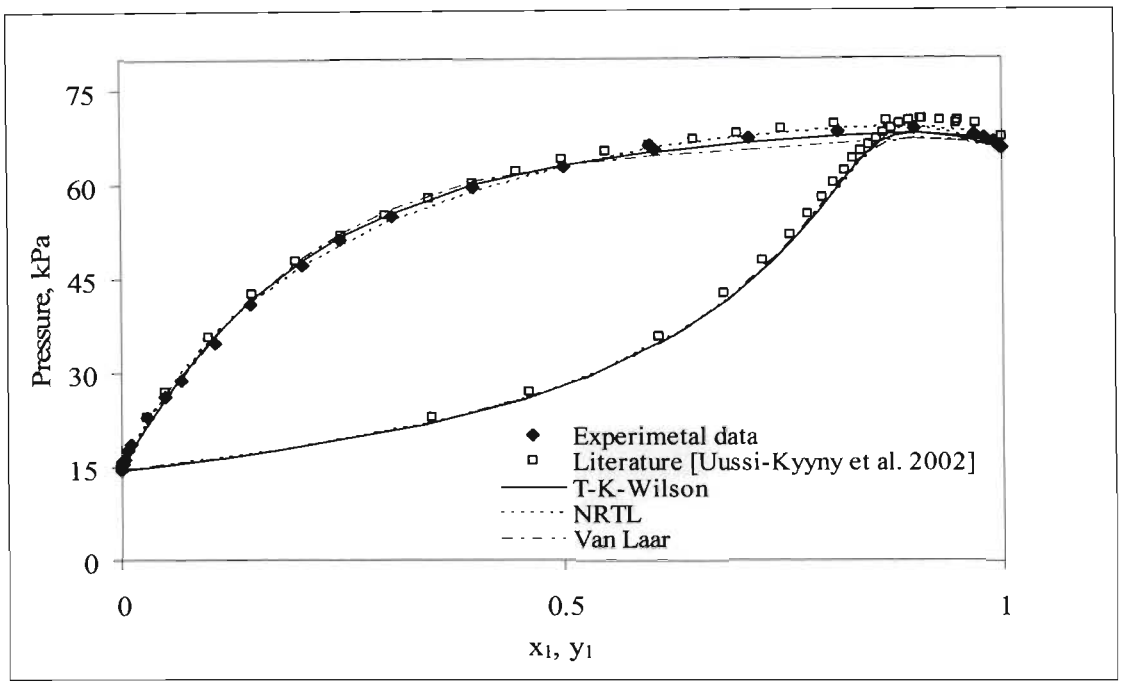

Figure 6-3: The P-x-y diagram for n-Hexane (1) + 2-Butanol (2) system at 329.22 K

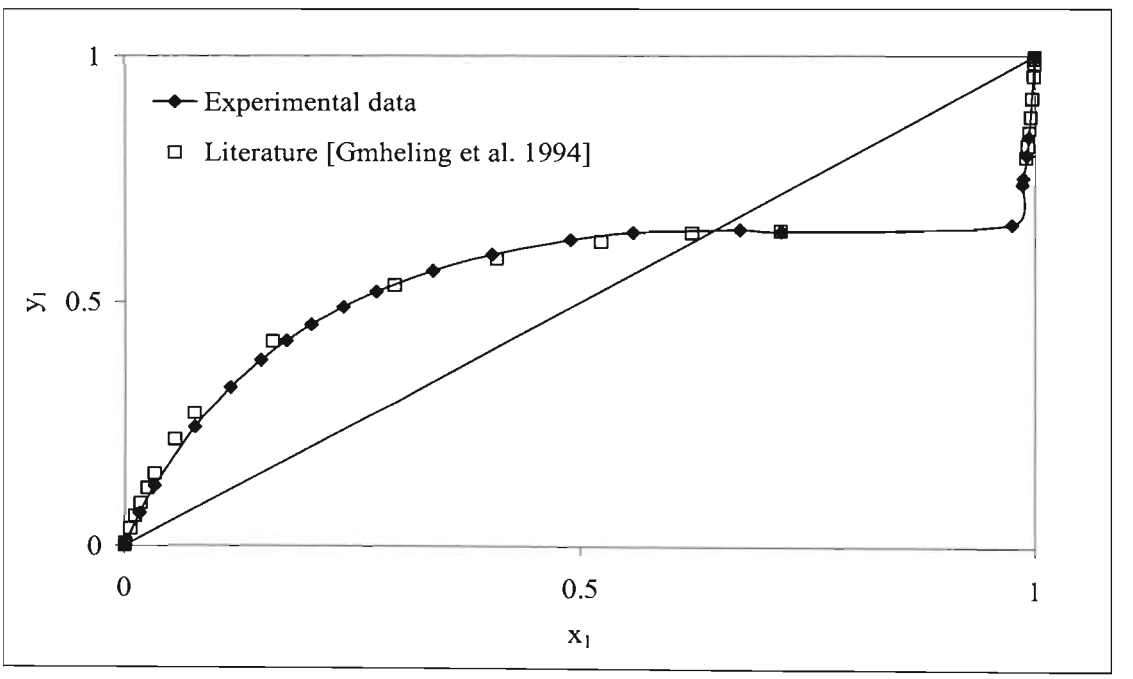

Figure 6-4: The x_1-y_1 diagram for Water (1) + 2-Butanol (2) system at 323.18 K

Table 6-5: Model parameters and deviations between experimental and calculated pressures for Water (1) + 1-Propanol (2) at 313.17 K; Water (1) + 2-Butanol (2) at 323.18 K and n-Hexane (1) + 2-Butanol (2) at 329.22 K.

Systems	Water (1) + 1-Propanol (2)	Water (1) + 2-Butanol (2)	n-Hexane (1) + 2-Butanol (2)
Equation	**313.17K**	**323.18 K**	**329.22 K**
NRTL			
$g_{12} - g_{11}$ (J/mol)	2377.135	2583.55	2637.126
$g_{12} - g_{22}$ (J/mol)	886.035	811.18	5595.866
a	-1.137	-1.300	0.619
Average ΔP (kPa)	0.002	0.0043	0.127
T-K Wilson			
$\lambda_{12} - \lambda_{11}$ (J/mol)	6163.698	7529.91	3915.624
$\lambda_{12} - \lambda_{22}$ (J/mol)	-3841.805	-5249.62	2463.320
Average ΔP (kPa)	0.0009	0.003	0.260
Van Laar			
A12	1.277	1.271	1.389
A21	2.838	3.618	1.942
Average ΔP (kPa)	0.006	0.0074	0.453

Since the process of data reduction was achieved by minimizing the pressure, the best model for the system was judged on the basis of the deviation between the calculated and the measured pressures. All the models (NRTL, T-K Wilson and Van Laar) fit the data well. It is evident from Table 6-5 that the Van Laar model is the least accurate but it could be preferred over the other two for mathematical simplicity.

Table 6-6: Best model for the test system isotherms

Systems	Best Model
Water (1) + 1-Propanol (2) at 313.17 K	T-K Wilson
Water (1) + 2-Butanol (2) at 323.18 K	T-K Wilson
n-Hexane (1) + 2-Butanol (2) at 329.22 K	NRTL

These test systems did not present any difficulty when VLE data were collected in the dilute regions. This could be due to the fact that the components had similar boiling points. Because the data for the test systems compared well with the literature data, a high degree of confidence was placed in the performance of the static assembly and the operating procedure. This gave confidence in measuring VLE for unknown systems.

6.4 New Systems Measured

The experimental VLE data for the new highly non-ideal systems (1-Propanol + n-Dodecane at 342.83 K and 352.68 K, 2-Butanol (1) + n-Dodecane at 342.83 K and 352.68 K; and Water (1) + o-Cresol (2) at 342.83 K) are presented in Chapter 5. Also available in Chapter 5 are the pure components' properties. The cross parameters were calculated using the Prausnitz [1986] mixing rules. This section deals with the reduction of the experimental data and the discussion of results. Like the test systems, these systems were regressed using the $\gamma - \phi$ approach of data reduction. The $\gamma - \phi$ approach was discussed in great detail in Chapter 2. The NRTL, T-K Wilson and Van Laar activity coefficient models were used to account for the liquid phase non-ideality (for the NRTL equation all the three parameters were obtained by regression) and the virial equation of state was used to account for the vapour phase non-ideality. The virial coefficients were estimated by using the Pitzer-Curl correlation and the Prausnitz mixing rule. The regressed data for the new systems are presented in Tables 6-7 to 6-11. (Note that only the data obtained using the NRTL equation for each system is presented here. The regressed data using the T-K Wilson and Van Laar equations can be found in Appendix B). Figures 6-5 to 6-9 are the P-x-y Diagrams. Figure 10 is the x_1-y_1 diagram for Propanol (1) + n-Dodecane (2) at 342.83 K. The x_1-y_1 diagrams for the other systems can be found in Appendix C.

For these systems, the data could not be compared to any data as there were none found in the open literature. Since all these systems exhibit similar behaviour, there will be only one discussion to avoid repetition.

Table 6-7: Regressed data for 1-Propanol (1) + n-dodecane (2) at 342.83 K using the NRTL model

Experimental		NRTL				
x_1	P/kPa	P_{cal}/kPa	ΔP/kPa	y_1 cal	γ_1	γ_2
0.0000	0.57	0.57	0.00	0.0000	3.807	1.000
0.1860	17.08	17.26	-0.18	0.9712	2.847	1.032
0.3107	23.88	23.37	0.51	0.9805	2.336	1.102
0.3763	25.60	25.42	0.18	0.9827	2.104	1.164
0.4467	26.86	26.93	-0.07	0.9843	1.882	1.259
0.5090	27.56	27.80	-0.24	0.9852	1.707	1.377
0.4511	27.03	27.01	0.02	0.9842	1.869	1.266
0.5073	27.52	27.78	-0.26	0.9851	1.712	1.373
0.6045	28.27	28.52	-0.25	0.9859	1.476	1.654
0.6990	28.75	28.81	-0.06	0.9863	1.291	2.130
0.7545	28.98	28.93	0.05	0.9866	1.201	2.581
0.8073	29.37	29.10	0.27	0.9869	1.129	3.215
0.8556	29.72	29.36	0.36	0.9877	1.076	4.081
0.9082	30.27	29.85	0.42	0.9895	1.033	5.560
0.9525	30.74	30.48	0.26	0.9927	1.009	7.569
0.9935	31.26	31.30	-0.04	0.9987	1.000	10.554
1.0000	31.45	31.45	0.00	1.0000	1.000	11.173

Table 6-8: Regressed data for 1-Propanol (1) + n-dodecane (2) at 352.68 K using the NRTL model

Experimental		NRTL				
x_1	P/kPa	P_{cal}/kPa	ΔP/kPa	y_1 cal	γ_1	γ_2
0.0000	0.77	0.77	0.00	0.0000	4.132	1.000
0.0744	13.24	13.31	-0.07	0.9448	3.349	1.008
0.1036	17.75	16.99	0.76	0.9575	3.114	1.015
0.1596	22.01	22.76	-0.75	0.9693	2.745	1.035
0.2912	30.67	32.12	-1.45	0.9799	2.155	1.110
0.3942	38.19	37.14	1.05	0.9837	1.851	1.201
0.4955	42.01	40.88	1.13	0.9862	1.627	1.332
0.5008	42.20	41.06	1.14	0.9862	1.617	1.341
0.5622	43.21	42.84	0.37	0.9874	1.506	1.454
0.6420	44.09	44.68	-0.59	0.9886	1.378	1.663
0.7126	45.08	45.90	-0.82	0.9896	1.277	1.953
0.7764	45.99	46.69	-0.70	0.9903	1.194	2.381
0.8593	47.33	47.43	-0.10	0.9911	1.097	3.505
0.8876	47.63	47.67	-0.04	0.9915	1.068	4.219
0.9242	48.34	48.08	0.26	0.9923	1.035	5.692
0.9542	48.99	48.57	0.42	0.9937	1.015	7.806
0.9753	49.55	49.04	0.51	0.9956	1.005	10.245
0.9881	49.67	49.41	0.26	0.9975	1.001	12.393
0.9974	49.73	49.71	0.02	0.9994	1.000	14.444
1.0000	49.80	49.80	0.00	1.0000	1.000	15.096

Table 6-9: Regressed data for 2-Butanol (1) + n-dodecane (2) at 342.83 K using the NRTL model

Experimental		NRTL				
x_1	P/kPa	P_{cal}/kPa	ΔP/kPa	y_1 *cal*	γ_1	γ_2
0.0000	0.54	0.54	0.00	0.0000	2.333	1.000
0.0848	5.96	5.84	0.12	0.9141	2.208	1.003
0.1107	7.35	7.33	0.02	0.9331	2.169	1.004
0.1512	9.34	9.55	-0.21	0.9505	2.109	1.009
0.2000	11.85	12.03	-0.18	0.9625	2.035	1.016
0.2995	16.45	16.44	0.01	0.9751	1.884	1.043
0.3960	20.23	19.88	0.35	0.9812	1.735	1.090
0.5050	23.15	22.80	0.35	0.9853	1.569	1.185
0.5034	22.93	22.77	0.16	0.9851	1.571	1.184
0.6015	24.17	24.58	-0.41	0.9875	1.423	1.338
0.6996	25.22	25.71	-0.49	0.9890	1.283	1.629
0.7996	26.30	26.37	-0.07	0.9901	1.152	2.257
0.8481	26.82	26.62	0.20	0.9907	1.097	2.839
0.8985	27.36	26.93	0.43	0.9916	1.049	3.877
0.9487	27.98	27.43	0.55	0.9937	1.015	5.853
0.9832	28.15	27.97	0.18	0.9971	1.002	8.426
0.9981	28.14	28.27	-0.13	0.9996	1.000	10.112
1.0000	28.31	28.31	0.00	1.0000	1.000	10.368

Table 6-10: Regressed data for 2-Butanol (1) + n-dodecane (2) at 352.68 K using the NRTL model

Experimental		NRTL				
x_1	P/kPa	P_{cal}/kPa	ΔP/kPa	y_1 cal	γ_1	γ_2
0.0000	0.79	0.79	0.00	0.0000	14.397	1.000
0.2646	28.57	28.67	-0.10	0.9733	2.376	1.230
0.3546	31.11	30.90	0.21	0.9760	1.917	1.353
0.4548	33.53	33.39	0.14	0.9789	1.621	1.515
0.5516	35.45	35.65	-0.20	0.9815	1.431	1.719
0.6521	37.33	37.72	-0.39	0.9839	1.285	2.024
0.7517	39.31	39.43	-0.12	0.9862	1.169	2.537
0.8054	40.22	40.25	-0.03	0.9875	1.115	2.994
0.8530	41.42	40.97	0.45	0.9888	1.073	3.609
0.9054	42.41	41.83	0.58	0.9908	1.035	4.716
0.9471	43.37	42.69	0.68	0.9933	1.012	6.229
0.9804	43.92	43.56	0.36	0.9968	1.002	8.240
1.0000	44.19	44.19	0.00	1.0000	1.000	10.028

Table 6-11: Regressed data for Water (1) + o-Cresol (2) at 342.83 K using the NRTL model

Experimental		NRTL				
x_1	P/kPa	P_{cal}/kPa	ΔP/kPa	y_1 cal	γ_1	γ_2
0.0000	0.83	0.83	0.00	0.0000	5.940	1.000
0.0536	5.81	5.91	-0.10	0.8642	3.094	1.016
0.0724	7.11	6.69	0.42	0.8844	2.655	1.027
0.1080	7.38	7.84	-0.46	0.9001	2.123	1.050
0.1556	9.12	9.02	0.10	0.9152	1.725	1.083
0.2112	10.51	10.29	0.23	0.9279	1.469	1.122
0.3049	12.41	12.41	0.00	0.9443	1.250	1.186
0.4045	15.16	14.77	0.39	0.9577	1.138	1.248
0.5446	17.50	18.25	-0.75	0.9720	1.060	1.328
1.0000	30.65	30.65	0.00	1.0000	1.000	1.576

Table 6-12: Model parameters and deviations between experimental and calculated pressure for 1-Propanol (1) + n-Dodecane (2) at 342.83 K and 352.68 K.

Equation	342.83 K	352.68 K
NRTL		
$g_{12} - g_{11}$ (J/mol)	3469.875	2465.4235
$g_{12} - g_{22}$ (J/mol)	321.167	6479.570
a	-0.523	0.607
Average ΔP (kPa)	0.0561	0.0707
T-K Wilson		
$\lambda_{12} - \lambda_{11}$ (J/mol)	7456.826	6669.793
$\lambda_{12} - \lambda_{22}$ (J/mol)	-2474.59	-2510.434
Average ΔP (kPa)	0.0205	0.316
Van Laar		
A12	1.325	1.274
A21	2.395	2.098
Average ΔP (kPa)	0.0618	0.384

A close look at Table 6-12 reveals that at 342.83 K, the T-K Wilson equation provides the best fit for the 1-Propanol (1) + n-Dodecane system followed by the NRTL and lastly the Van Laar equation. At 352.68 K for the same system, the NRTL equation provides the best fit.

Table 6-13: Model parameters and deviations between experimental and calculated pressure for 2-Butanol (1) + n-Dodecane (2) at 342.83 K and 352.68 K.

Equation	342.83 K	352.68 K
NRTL		
$g_{12} - g_{11}$ (J/mol)	41.7929	1625.458
$g_{12} - g_{22}$ (J/mol)	6624.8151	1800.511
a	0.442	-2.013
Average ΔP (kPa)	0.0494	0.1317
T-K Wilson		
$\lambda_{12} - \lambda_{11}$ (J/mol)	10002.303	5393.665
$\lambda_{12} - \lambda_{22}$ (J/mol)	-3403.84	-911.506
Average ΔP (kPa)	0.0138	0.3349
Van Laar		
A12	0.845	1.340
A21	2.330	1.824
Average ΔP (kPa)	0.0507	0.4147

Table 6-14: Model parameters and deviations between experimental and calculated pressure for Water (1) + o-Cresol (2) at 342.83 K

Equation	342.83 K
NRTL	
$g_{12} - g_{11}$ (J/mol)	4814.6296
$g_{12} - g_{22}$ (J/mol)	290.1578
a	0.926
Average ΔP (kPa)	0.017
Van Laar	
A12	1.705
A21	0.414
Average ΔP (kPa)	0.014

For the Water (1) + o-Cresol (2) system, only the NRTL and the Van Laar equations fitted the data well. And the Van Laar equations gave the best fit.

Table 6-15: Best model for the new isotherms measured in this work

Systems	Temperature	Best Model
1-Propanol (1) + n-Dodecane(2)		
	342.83 K	T-K Wilson
	352.68 K	NRTL
2-Butanol (1) + n-Dodecane(2)		
	342.83 K	T-K Wilson
	352.68 K	NRTL
Water (1) + o-Cresol (2)	342.83 K	Van Laar

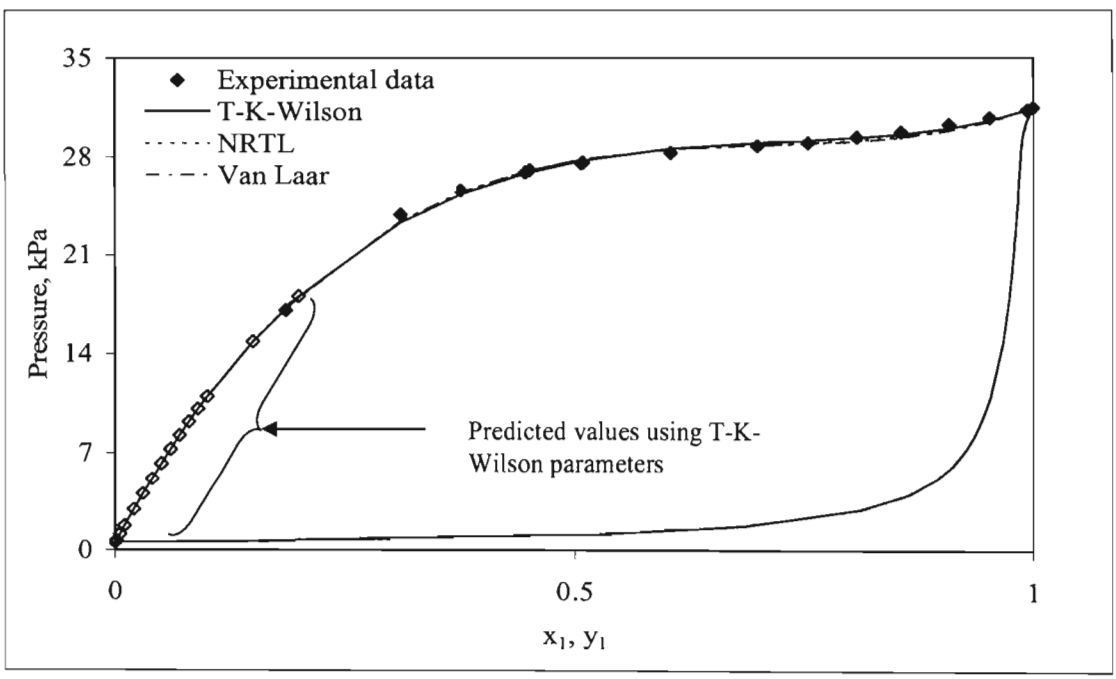

Figure 6-5: The P-x-y diagram for 1-Propanol (1) + n-Dodecane (2) system at 342.83 K

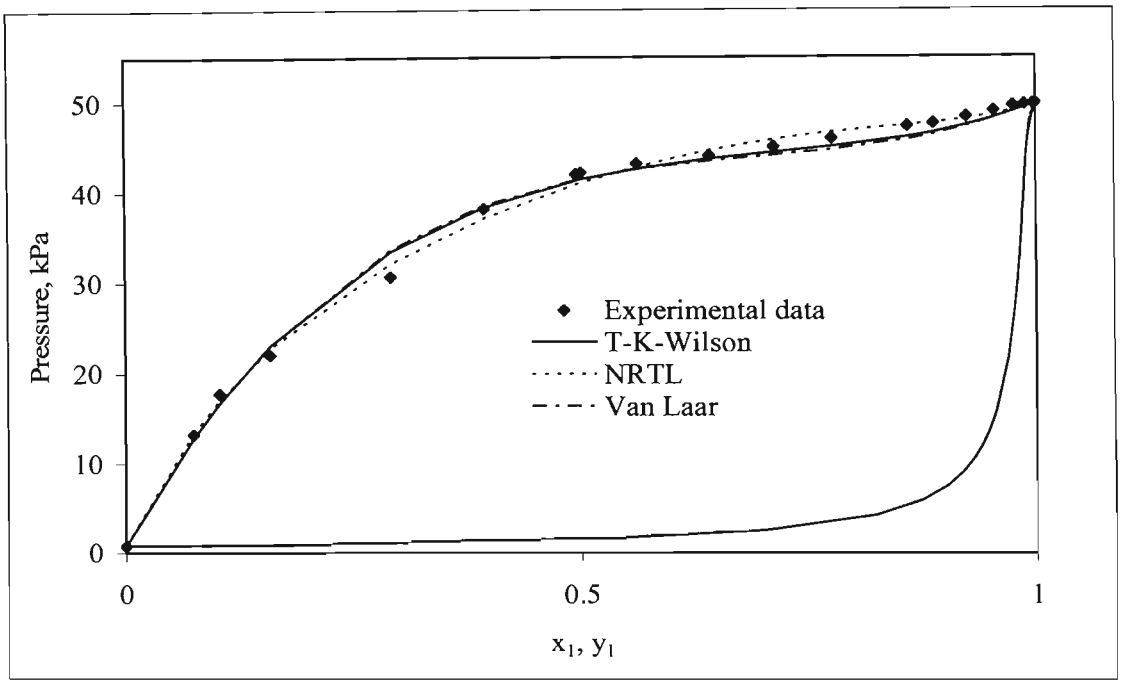

Figure 6-6: The P-x-y diagram for 1-Propanol (1) + n-Dodecane (2) system at 352.68 K

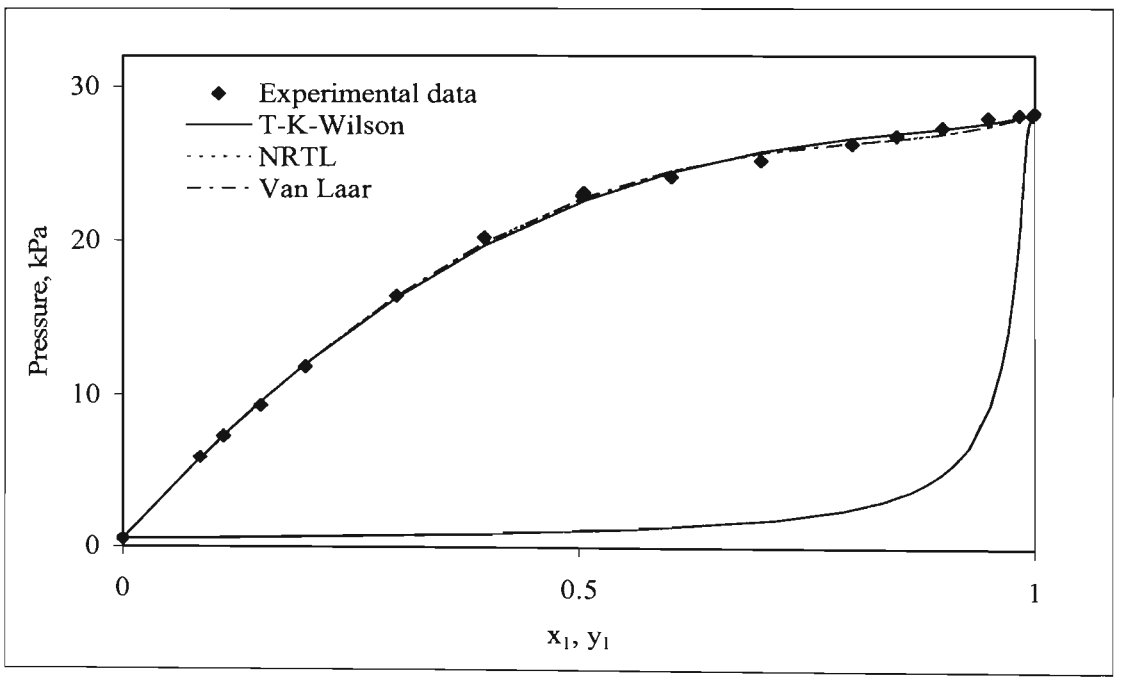

Figure 6-7: The P-x-y diagram for 2-Butanol (1) + n-Dodecane (2) system at 342.83 K

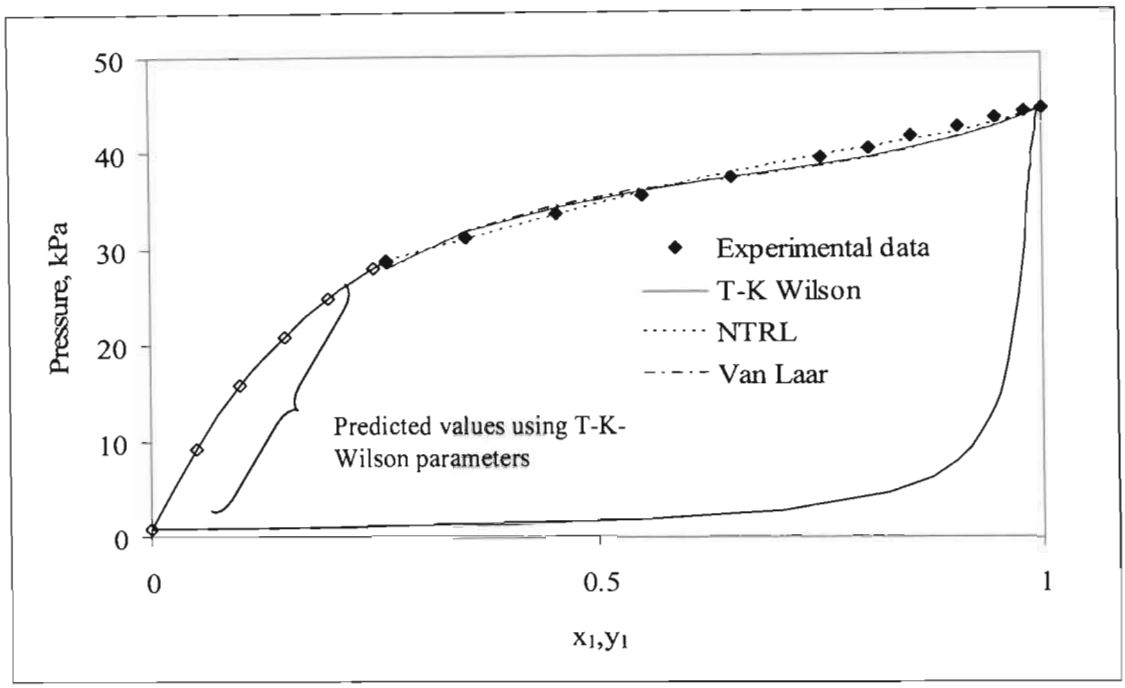

Figure 6-8: The P-x-y diagram for 2-Butanol (1) + n-Dodecane (2) system at 352.68 K

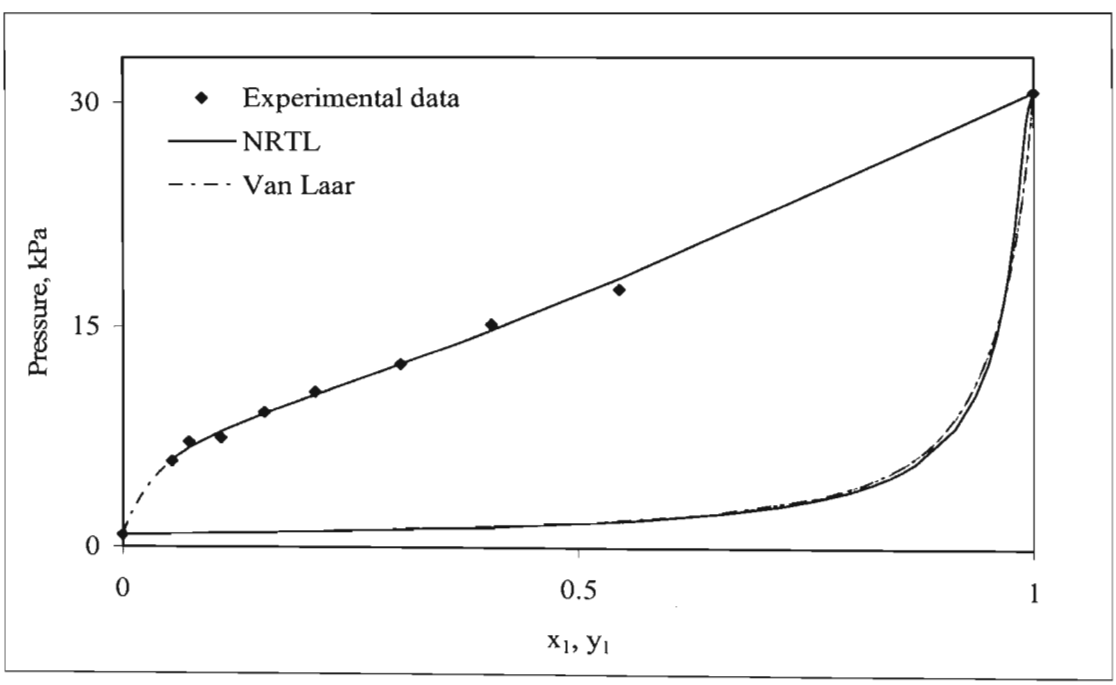

Figure 6-9: The P-x-y diagram for Water (1) + o-Cresol (2) system at 342.83 K

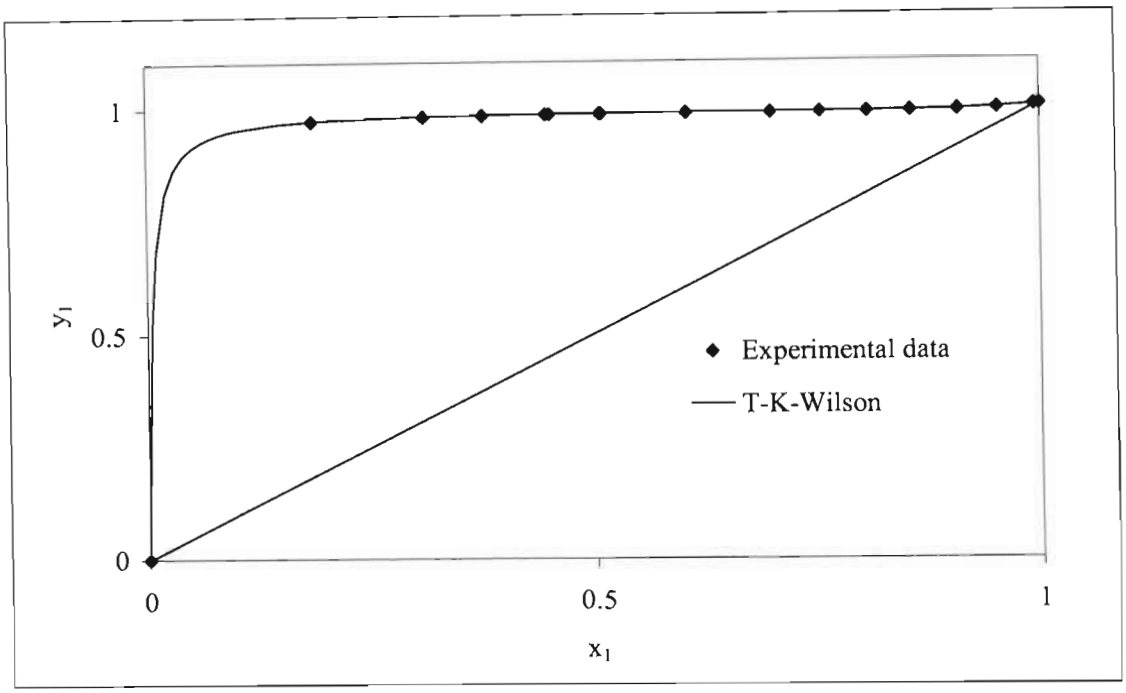

Figure 6-10: The x_1-y_1 diagram for 1-Propanol (1) + n-Dodecane at 342.83 K

The new systems measured in this work were very challenging systems. The difficulty was due to the large relative volatilities of the systems which was a result of the large boiling point differences between the binaries' constituents. VLE data in the n-Dodecane rich region and the o-Cresol rich region were very difficult to measure; It was observed during the measurements that the equilibrium pressure would not stabilize regardless of how long the system was left to attain equilibrium. The pressure fluctuations can then be explained in terms of flashing of the more volatile component (Water, 1-Propanol and 2-Butanol in this case). One way of getting around this problem would be to measure large amounts of data starting from the lower boiling chemicals (Water, 1-Propanol or 2-Butanol) and extrapolate the data to the n-Dodecane and o-Cresol rich regions. This approach was used for 2-Butanol (1) + n-Dodecane (2) system at 352.68 K.

The Water (1) + o-Cresol (2) system had an additional difficulty; o-Cresol is solid at room temperature and therefore had to be melted and kept at temperatures above 40 °C to avoid solidification. The piston-injector as well as the line leading to the equilibrium cell had to be kept at temperatures above the melting point of the o-Cresol. This was achieved by circulating water (45 °C) around the removable cylinder water-jacket and heating the line leading to the cell using nichrome wire. Very few data points were measured for this system due to the toxicity of o-Cresol and the lack of adequate safety features on the apparatus to work with such chemicals. Due to time

constraint, it was impossible to add additional safety features on the apparatus to work with toxic chemicals such as o-Cresol. Building a fume-hood above the apparatus set-up would help.
The two halves of the equilibrium curves, starting from different ends, matched seamlessly for all systems. None of the new systems measured in this work exhibited azeotropic behaviour as can be seen from Figures 6-5 to 6-9; as a result ordinary distillation can therefore be considered as a separation technique for these binary pairs.

6.5 Infinite Dilution Activity Coefficients

The evaluation of infinite dilution activity coefficients is discussed in detail in Appendix A. Infinite dilution activity coefficients (γ_i^∞) were determined for the following systems: Water (1) + 1-Propanol (2) at 313.17 K, Water (1) + 2-Butanol (2) at 323.18 K and n-Hexane (1) + 2-Butanol (2) at 329.22 K. As discussed by Fischer and Gmheling [1996], derivation of γ^∞ values from P-x data are more difficult for high boiling substances (such as n-Dodecane) in low boiling components than otherwise. Due to the scarcity of data points in the dilute n-Dodecane rich region, even γ_1^∞ could not be calculated for new unmeasured systems. Determination of the limiting values, $\left(P_D/x_i x_j\right)^\infty$, according to the method of Maher and Smith [1979] is demonstrated for the Water (1) + Propanol (2) system at 313.17 K. Figures 6-11 and 6-12 show the plot of $\left(P_D/x_1x_2\right)$ vs x_1 as $x_1 \to 0$ and $\left(x_1x_2/P_D\right)$ vs x_1 as $x_1 \to 1$ respectively and the plots for the other systems can be found in Appendix A. The excellent linearity in the dilute regions for all the systems may be noted.

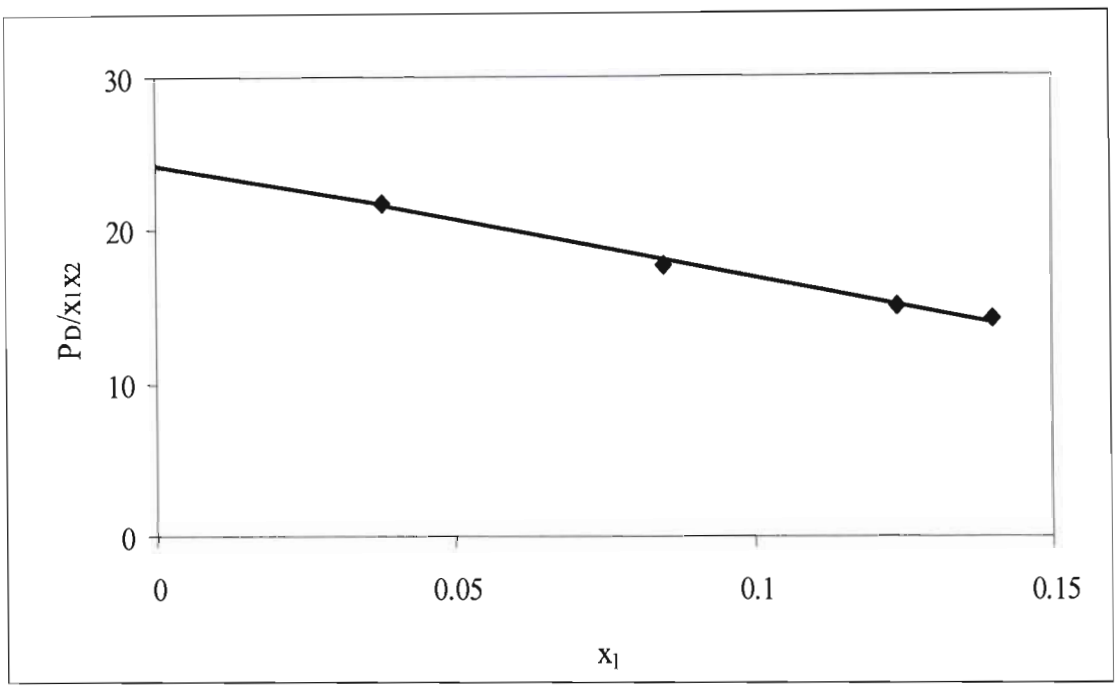

Figure 6-11: Plot of (P_D/x_1x_2) vs x_1 as $x_1 \to 0$ for Water (1) + 1-Propanol (2) at 313.17 K

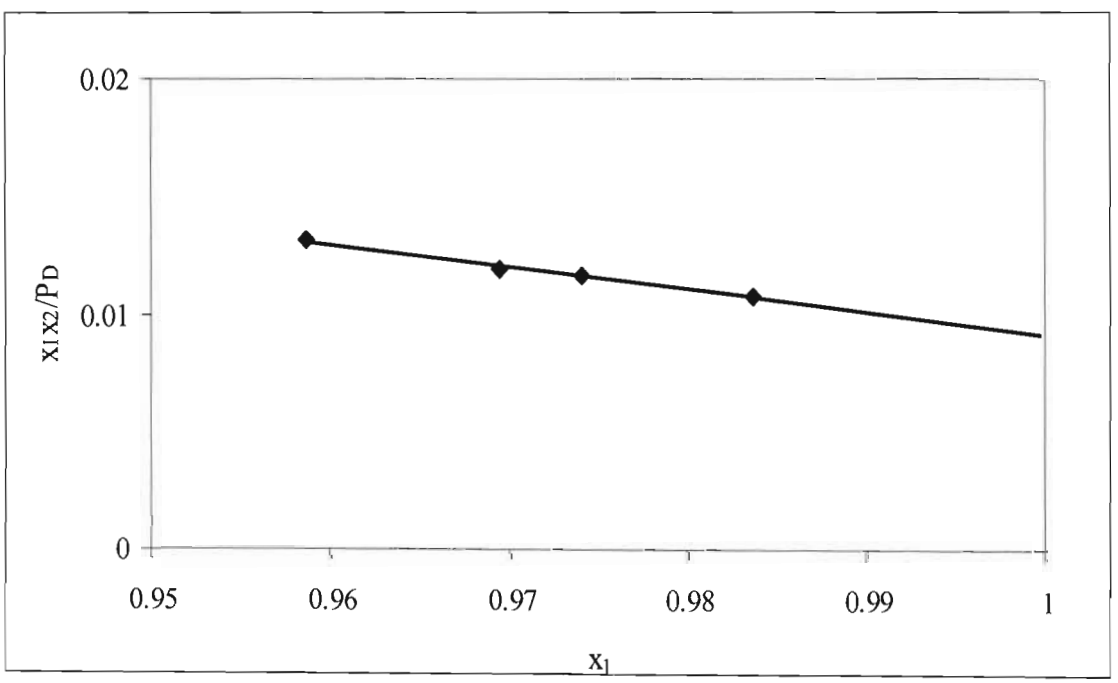

Figure 6-12: Plot of (x_1x_2/P_D) vs x_1 as $x_1 \to 1$ for Water (1) + 1-Propanol (2) at 313.17 K

Table 6-16 shows the limiting values obtained from the plots in Figures 6-11, 6-12 and A-1 to A-4 while Table 6-17 compares the infinite dilution activity coefficient values obtained by extrapolation

of the experimental γ_i with values calculated by the method of Maher and Smith [1979]. Note that γ_i^{∞} values were calculated for the model that gave the best fit for each system.

Table 6-16: Limiting values obtained from the plots of (P_D/x_1x_2) vs x_1 as $x_1 \to 0$ and (x_1x_2/P_D) vs x_1 as $x_1 \to 1$

System	T (K)	P_D/x_1x_2		x_1x_2/P_D	
		$x_1=0$	$x_1=1$	$x_1=0$	$x_1=1$
Water (1) + 1-Propanol (2)	313.17	24.38	-	-	0.0091
Water (1) + 2-Butanol (2)	323.18	34.60	-	-	0.0016
n-Hexane (1) + 2-Butanol (2)	329.22	271.42	-	-	0.0055

Table 6-17: Activity coefficients at infinite dilution (γ_i^{∞} values)

		Activity coefficients at infinite dilution					
		a		b		c	
System	T (K)	γ_1^{∞}	γ_2^{∞}	γ_1^{∞}	γ_2^{∞}	γ_1^{∞}	γ_2^{∞}
Water (1) + 1-Propanol (2)	313.17	3.83	18.42	4.30	16.80	-	-
Water (1) + 2-Butanol (2)	323.18	3.75	39.09	3.82	59.27	[d]4.71	[d]39.30
n-Hexane (1) + 2-Butanol (2)	329.22	4.66	13.13	5.25	19.27	[e]4.41	[e]10.54

a : Extrapolated γ_i^{∞} from experimental γ_i;

b : Calculated γ_i^{∞} by the method of Maher and Smith [1979];

c : Reference values;

[d] : Values obtained by Fischer and Gmehling [1994],

[e] : Values obtained by extrapolation by Uussi-Kyyny et al. [2002].

A close look at Table 6-17 reveals that the γ_i^{∞} values obtained by extrapolation of experimental γ_i is significantly different from that obtained by the Maher and Smith [1979] method especially as far as γ_2^{∞} is concerned. It is also important to keep in mind that γ_i^{∞} is dependent upon the equation of state used (Maher and Smith [1979]). Figures 6-13 to 6-15 are the plots of $\ln \gamma_i$ vs x_1.

The discrepancies between the measured γ_i^{∞} and literature values are not unexpected. For highly non-ideal systems with very large γ_i^{∞} (as in this study), literature values frequently show considerable discrepancies and specialized measurement techniques such as differential ebulliometry or inert gas stripping are usually preferred. The values from the Maher and Smith procedure in Table 6-17 should be more reliable than those from the less attractive activity coefficient extrapolation, particularly in view of the excellent linearity of the plots such as in Figures 6-11 and 6-12.

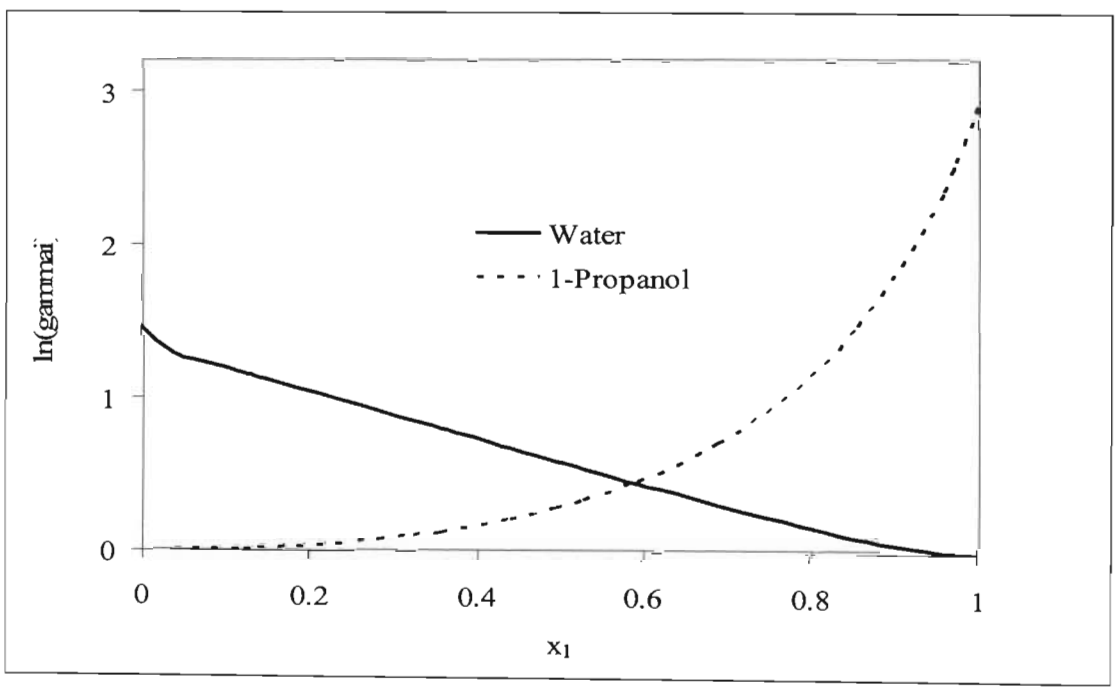

Figure 6-13: Plot of $\ln \gamma_i$ vs x_1 for Water (1) + 1-Propanol (2) at 313.17 K

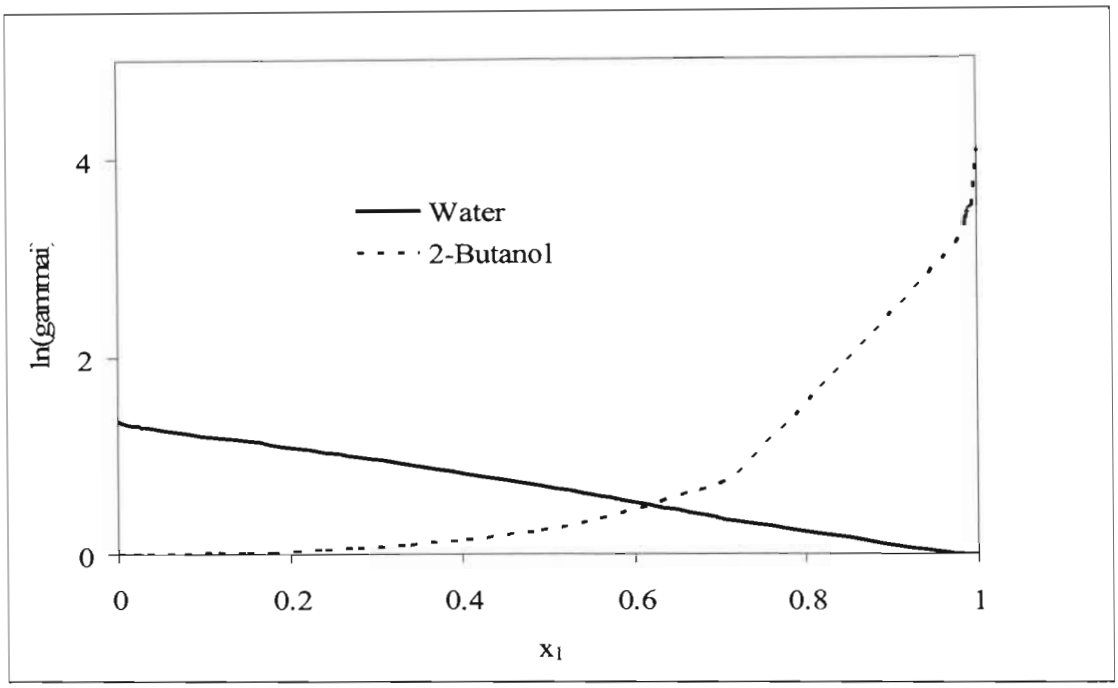

Figure 6-14: Plot of $\ln \gamma_i$ vs x_1 for Water (1) + 2-Butanol (2) at 323.18 K

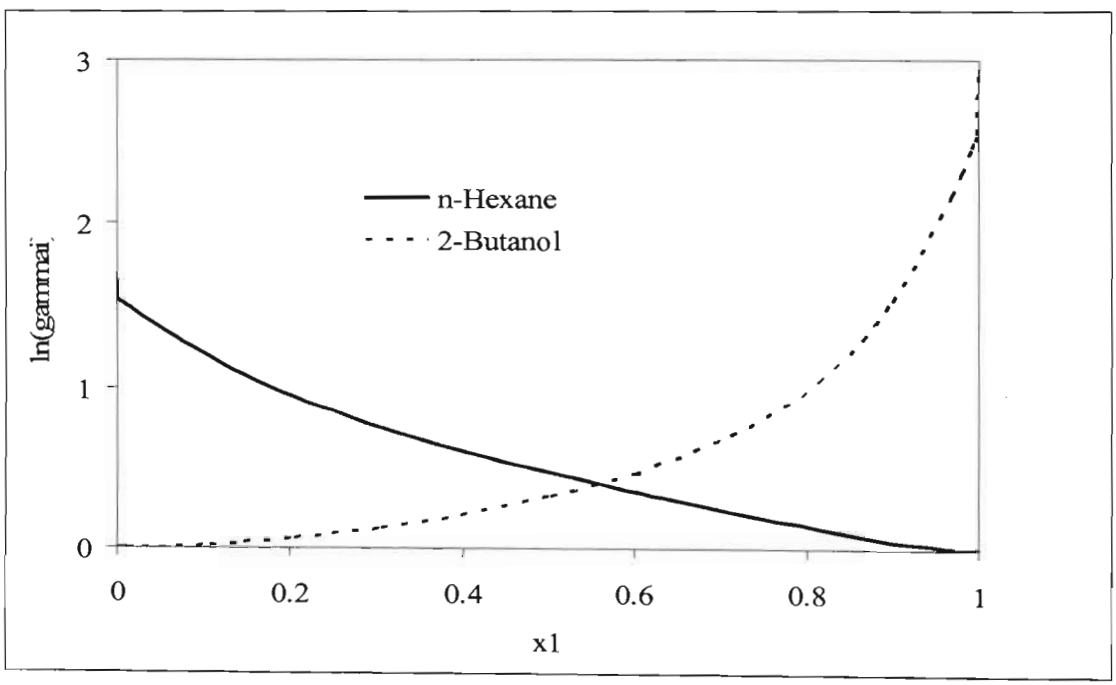

Figure 6-15: Plot of $\ln \gamma_i$ vs x_1 for n-Hexane (1) + 2-Butanol (2) at 329.22 K

CHAPTER SEVEN

CONCLUSIONS AND RECOMMENDATIONS

7.1 Conclusions

The main objective of this project was to develop a new static synthetic apparatus with operating capabilities of ± 15 bar pressure and ± 150 °C temperature. An intensive literature survey of the experimental methods that have been used previously for measuring VLE provided the basis for the current design. The static synthetic apparatus was chosen for its relative simplicity and it was built in the workshop of the School of Chemical Engineering, University of Kwa-Zulu Natal. The apparatus developed in this work operates according to the principles of the apparatus of Gibbs and Van Ness [1972] and incorporates novel dual-action [Raal 1999] precision injector pistons, with the micro- or macro-mode selectable by solenoid operation. The dual mode permits accurate injection of very small volumes when used in the micro-mode for increased accuracy in the difficult very dilute regions. A full description of the static apparatus is presented in Chapter 3. Prior to making the measurements, the measuring devices (temperature probes in this case Pt-100s, piston-injectors) were calibrated. The Wika D-10-P, 0-1 bar absolute pressure transmitter was not calibrated since the pressure standard was used for measuring pressures. The estimated uncertainties on the temperature and the pressure were ± 0.2 °C and ± 0.01 kPa respectively and the estimated uncertainty of the injected volumes was ± 0.002 cm^3.

VLE data on three test systems namely, Water (1) + 1-Propanol (2) at 313,17 K, Water (1) + 2-Butanol (2) at 323.18 K and n-Hexane (1) + 2-Butanol (2) at 329.22 K, were measured to test the

performance of the apparatus and to validate the experimental procedure. The data obtained were compared with literature data and excellent agreement was found. A high degree of confidence was therefore placed in the performance of the static apparatus and the operating procedure and the VLE data for unknown systems were then measured.

New previously unmeasured vapour-liquid equilibrium data were measured for the following binary systems:

- 1-Propanol (1) + n-Dodecane at 342.83K and 352.68 K
- 2-Butanol (1) + n-Dodecane at 342.83 K and 352.68 K
- Water (1) + o-Cresol at 342.83 K

The VLE measurements for these binary systems were very challenging. The difficulties arose from the exceptionally large boiling point differences between the systems' constituents.

The combined method ($\gamma - \phi$ approach) was used for the reduction of experimental data. The experimental isothermal P-z_i data were reduced using Barker's method. The Barker's method was implemented to convert the moles of each component injected into the cell to mole fraction of the vapour and liquid phase (Uusi-Kyyny et al.[2002]). Although the pressures measured were below atmospheric pressure, the vapour phase non-ideality was taken into account and allowance was made for the effect of vapour volume in the computation of true liquid equilibrium compositions from the injected liquid volumes. The second virial coefficients were estimated using the Pitzer-Curl [1957] correlation. Three activity coefficient models were used to account for the non-idealities in the liquid phase namely, NRTL (Renon and Prausnitz [1968]), T-K Wilson (Tsuboka and Katayama [1975]) and Van Laar (Van Laar [1910]). The fit of these models to the experimental data gave low deviation between the calculated and the experimental pressure. The T-K Wilson and the NRTL activity coefficients equations gave the overall best fit for the systems studied. The temperature-dependent modeling parameters in Tables 6-5, 6-12, 6-13 and 6-14 permit VLE data interpolation and limited extrapolation to temperatures outside the measured ranges. Infinite dilution activity coefficients were calculated using the method proposed by Maher and Smith [1979] for the three test systems and the values obtained are presented in Table 6-16.

7.2 Recommendations

1. Construct a fume hood above the apparatus to extract fumes from toxic chemicals.
2. The equilibrium temperature should be measured inside the equilibrium cell since very accurate temperature measurements are desirable for good quality VLE data.
3. Generate replicate measurements of temperature, pressure and composition to provide statistical estimates of the variances of these measurements and hence give a more conclusive evaluation of the performance of the equipment.
4. P-x_i data should be measured in the very dilute region for the binary systems with n-Dodecane as one of the constituents, so that activity coefficients at infinite dilution could be easily calculated using the Maher and Smith [1979] method.
5. Data reduction using the equation of state approach could be investigated.

REFERENCES

Abbott. M M (1986), "Low Pressure Phase Equilibria: Measurement of VLE", *Fluid Phase Equilibria*, Vol 29, p 193 -207.

Abrams, D S, and Prausnitz, J M, (1975), "Statistical Thermodynamics of Liquid Mixtures: A New Expression for the Excess Gibbs Energy of Partly or Completely Miscible Systems", *American Institute of Chemical Engineers Journal*, Vol. 21 pp 116 -128.

Aim, K, (1978), "Measurement of vapor-liquid equilibrium in systems with components of very different volatility by total pressure static method", *Fluid Phase Equilibria*, Vol 2, p 119 -142.

Barker, J A, (1953), "Determination of Activity Coefficients from Total Pressure Measurements", *Australian Journal Chemistry*, Vol. 6 pp 207 – 210.

Beattie, J A, (1949), Chem. Rev., Vol. 44, pp 141 as in Prausnitz et al. (1967).

Bell, T N, Cussler, E L, Harris, K R, Pepela, C N, Dunlop, P J, (1968), "An apparatus for degassing liquids by vacuum sublimation", *J. Phys. Chem.* Vol. 72, pp 4693-4695.

Christiansen, L J, and Fredenslund, A, (1975), "Thermodynamic Consistency Using Orthogonal Collocation or Computation of Equilibrium Vapour Compositions at High Pressures", *American Institute of Chemical Engineers Journal*, Vol. 21pp 49-57.

Chueh, P H, Muirbrook, N K and Prausnitz, J M, (1965), *AIChE J.* Vol.11 pp 1097 as in Raal and Mühlbauer (1998).

Dortmund Data Bank Software purchased 1998.

Figuiere, P, Hom, J, Laugier, S, Renon, H, Richon, D and Szwarc, H, 1980, "Vapour-Liquid Equilibria up to 40 000 kPa and 400oC: A New Static Method", *AIChE J.* Vol. 26, pp 872-875

Fischer, K and Gmehling, J (1994), "P-x and γ^{∞} Data for the Different Binary Butanol-Water Systems at 50 °C." *Journal of Chemical Engineering Data*, Vol. 39, pp. 309-315.

Fischer, K and Gmehling, J (1996), "Vapour-liquid equilibria, activity coefficients at infinite dilution and heats of mixing for mixtures of N-methyl pyrrolidone-2 with C5 or C6 hydrocarbons and for hydrocarbon mixtures", *Fluid Phase Equilibria*, vol. 119, pp. 113-130.

Gaube, (1988), *Private communication between Gaube and Rarey*, as reported by Harris (2003).

Gess, M A, Danner, R P and Nagvekar, M, (1991), "Thermodynamics Analysis of Vapour Liquid Equilibria: recommended Models and a Standard Data Base", Design Institute for Physical Property Data, American Institute of Chemical Engineers.

Gibbs, R E & Van Ness, H C (1972), "Vapour – Liquid Equilibria from Total Pressure Measurements. A New Apparatus", *Industrial and Engineering Chemistry-Fundamentals*, Vol 11, p 410 – 413.

Guillevic, J, Richon, D and Renon, H, (1983), "Vapour-liquid equilibrium measurements up to 558 K and 7 MPa: a new apparatus", *Ind. Eng. Chem. Fundam.*, Vol. 22, pp 495-499.

Hala, E, Pick, J. Fried, V & Vilim.O (1958) "Vapour-Liquid Equilibrium", 1st Edition, Pergamon Press , Oxford.

Hala, E, Pick, J. Fried, V & Vilim.O (1967) "Vapour-Liquid Equilibrium", 2nd Edition, Pergamon Press , Oxford.

Harris, R A, (2004), "Robust Equipment for the Measurement of Vapour-Liquid Equilibrium at High Temperatures and High Pressures", Ph.D Thesis, University of Kwa-Zulu Natal.

Hartwick, R P and Howat, C S, (1995), "Infinite Dilution Activity Coefficients of Acetone in Water. A New Experimental Method and Verification", *J. Chem. Eng. Data*, Vol. 40, pp 738-745.

Hayden, J G, and O'Connell, J P, (1975), "A Generalised Method for Predicting Second Virial Coefficients", *Industrial and Engineering Chemistry. Process Design and Development*, Vol. 14,

pp. 209 – 216.

Inoue, M, Azumi, K & Suzuki, N (1975), "A new Vapour Pressure Assembly for Static vapour Liquid Equilibrium", *Industrial and Engineering Chemistry Fundamentals*, Vol 14, pp. 312 – 314.

Joseph, M A, (2001), Master of Science in Engineering (Chemical Engineering) Thesis. University of Natal Durban campus.

Joseph, M A, Raal, J D & Ramjugernath, D , (2001), " Phase Equilibrium Properties of Binary Systems with Diacetyl from a computer controlled Vapour – Liquid Equilibrium still", *Fluid Phase Equilibria*, Vol 182, p 157 – 176.

Karla, H, Kubota, H, Robinson, D and Ng, H, (1978), "Equilibrium phase properties of the carbon dioxide-n-heptane system", *Journal of Chemical Engineering Data*, Vol. 23, pp. 317-321.

Kolbe, B and and Gmehling , J, (1985), "Thermodynamic Properties of Ethanol + Water. I. Vapour-Liquid Equilibria Measurements from 90 to 150 °C by the Static Method." *Fluid Phase Equilibria*, Vol. 23, pp.213-226.

Ljunglin, J J, and Van Ness, H C, (1962), "Calculation of Vapour Liquid Equilibria from Vapour Pressure Data", *Chemical Engineering Science* Vol.17, pp. 531 – 539.

Loehe, J, Van Ness, H C & Abbott, M M, (1983), "vapour- Liquid – Liquid Equilibrium. Total – Pressure data and GE for water – Methyl Acetate at 50°C", *Journal of Chemical and Engineering Data*, Vol 28, pp 405 – 407.

Lorenzo, L M, Montero, E A, Martin, M C and Villamanan, M A, (1997), "Isothermal vapor-liquid equilibria for binary mixtures containing methyl *tert*-butyl ether (MTBE) and /or substitution hydrocarbons" *Fluid Phase Equilibria*, Vol. 133, pp.155-162.

Maher, P J and Smith, B D, (1979), "A New Total Pressure Vapour-Liquid Equilibrium Apparatus. The Ethanol + Aniline system at 313.15 K, 350.81 K, and 386.67 K", *Journal of Chemical and Engineering Data,* Vol. 24, pp. 16-22.

Maher, P J and Smith, B D, (1979), "Infinite Dilution Activity Coefficient from Total Pressure VLE data. Effect of equation of state used", *Industrial and Engineering Chemistry Fundamentals*, Vol. 18, pp 354-357.

Malanowski, S, (1982a), "Experimental Methods for vapour Liquid Equilibria. Part I. Circulation Methods", *Fluid Phase Equilibria*, Vol 8, p197 -219.

Malanowski, S, (1982b), "Experimental Methods for Vapour Liquid Equilibria. Part II, Dew and Bubble Point Method", *Fluid Phase Equilibria*, Vol, 9, pp 311-317.

Malanowski, S and Anderko, A, (1992) "Modelling Phase Equilibrium: Thermodynamic Background and Practical Tools, John Wiley and Sons, Inc, New York, USA.

Marquadt, D W, (1963), "An Algorithm for Least-Squares Estimation of Non-Linear Parameters", *Journal Society of Industrial and Applied Mathematics*, Vol. 11, pp 431-441.

Mentzer, R A, Greenkorn, R A, Chao, K C, (1982), "Bubble pressures and vapor-liquid equilibrist for four binary hydrocarbon mixtures" *J. Chem. Thermodynamics*, Vol. 14, pp 817-830.

Mühlbauer, A L and Raal, J D, (1991), " Measurement and thermodynamic interpretation of high-pressure vapour-liquid equilibria in the toluene---CO2 system", *Fluid Phase Equilibria*, Vol. 64, pp 213-236.

Ng, H and Robinson, D, (1978), "Equilibrium-phase properties of the toluene-carbon dioxide system", J. Chem. Eng. Data", Vol. 23, pp 325-327.

Perry, R H and Green, D W, (1997), "Perry's Chemical Engineers' Handbook", McGraw-Hill Book Company, Singapore.

Pitzer, K S, and Curl, R F, (1957), "Empirical Equation for the Second Virial Coefficients", *Journal of the American Chemical Society*, Vol. 79, pp 2369 – 2370.

Prausnitz, J M, Anderson, T F, Grens, E A, Eckert, CA, O'Connell, J P (1967) "Computer Calculations for Multicomponent Vapour Liquid Equilibria" Prentice- Hall, Englewood Cliffs, N.J.

Prausnitz, J M, Anderson, T F, Grens, E A, Eckert, CA, O'Connell, J P (1980) "Computer Calculations for Multicomponent Vapour Liquid Equilibria" Prentice- Hall, Englewood Cliffs, N.J.

Prausnitz, J M, Lichtenthaler, R N and De Azevedo, E G (1986) "Molecular Thermodynamics of Fluid Phase Equilibria", 2nd Edition, Prentice Hall, Englewood Cliffs, New Jersey.

Raal, J D, Jeffery, G and Tonkin, T, (1980), *Chemical Engineering Research Group Report CENG 331,* CSIR, Pretoria, South Africa.

Raal, J D and Mühlbauer, A L, (1994), *Dev. Chem. Eng. Mineral Proc.* Vol. 2, pp 69-88.

Raal, J D and Mühlbauer, A L, (1998), "Phase Equilibria: Measurement and Computation", Taylor and Francis, Bristol PA

Raal, J D and Ramjugernath, D, (2005), "Measurement of the Thermodynamic Properties of Multiple Phases", Chapter 5, *Vapour –Liquid Equilibrium at Low Pressures*, Elsevier, pp 71-86.

Raal, J D, (1999) US patent 09/041/747.

Rackett, H G, (1970), "Equation of state for saturated Liquids", *Journal of Chemical and Engineering Data*, Vol. 15 pp 514-517.

Rarey, J R, (1991), *Ph.D. Thesis*, University of Dortmund, Federal Republic of Germany as in Harris 2003.

Rarey, J R and Gmehling, J, (1993), "Computer-Operated Differential Static Apparatus for the Measurement of Vapour-Liquid Equilibrium Data", Fluid Phase Equilibrium, Vol. 83, pp. 279-287.

Reid, C R, Prausnitz, J M, and Polling, B E, (1988), "The Properties of Gases and Liquids", 4th Edition, McGraw Hill Book Company, Singapore

Renon, H and Prausnitz, J M, (1968), "Local Composition in Thermodynamic Excess Functions for Liquids Mixtures", *AIChE J.* Vol 14, pp 135-142.

Rigas, T, Mason, D and Thodos, D, (1958), "Vapour-Liquid Equilibria. Microsampling Technique Applied to a New Variable-Volume Cell", *Ind. Eng. Chem.*, Vol 50, pp 1297-1300.

Robinson, C S and Gilliland, E R,(1950), "Element of Fractional Distillation", 4th edition, McGraw-Hill, New York.

Ronc, M and Ratcliff, G R, (1976), " Measurement of vapor-liquid equilibria using a semi-continuous total pressure static equilibrium cell", Can. J. Chem. Eng., Vol. 54 pp 326-332.

Sandler, S I, Orbey, H, and Lee, B, (1994), "Models for Thermodynamic and Phase Equilibria Calculations. Marcel Dekker, New York.

Scatchard, G (1949), "Equilibrium in Non-Electrolyte Mixtures", *Chemical Reviews*, Vol. 44, pp 7–35.

Seader, J D and Henley, E J, (1998),"Separation Process Principles", John Wiley & Sons, Inc.

Smith J M and Van Ness, H C, (1987), "Introduction to Chemical Engineering Thermodynamics" 4th Edition, McGraw-Hill, Singapore

Smith J M, Van Ness, H C and Abbott, M M, (1996), "Introduction to Chemical Engineering Thermodynamics" 5th Edition, McGraw-Hill International Editions, New York.

Tamir, A, Apelblat, A and Wagner, M, (1981), *Fluid Phase Equilibria*, Vol. 6 pp 237 as in Kolbe and Gmehling (1985).

Tomlins, R P and Marsh, K N, (1976), " A new apparatus for measuring the vapour pressure of liquid mixtures Excess Gibbs free energy of octamethylcyclotetrasiloxane + cyclohexane at 308.15 K", *J. Chem. Thermodynamics*, Vol. 8 pp 1185-1194.

Tsonopoulos, C (1974), "An Empirical Correlation of the Second Virial Coefficients", *American Institute of Chemical Engineers Journal*, Vol. 20, pp 263 – 272.

Tsuboka, T and Katayama, T, (1975), "Modified Wilson Equation for Vapour Liquid and Liquid

Liquid Equilibria", *Journal of Chemical Engineering of Japan*, Vol.8 No. 5, pp 181 -187.

Uusy-Kyyny, P, Pokki, J-P, Laakkonen, M, Aittamaa, J and Liukkonen, S, (2003), "Vapor liquid equilibrium for the binary systems 2-methylpentane + 2-butanol at 329.2 K and n-hexane + 2-butanol at 329.2 and 363.2 K with a static apparatus", *Fluid Phase Equilibrium*, Vol. 201, issue 2, pp 343-358.

Van laar, J J , (1910), " The Vapour Pressure of binary mixtures", *Zeitschrift feur Physik Chemie*, Vol 72. pp 723 -751.

Van Ness, H C, Soczek, C A and Kochar, N K, (1967a), " Thermodymanic excess properties for ethanol-n-heptane", *Journal of Chemical Engineering Data*, Vol. 12, pp 346-351.

Van Ness, H C, Soczek, C A, Peloquin, G L and Machado, R L, (1967b), " Thermodymanic excess properties of three alcohol-hydrocarbon systems", *Journal of Chemical Engineering Data*, Vol. 12, pp 346-351.

Van Ness, H. C.; Byer, S. M.; Gibbs, R. E.; (1973); Vapor-Liquid Equilibrium: Part I An Appraisal of Data Reduction Methods, *American Institute of Chemical Engineers Journal.* Vol 19, pp 238-244.

Van Ness, H C and Abbott, M M, (1975), "Vapour Liquid Equilibrium: Part III- Data Reduction with Precise Expressions for GE", *American Institute of Chemical Engineers Journal*, Vol 21, No.1 pp 62 – 71

Van Ness, H C and Abbott, M M, (1978), " A Procedure for Rapid Degassing of Liquids", Ind. Eng. Chem. Fundamentals, Vol. 17, no. 1, pp 66-67.

Van Ness, H C, and Abbott, MM, (1982), "Classical Thermodynamics of Non-Electrolyte Solutions: With Applications to Phase Equilibria", McGraw Hill, New York.

Van Ness, H C (1995), "Thermodynamics in the Treatment of Vapour Liquid Equilibrium Data" *Journal of Pure and Applied Chemistry*, Vol. 67. No 6 pp 859 – 872.

Walas, S M (1985), " Phase Equilibrium in Chemical Engineering" Butterworth, Boston Weast, R C (Editor) "Handbook of Chemistry and Physics, 64th Edition, (1983 -1984) CRC Press, London.

Wichterle, I, (1987a), "High-Pressure Vapour-Liquid Equilibrium IV: Quantitative Description. Part 2" *Fluid Phase Equilibrium*, Vol. 2, pp. 59-78.

Wichterle, I, (1987b), "High-Pressure Vapour-Liquid Equilibrium V: Quantitative Description. Part 3" *Fluid Phase Equilibrium*, Vol. 2, pp. 143-159.

Wilson, G M, (1964), "Vapour Liquid Equilibrium, A New Expression for the Excess Free Energy of Mixing", *Journal of American Chemical Society*, Vol. 86, pp 127 – 130.

Won, K W and Prausnitz, J M, (1973), *Ind. Eng. Chem. Fundam.* Vol. 12, pp 238 as in Raal and Mühlbauer (1998).

Zielkiewicz, J and Konitz, A, (1991) *J. Chem. Thermodyn.*,Vol. 23 pp 59 as reported in the DDB (1998).

Zimmerman, A and Keller, J, (1989), "VLE in the system water-ammonia-lithium bromide", *Fluid Phase Equilibria*, Vol. 53, pp 229-234.

APPENDIX A

A.1 Evaluation of Infinite Dilution Activity Coefficient

Infinite Dilution Activity coefficients can be obtained by extrapolating experimental data obtained in the dilute region. This technique has been ruled incorrect and inaccurate by many authors. Hartwick and Howard [1995] show that extrapolation of binary activity coefficient curves to the end points seldom gives accurate values for γ_i^{∞}. The method described below for evaluating the infinite dilution activity coefficient is the well-accepted Maher and Smith [1979] method.

$$\gamma_i^{\infty} = \varepsilon_i^{\infty} \frac{P_j^{sat}}{P_i^{sat}} \left[1 + \beta_j \frac{1}{P_j^{sat}} \left(\frac{\partial P}{\partial x_1} \right)_{x_1=0}^{\infty} \right]_T^{x_i \to 0} \tag{A-1}$$

where

$$\varepsilon_i^{\infty} = \exp\left[\frac{\left(B_{ii} - V_i^L\right)\left(P_j^{sat} - P_i^{sat}\right) + \delta_{ij} P_j^{sat}}{RT} \right] \tag{A-2}$$

$$\beta_j = 1 + P_j^{sat} \left[\frac{B_{jj} - V_j^L}{RT} \right] \tag{A-3}$$

Where $\delta_{ij} = 2B_{ij} - B_{ii} - B_{jj}$

The parameters B_{ii} and B_{jj} are the second virial coefficients of the pure components. B_{ij} is the mixture virial coefficient, it accounts for the i-j interaction. The virial coefficients can be obtained from such correlation as the Pitzer and Curl.

$$P_D = P - \left[P_2^{sat} + \left(P_1^{sat} - P_2^{sat} \right) x_1 \right] \tag{A-4}$$

$$\left(\frac{P_D}{x_1 x_2} \right)_{x_1=0} = \left(\frac{\partial P}{\partial x_1} \right)_{x_1=0} - P_1^{sat} + P_2^{sat} \tag{A-5}$$

The term on the left hand side of Equation (A-5) is determined by the extrapolation of a plot of P_D/x_1x_2 vs x_1 to $x_1 = 0$.If the curve is not linear, Maher and Smith [1979] suggest a plot of x_1x_2/P_D against x_1. Thus the partial derivative and hence γ_1^{∞} can be determined. A similar procedure is used to determine γ_2^{∞}. P_D is the deviation pressure, which refers to the degree to which a system deviates from ideality defined in Equation (A-4).

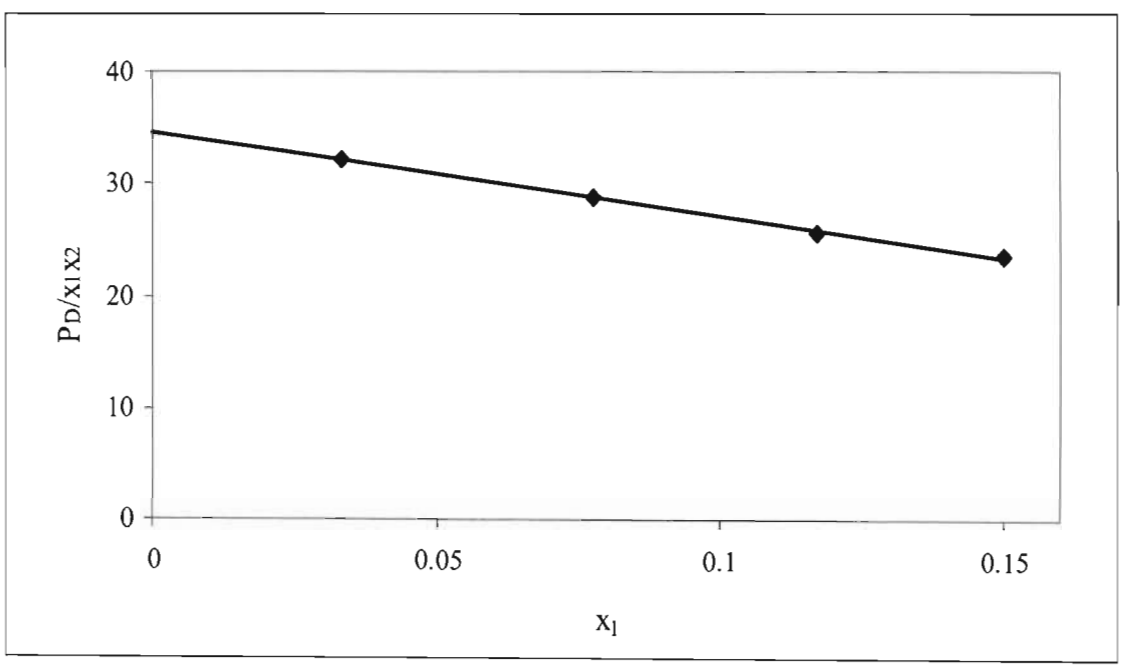

Figure A-1: Plot of $\left(P_D/x_1x_2\right)$ vs x_1 as $x_1 \to 0$ for Water (1) + 2-Butanol (2) at 323.18 K

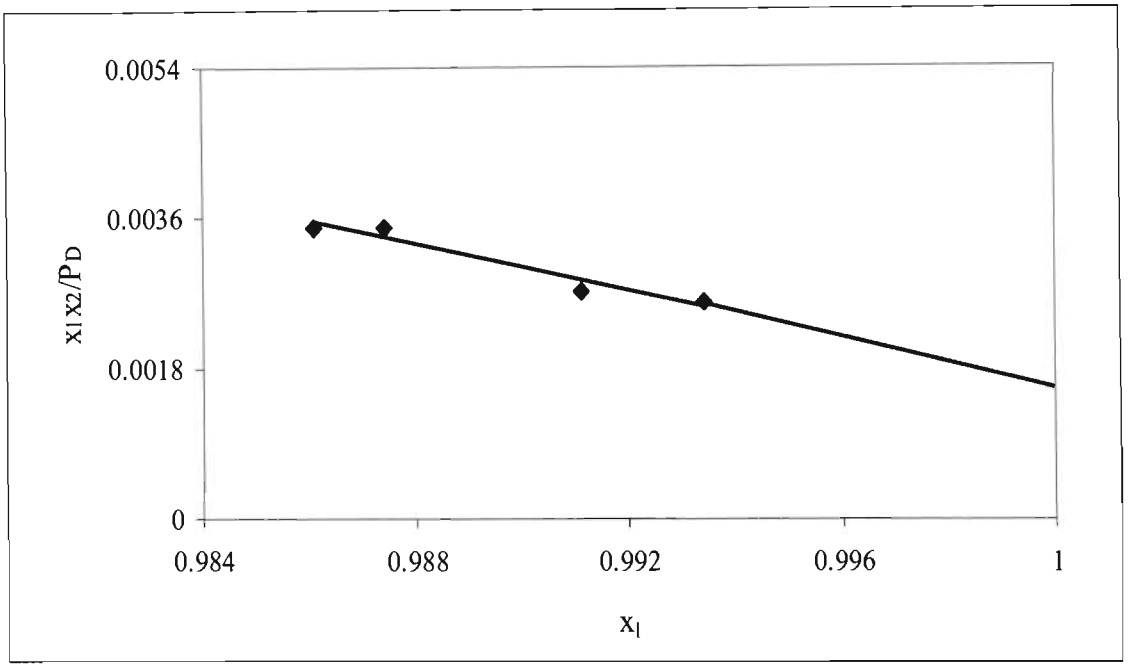

Figure A-2: Plot of $(x_1 x_2 / P_D)$ vs x_1 as $x_1 \to 1$ for Water (1) + 2-Butanol (2) at 323.18 K

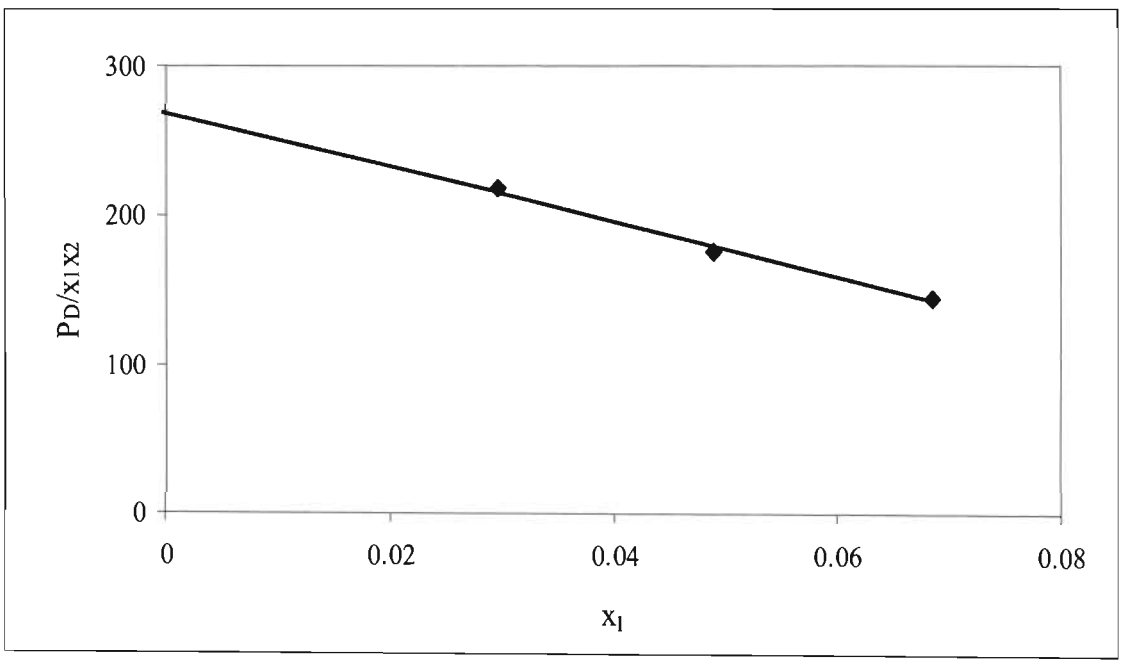

Figure A-3: Plot of $(P_D / x_1 x_2)$ vs x_1 as $x_1 \to 0$ for n-Hexane + 2-Butanol (2) at 329.22 K

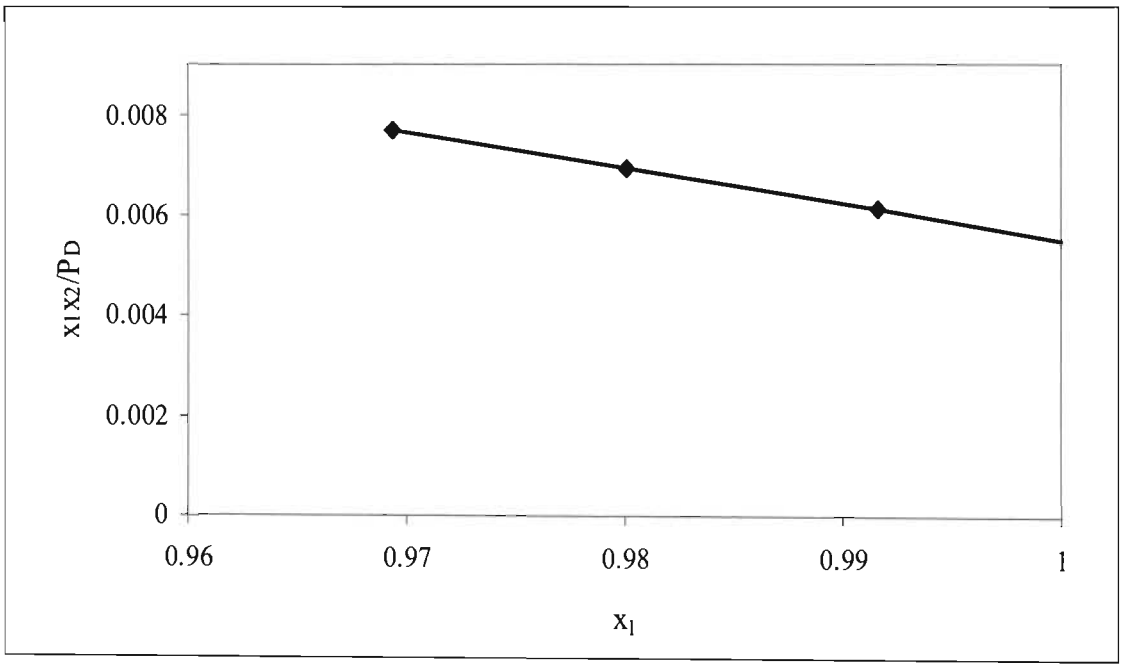

Figure A-4: Plot of $(x_1 x_2 / P_D)$ vs x_1 as $x_1 \to 1$ for n-Hexane + 2-Butanol (2) at 329.22 K

A.2 Low Pressure VLE Data regression

The measured VLE data was regressed using the following iterative bubble point pressure calculations.

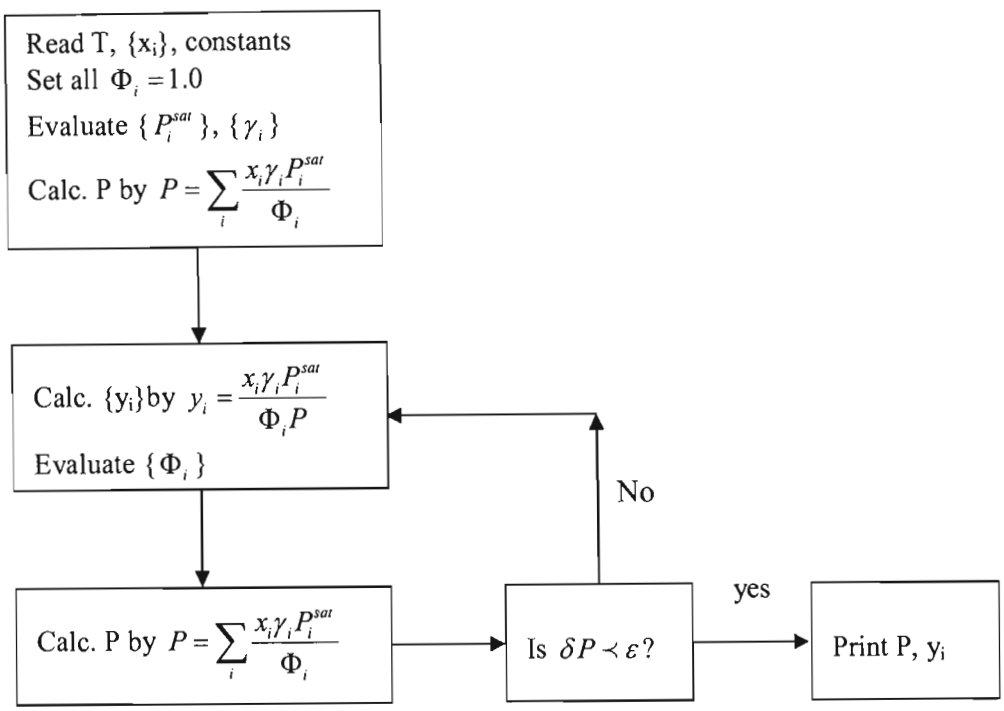

Figure A-1: Block diagram for the bubble point pressure calculation (Combined method) Smith and Van Ness [1996].

A-3 Sample computer programs for the Water (1) + 1-Propanol at 313.17 K

%system water (1) + 1-propanol (2) at 40.02 °C , 313.17 K

```
Pexp = [6.99 7.86 8.65 9.15 9.35 9.84 10.28 10.63 10.83 10.93 11.21 11.28 11.2 11.35...
     11.38 11.41 11.31 11.25 11.35 11.35 11.17 10.36 9.83 9.52 8.85 8.32 7.82 7.42 7.36]; % kpa
n1 = [ 0 0.01827 0.04301 0.06564 0.07564 0.1064 0.1404 0.1832 0.2241 0.2599 0.3662 0.4583...
     0.5220 1.02 1.02 1.02 1.02 1.02 1.02 1.02 1.02 1.02 1.02 1.02 1.02 1.02...
     1.02 1.02 1.02]; % Total moles for component 1
n2 = [ 0.4639 0.4639 0.4639 0.4639 0.4639 0.4639 0.4639 0.4639 0.4639 0.4639 0.4639 0.4639...
     0.4639 0.9688 0.6922 0.5716 0.4571 0.3430 0.2282 0.1702 0.1016 0.04428 0.03234 ...
     0.02737 0.01708 0.009311 0.003528 0.000557 0]; % total moles for component 2
z1 = [0 0.03789 0.08484 0.1240 0.1402 0.1865 0.2323 0.2831 0.3257 0.3590 0.4411 0.4970 ...
```

```
    0.5294 0.5129 0.5957 0.6409 0.6906 0.7483 0.8171 0.8570 0.9094 0.9584 0.9689 0.9739...
    0.9835 0.9910 0.9966 0.9995 1];

P1sat = 7.36;
P2sat = 6.99;
T = 313.15; % K

Vi_1 = 16.53e-6;
Vi_2 = 74.94e-6; % liquid molar volumes in m3/mol
R = 8.3144;
param = [0.5 0.5  0.3]; % initial guess of NRTL parameters

Tc = [647.3 536.7]; %in K
Pc = [22048.2 5167.6]; % in kPa
Vc = [56.00 218.50]; % cm3/mol

omega = [0.344 0.624];



%-------------------------------------------------------------------------
% A program to determine the  coefficients in Renon' s NRTL equation from
% measured P-x data using the Nelder-Mead simplex method'
%-------------------------------------------------------------------------

clear all
close all
clc;
global T P1sat P2sat x1 x2 param Pexp y1cal Pcal B
   Vi_1 Vi_2 y2cal y1cal phi_1 phi_2 Zc Tc Pc Vc omega R n1 n2 z1 ln_gammai_1 ln_gammai_2

%Program Header
disp(' A program to determine the NRTL coefficients from ')
disp('measured P-x data using the Nelder-Mead simplex method')
disp( ' in the process the program computes equlibrium x and y values from total composition ')
disp(' ')

%data_input3; % Call a script to enter the measured data and other constants

Pexp = 1000 * Pexp; % converting Pressure from Kpa  to Pa
P1sat = 1000 * P1sat;
P2sat = 1000 * P2sat;

% Compute the Virial coeficients
Zc = (Pc .* Vc * 1e-3)./ (R * Tc);
B = Virial(T);

 %initial values of phi_1 and phi_2

 for h = 1:length(n1)
   phi_1(h) = 1;
```

```
   phi_2(h) = 1;
end

% set new optimisation parameters
mk = optimset('MaxFunEvals',500,'MaxIter',500,'Display', 'iter');

% Call a routine (fminsearch) to find the parameters % ----------

    [param,FVAL,EXITFLAG,OUTPUT] = fminsearch('regressnpx', param, mk);
    %[param,FVAL,EXITFLAG,OUTPUT] = fminsearch('regresstkwil', param, mk);
% Print the coefficients ---------------------------------------------
    A1_2 = param(1);
    A2_1 = param(2);
    alpha1_2 = param(3);
     A1_2 = param(1);
    A2_1 = param(2);
    g12_g11 =  A2_1 * R * T;
    g12_g22 =  A1_2 * R * T;

    disp('The  fitted coefficients are:')
    disp('  ')
     disp(['  A12 = ', num2str(A1_2) ])
     disp(['  A21 = ', num2str(A2_1) ])
     disp(['  apha12 = ', num2str(alpha1_2)])
     disp(' ')
     disp('or')
     disp('  ')
     disp(['g12_g11 in J/mol:  ', num2str(g12_g11)])
     disp(['g12_g22 in J/mol:  ', num2str(g12_g22)])
     disp(['  apha12 = ', num2str(alpha1_2)])
     disp('  ')


    figure(1)
    plot(x1,Pexp/1000,'ro',x1,Pcal/1000,'g-')
    grid on
    xlabel ('x1')
    ylabel('Pressure kPa')
    legend('Experimental ', 'Calculated')
    hold on
    plot( y1cal,Pcal/1000,'gd')
    title('Pxy Curve from PTX data')

    % Display experimental and Calculated values

    disp(['      x1   ''x2  ''  y1cal ' '  y2cal  ' '  Pexp  ' 'Pcal' '  deltap' '  Gam1 ' '
Gam2' '  phi_1' '  phi_2' ])
    [x1' x2' y1cal' y2cal' (Pexp/1000)' (Pcal/1000)' (Pexp - Pcal)'/1000   exp(ln_gammai_1)'
exp(ln_gammai_2)']
```

```
function r = regressnpx(param)
%-------------------------------------------------------------------
% Evaluate the function (which is r) to be minimized
% Objective function = sum(Pexp - Pcal)^2
% -------------------------------------------------------------------
global  x1 x2 Pexp n1 n2 z1 P1sat P2sat y2cal y1cal Pcal phi_1 phi_2 Vi_1 Vi_2 R T ln_gammai_1
ln_gammai_2

 % Use my own variables
     A1_2 = param(1);
     A2_1 = param(2);
     alpha1_2 = param(3);


    x1 = z1; % initial guess
    x2 = 1-x1;
    counter = 0 ;% initialising counter

    while counter <= 150
     [ln_gammai_1, ln_gammai_2] = active(A1_2, A2_1, alpha1_2,x1); % calculating the log of
activity coefficient

    for k = 1:length(x1)

     volvap(k) =  R * T /Pexp(k) ;

   Pcal(k) = (x1(k) * exp(ln_gammai_1(k)) * P1sat)/phi_1(k) + (x2(k)*exp(ln_gammai_2(k)) *
P2sat)/phi_2(k);
    y1cal(k) = (x1(k) * exp(ln_gammai_1(k)) * P1sat) /(Pcal(k) * phi_1(k));

    y2cal(k) = 1-y1cal(k);

    % compute the amount of moles in vapour phase
    liquidMolarVol(k) = x1(k) * Vi_1 + (1-x1(k))* Vi_2;
    molesvap(k) = (190e-6 - liquidMolarVol(k) * (n1(k) + n2(k)))/(volvap(k) - liquidMolarVol(k));

    % compute moles of each component in vapour and liquid phases

    n1_vap(k) = y1cal(k) * molesvap(k) ;
    n2_vap(k) = y2cal(k) * molesvap(k) ;

    n1_liq(k) = n1(k) - n1_vap(k);
    n2_liq(k) = n2(k) - n2_vap(k);

    % compute new xi

    %x1(k) = n1_liq(k)/((n1(k) + n2(k)) - molesvap(k)); % Alternative way
    %for computing the liquid composition

    x1(k) = n1_liq(k) / (n1_liq(k) + n2_liq(k));
```

```
  end % for
[phi_1, phi_2] = phi(Pcal, y1cal);% Obtaining a better estimate of the vapour fugacity coefficients
 counter  = counter + 1;
  end % while

 err = (Pexp - Pcal)./ Pexp;
 r = sum(err.^2);
```

Evalation of the virial coefficient

```
% function to calculate the virial coefficients from a given T
% using the Pitzer - Curl correlation and the Mixing rules
% proposed by Prausnitz etal (1986): Molecular Thermodynamics of Fluid Phase
% Equilibria. 2nd Edition, Prentice Hall.

function r = Virial(a)
global Vc Pc Tc Zc R omega

% Use my own variables
T = a;
Pcnew = Pc*1000; % converting Pc to Pa

%Zc = Pcnew .* Vc ./ (R * Tc);

omegaij = sum(omega)/2;
Zcij = sum(Zc)/2;
Vcij =  (sum (Vc .^ (1/3))/2)^3;
Tcij = sqrt(Tc(1)* Tc(2));
Pcij = ( R * 1e6 * Zcij .* Tcij ) ./ Vcij;

TcNew = [ Tc Tcij];
PcNew = [ Pcnew Pcij];
omegaNew = [omega omegaij];
Tr = T ./ TcNew;
Bo = 0.083 - 0.422 ./ (Tr.^ 1.6);
B1 = 0.139 - 0.172 ./ (Tr .^ 4.2);


r = (R * TcNew .* (Bo + omegaNew .* B1)) ./ PcNew


%-------------------------------------------------------------------------
% A  function tom evaluate the correction factor
% Phi = exp((Vii - Bii)(P - Pisat) + Pyi^2 dij)/RT
%-------------------------------------------------------------------------

function  [r1, r2] = phi(a,b)

global B Vi_1 Vi_2 P1sat P2sat T
```

```
%use my own variables
Pcalc = a;
y1calc = b;
y2calc = 1 - y1calc;

B11 = B(1);
B22 = B(2);
B12 = B(3);

del_12 = 2 * B12 - B11 - B22;

for k = 1:length(y1calc)
ln_phi_1(k) = ((B11 - Vi_1) * (Pcalc(k) - P1sat) + Pcalc(k)* y1calc(k) * y1calc(k) * del_12) /
(8.314 * T);
ln_phi_2(k) = ((B22 - Vi_2) * (Pcalc(k) - P2sat) + Pcalc(k)* y2calc(k) * y2calc(k) * del_12) /
(8.314 * T);
end

r1 = exp(ln_phi_1);
r2 = exp(ln_phi_2);
```

APPENDIX B

Table B-1: Regressed data for Water (1) + 2-Butanol (2) at 323.18 K using the NRTL model

Experimental		NRTL				
x_1	P/kPa	P_{cal}/kPa	ΔP/kPa	y_1 cal	γ_1	γ_2
0.0000	10.74	10.74	0.00	0.0000	4.090	1.000
0.0168	11.54	11.37	0.17	0.0714	3.964	1.000
0.0334	11.90	11.96	-0.06	0.1307	3.847	1.001
0.0776	13.27	13.34	-0.07	0.2524	3.562	1.006
0.1170	14.30	14.38	-0.08	0.3307	3.337	1.013
0.1502	15.11	15.13	-0.02	0.3828	3.164	1.021
0.1782	15.64	15.69	-0.05	0.4193	3.030	1.030
0.2056	16.27	16.18	0.09	0.4501	2.907	1.040
0.2404	16.82	16.73	0.09	0.4837	2.761	1.055
0.2767	17.31	17.22	0.09	0.5132	2.620	1.075
0.3385	18.01	17.88	0.13	0.5542	2.402	1.117
0.4035	18.50	18.38	0.12	0.5875	2.195	1.178
0.4897	18.77	18.79	-0.02	0.6198	1.950	1.297
0.5581	18.77	18.94	-0.17	0.6371	1.773	1.441
0.6751	18.90	18.99	-0.09	0.6498	1.499	1.895
0.7205	19.01	19.00	0.01	0.6481	1.401	2.215
0.7945	18.95	19.13	-0.18	0.6350	1.254	3.144
0.9745	18.52	18.21	0.31	0.6570	1.007	22.414
0.9861	16.10	16.35	-0.25	0.7365	1.002	28.399
0.9874	15.74	16.08	-0.34	0.7498	1.002	29.182
0.9911	15.42	15.18	0.24	0.7963	1.001	31.622
0.9934	14.70	14.52	0.18	0.8341	1.001	33.308
1.0000	12.18	12.18	0.00	1.0000	1.000	38.812

Table B-2: Regressed data for Water (1) + 2-Butanol (2) at 323.18 K T-K using the T-K Wilson model

Experimental		T-K Wilson				
x_1	P/kPa	P_{cal}/kPa	ΔP/kPa	y_1 cal	γ_1	γ_2
0.0000	10.74	10.74	0.00	0.0000	3.747	1.000
0.0168	11.54	11.32	0.22	0.0666	3.676	1.000
0.0334	11.90	11.86	0.04	0.1236	3.607	1.001
0.0776	13.27	13.20	0.07	0.2454	3.425	1.004
0.1170	14.30	14.25	0.05	0.3269	3.268	1.009
0.1502	15.11	15.04	0.07	0.3821	3.138	1.015
0.1782	15.64	15.63	0.01	0.4211	3.032	1.022
0.2055	16.27	16.16	0.11	0.4541	2.930	1.030
0.2404	16.82	16.76	0.06	0.4900	2.802	1.044
0.2766	17.31	17.30	0.01	0.5214	2.674	1.061
0.3385	18.01	18.02	-0.01	0.5640	2.463	1.101
0.4035	18.50	18.55	-0.05	0.5973	2.252	1.160
0.4897	18.77	18.96	-0.19	0.6274	1.992	1.282
0.5581	18.77	19.09	-0.32	0.6418	1.801	1.433
0.6751	18.90	19.13	-0.23	0.6480	1.506	1.919
0.7205	19.01	19.15	-0.14	0.6438	1.403	2.259
0.9745	18.52	18.17	0.35	0.6584	1.007	22.542
0.9861	16.10	16.31	-0.21	0.7385	1.002	28.540
0.9874	15.74	16.04	-0.30	0.7518	1.002	29.328
0.9911	15.42	15.14	0.28	0.7984	1.001	31.787
0.9934	14.70	14.48	0.22	0.8359	1.001	33.492
1.0000	12.18	12.18	0.00	1.0000	1.000	39.086

Table B-3: Regressed data for Water (1) + 2-Butanol (2) at 323.18 K using the Van Laar model

Experimental		Van Laar				
x_1	P/kPa	P_{cal}/kPa	ΔP/kPa	y_1 *cal*	γ_1	γ_2
0.0000	10.74	10.74	0.00	0.0000	3.566	1.000
0.0168	11.54	11.28	0.26	0.0638	3.513	1.000
0.0334	11.90	11.80	0.10	0.1192	3.460	1.001
0.0776	13.27	13.09	0.18	0.2398	3.319	1.003
0.1170	14.30	14.12	0.18	0.3222	3.193	1.007
0.1502	15.11	14.92	0.19	0.3788	3.087	1.013
0.1782	15.64	15.53	0.11	0.4193	2.998	1.018
0.2055	16.27	16.07	0.20	0.4537	2.911	1.026
0.2404	16.82	16.70	0.12	0.4915	2.800	1.037
0.2766	17.31	17.27	0.04	0.5246	2.686	1.052
0.3384	18.01	18.05	-0.04	0.5699	2.493	1.088
0.4035	18.50	18.64	-0.14	0.6052	2.293	1.143
0.4897	18.77	19.10	-0.33	0.6367	2.036	1.259
0.5580	18.77	19.24	-0.47	0.6509	1.841	1.408
0.6751	18.90	19.27	-0.37	0.6532	1.529	1.905
0.7205	19.01	19.31	-0.30	0.6459	1.419	2.265
0.9745	18.52	18.28	0.24	0.6541	1.006	22.965
0.9861	16.10	16.28	-0.18	0.7396	1.002	28.366
0.9874	15.74	16.00	-0.26	0.7534	1.002	29.056
0.9911	15.42	15.08	0.34	0.8014	1.001	31.182
0.9934	14.70	14.42	0.28	0.8394	1.000	32.633
1.0000	12.18	12.18	0.00	1.0000	1.000	37.271

Table B-4: Regressed data for n-Hexane (1) + 2-Butanol (2) at 329.22 K using the NRTL model

Experimental		NRTL				
x_1	P/kPa	P_{cal}/kPa	ΔP/kPa	y_1 cal	γ_1	γ_2
0.0000	14.55	14.55	0.00	0.0000	4.663	1.000
0.0002	15.31	14.62	0.69	0.0048	4.659	1.000
0.0011	15.52	14.85	0.67	0.0214	4.644	1.000
0.0019	15.84	15.10	0.74	0.0378	4.629	1.000
0.0029	16.16	15.37	0.79	0.0559	4.612	1.000
0.0073	17.58	16.57	1.01	0.1272	4.537	1.000
0.0118	18.67	17.76	0.91	0.1891	4.461	1.000
0.0297	22.75	22.14	0.61	0.3591	4.183	1.002
0.0489	26.08	26.27	-0.19	0.4680	3.919	1.004
0.0685	28.76	29.96	-1.20	0.5405	3.680	1.008
0.1073	34.81	36.09	-1.28	0.6292	3.281	1.019
0.1482	40.95	41.23	-0.28	0.6845	2.945	1.036
0.2062	47.17	46.95	0.22	0.7333	2.573	1.066
0.2488	51.15	50.33	0.82	0.7580	2.358	1.094
0.3074	55.03	54.18	0.85	0.7834	2.118	1.140
0.3991	59.44	58.91	0.53	0.8124	1.835	1.233
0.5026	62.96	62.91	0.05	0.8366	1.598	1.381
0.6063	65.56	65.80	-0.24	0.8556	1.415	1.608
0.6009	66.12	65.66	0.46	0.8550	1.423	1.594
0.7132	67.40	67.71	-0.31	0.8718	1.260	2.019
0.8147	68.40	68.71	-0.31	0.8850	1.135	2.843
0.9004	68.83	69.07	-0.24	0.9002	1.050	4.598
0.9694	67.96	68.16	-0.20	0.9405	1.006	8.724
0.9801	67.46	67.58	-0.12	0.9555	1.003	9.953
0.9916	66.58	66.63	-0.05	0.9777	1.001	11.616
0.9952	66.10	66.25	-0.15	0.9864	1.000	12.232
0.9984	65.67	65.84	-0.17	0.9953	1.000	12.823
1.0000	65.63	65.63	0.00	1.0000	1.000	13.128

Table B-5: Regressed data for n-Hexane (1) + 2-Butanol (2) at 329.22 K using the T-K Wilson model

Experimental		T-K Wilson				
x_1	P/kPa	P*cal*/kPa	ΔP/kPa	y_1 *cal*	γ_1	γ_2
0.0000	14.55	14.55	0.00	0.0000	4.225	1.000
0.0002	15.31	14.61	0.70	0.0044	4.223	1.000
0.0011	15.52	14.83	0.69	0.0195	4.214	1.000
0.0019	15.84	15.05	0.79	0.0346	4.204	1.000
0.0029	16.16	15.30	0.86	0.0513	4.194	1.000
0.0073	17.58	16.39	1.19	0.1179	4.147	1.000
0.0118	18.67	17.50	1.17	0.1769	4.100	1.000
0.0298	22.75	21.66	1.09	0.3446	3.920	1.001
0.0490	26.08	25.72	0.36	0.4566	3.741	1.003
0.0685	28.76	29.48	-0.72	0.5331	3.571	1.006
0.1073	34.81	35.96	-1.15	0.6286	3.266	1.015
0.1481	40.95	41.59	-0.64	0.6884	2.987	1.028
0.2061	47.17	47.90	-0.73	0.7403	2.649	1.055
0.2488	51.15	51.56	-0.41	0.7655	2.438	1.081
0.3074	55.03	55.53	-0.50	0.7902	2.188	1.127
0.3991	59.44	59.93	-0.49	0.8159	1.873	1.227
0.5026	62.96	63.14	-0.18	0.8350	1.601	1.397
0.6063	65.56	65.20	0.36	0.8492	1.392	1.663
0.6010	66.12	65.11	1.01	0.8485	1.401	1.646
0.7133	67.40	66.63	0.77	0.8624	1.227	2.127
0.8147	68.40	67.62	0.78	0.8780	1.109	2.959
0.9004	68.83	68.08	0.75	0.9022	1.038	4.440
0.9693	67.96	67.30	0.66	0.9505	1.005	7.221
0.9800	67.46	66.88	0.58	0.9643	1.002	7.953
0.9915	66.58	66.25	0.33	0.9829	1.000	8.900
0.9952	66.10	66.00	0.10	0.9899	1.000	9.241
0.9984	65.67	65.76	-0.09	0.9965	1.000	9.564
1.0000	65.63	65.63	0.00	1.0000	1.000	9.729

Table B-6: Regressed data for n-Hexane (1) + 2-Butanol (2) at 329.22 K using the Van Laar model

Experimental		Van Laar				
x_1	P/kPa	P_{cal}/kPa	ΔP/kPa	y_1 cal	γ_1	γ_2
0.0000	14.55	14.55	0.00	0.0000	4.012	1.000
0.0002	15.31	14.61	0.70	0.0041	4.010	1.000
0.0011	15.52	14.81	0.71	0.0186	4.003	1.000
0.0019	15.84	15.02	0.82	0.0330	3.996	1.000
0.0029	16.16	15.26	0.90	0.0490	3.989	1.000
0.0073	17.58	16.31	1.27	0.1132	3.954	1.000
0.0119	18.67	17.37	1.30	0.1706	3.919	1.000
0.0298	22.75	21.39	1.36	0.3368	3.782	1.001
0.0490	26.08	25.40	0.68	0.4502	3.641	1.003
0.0685	28.76	29.17	-0.41	0.5288	3.504	1.005
0.1073	34.81	35.80	-0.99	0.6278	3.248	1.012
0.1481	40.95	41.67	-0.72	0.6902	3.001	1.024
0.2061	47.17	48.34	-1.17	0.7440	2.686	1.049
0.2488	51.15	52.18	-1.03	0.7697	2.480	1.074
0.3074	55.03	56.24	-1.21	0.7941	2.227	1.119
0.3991	59.44	60.45	-1.01	0.8179	1.894	1.223
0.5026	62.96	63.09	-0.13	0.8336	1.597	1.408
0.6063	65.56	64.54	1.02	0.8439	1.370	1.705
0.6010	66.12	64.48	1.64	0.8434	1.380	1.686
0.7133	67.40	65.58	1.82	0.8544	1.197	2.217
0.8148	68.40	66.52	1.88	0.8719	1.084	3.060
0.9003	68.83	67.06	1.77	0.9041	1.025	4.291
0.9692	67.96	66.55	1.41	0.9588	1.003	5.934
0.9799	67.46	66.30	1.16	0.9715	1.001	6.269
0.9915	66.58	65.95	0.63	0.9871	1.000	6.662
0.9952	66.10	65.82	0.28	0.9925	1.000	6.794
0.9984	65.67	65.69	-0.02	0.9975	1.000	6.914
1.0000	65.63	65.63	0.00	1.0000	1.000	6.974

Table B-7: Regressed data for 1-Propanol (1) + n-Dodecane (2) at 342.83 K using the T-K Wilson model

Experimental		T-K Wilson				
x_1	P/kPa	P_{cal}/kPa	ΔP/kPa	y_1 *cal*	γ_1	γ_2
0.0000	0.57	0.57	0.00	0.0000	3.965	1.000
0.1860	17.08	17.38	-0.30	0.9710	2.867	1.035
0.3107	23.88	23.31	0.57	0.9801	2.328	1.109
0.3763	25.60	25.30	0.30	0.9823	2.093	1.173
0.4467	26.86	26.81	0.05	0.9840	1.873	1.268
0.5090	27.56	27.72	-0.16	0.9849	1.702	1.384
0.4511	27.03	26.89	0.14	0.9840	1.860	1.275
0.5073	27.52	27.70	-0.18	0.9849	1.706	1.381
0.6045	28.27	28.56	-0.29	0.9859	1.478	1.654
0.6990	28.75	28.98	-0.23	0.9865	1.298	2.112
0.7545	28.98	29.15	-0.17	0.9868	1.210	2.547
0.8073	29.37	29.33	0.04	0.9871	1.139	3.168
0.8556	29.72	29.57	0.15	0.9878	1.084	4.041
0.9082	30.27	29.99	0.28	0.9894	1.038	5.616
0.9525	30.74	30.55	0.19	0.9923	1.011	7.945
0.9935	31.26	31.31	-0.05	0.9985	1.000	11.863
1.0000	31.45	31.45	0.00	1.0000	1.000	12.748

Table B-8: Regressed data for 1-Propanol (1) + n-Dodecane (2) at 342.83 K using the Van Laar model

Experimental		Van Laar				
x_1	P/kPa	P_{cal}/kPa	ΔP/kPa	y_1 *cal*	γ_1	γ_2
0.0000	0.57	0.57	0.00	0.0000	3.763	1.000
0.1860	17.08	17.23	-0.15	0.9709	2.842	1.031
0.3107	23.88	23.39	0.49	0.9803	2.337	1.100
0.3763	25.60	25.45	0.15	0.9826	2.106	1.162
0.4467	26.86	26.95	-0.09	0.9842	1.883	1.257
0.5090	27.56	27.81	-0.25	0.9851	1.708	1.375
0.4511	27.03	27.03	0.00	0.9842	1.870	1.264
0.5073	27.52	27.79	-0.27	0.9851	1.712	1.371
0.6045	28.27	28.51	-0.24	0.9859	1.475	1.654
0.6990	28.75	28.78	-0.03	0.9862	1.289	2.133
0.7545	28.98	28.90	0.08	0.9865	1.199	2.585
0.8073	29.37	29.07	0.30	0.9868	1.128	3.219
0.8556	29.72	29.34	0.39	0.9876	1.075	4.080
0.9082	30.27	29.83	0.44	0.9895	1.032	5.539
0.9525	30.74	30.47	0.27	0.9928	1.009	7.500
0.9935	31.26	31.30	-0.04	0.9987	1.000	10.373
1.0000	31.45	31.45	0.00	1.0000	1.000	10.964

Table B-9: Regressed data for 1-Propanol (1) + n-Dodecane (2) at 352.68 K using the T-K Wilson model

Experimental		T-K Wilson				
x_1	P/kPa	P_{cal}/kPa	ΔP/kPa	y_1 cal	γ_1	γ_2
0.0000	0.77	0.77	0.00	0.0000	3.661	1.000
0.0744	13.24	12.83	0.41	0.9424	3.217	1.005
0.1036	17.75	16.71	1.04	0.9566	3.060	1.010
0.1596	22.01	23.07	-1.06	0.9696	2.784	1.025
0.2912	30.67	33.44	-2.77	0.9807	2.246	1.091
0.3942	38.19	38.34	-0.15	0.9841	1.913	1.187
0.4955	42.01	41.34	0.67	0.9861	1.646	1.340
0.5008	42.20	41.46	0.74	0.9862	1.633	1.350
0.5622	43.21	42.63	0.58	0.9869	1.498	1.490
0.6420	44.09	43.72	0.37	0.9877	1.347	1.750
0.7126	45.08	44.45	0.63	0.9883	1.235	2.101
0.7764	45.99	45.09	0.90	0.9890	1.151	2.583
0.8593	47.33	46.14	1.19	0.9904	1.066	3.653
0.8876	47.63	46.63	1.00	0.9912	1.044	4.223
0.9242	48.34	47.40	0.94	0.9928	1.021	5.217
0.9542	48.99	48.20	0.79	0.9948	1.008	6.362
0.9753	49.55	48.88	0.67	0.9967	1.003	7.429
0.9881	49.67	49.34	0.33	0.9983	1.001	8.219
0.9974	49.73	49.70	0.03	0.9996	1.000	8.883
1.0000	49.80	49.80	0.00	1.0000	1.000	9.078

Table B-10: Regressed data for 1-Propanol (1) + n-Dodecane (2) at 352.68 K using the Van Laar model

Experimental		Van Laar				
x_1	P/kPa	P_{cal}/kPa	ΔP/kPa	y_1 cal	γ_1	γ_2
0.0000	0.77	0.77	0.00	0.0000	3.576	1.000
0.0744	13.24	12.71	0.53	0.9419	3.185	1.005
0.1036	17.75	16.62	1.13	0.9564	3.042	1.009
0.1596	22.01	23.08	-1.07	0.9697	2.785	1.023
0.2912	30.67	33.66	-2.99	0.9809	2.262	1.087
0.3941	38.19	38.57	-0.38	0.9843	1.925	1.183
0.4955	42.01	41.41	0.60	0.9861	1.649	1.340
0.5008	42.20	41.52	0.68	0.9862	1.636	1.351
0.5622	43.21	42.56	0.65	0.9869	1.495	1.496
0.6420	44.09	43.49	0.60	0.9875	1.339	1.769
0.7126	45.08	44.12	0.96	0.9881	1.225	2.134
0.7764	45.99	44.73	1.26	0.9887	1.141	2.626
0.8593	47.33	45.86	1.47	0.9903	1.059	3.675
0.8876	47.63	46.40	1.23	0.9912	1.039	4.207
0.9242	48.34	47.26	1.08	0.9929	1.018	5.096
0.9542	48.99	48.13	0.86	0.9950	1.007	6.063
0.9753	49.55	48.84	0.71	0.9970	1.002	6.914
0.9881	49.67	49.32	0.35	0.9984	1.001	7.519
0.9974	49.73	49.69	0.04	0.9996	1.000	8.010
1.0000	49.80	49.80	0.00	1.0000	1.000	8.152

Table B-11: Regressed data for 2-Butanol (1) + n-Dodecane (2) at 342.83 K using the T-K Wilson model

Experimental		T-K Wilson				
x_1	P/kPa	P_{cal}/kPa	ΔP/kPa	y_1 *cal*	γ_1	γ_2
0.0000	0.54	0.54	0.00	0.0000	2.376	1.000
0.0848	5.96	5.89	0.07	0.9145	2.228	1.003
0.1107	7.35	7.37	-0.02	0.9333	2.183	1.005
0.1512	9.34	9.57	-0.23	0.9504	2.114	1.010
0.2000	11.85	12.02	-0.17	0.9622	2.032	1.019
0.2995	16.45	16.32	0.13	0.9746	1.869	1.048
0.3960	20.23	19.68	0.55	0.9808	1.717	1.096
0.5050	23.15	22.59	0.56	0.9850	1.554	1.191
0.5034	22.93	22.56	0.37	0.9850	1.556	1.189
0.6015	24.17	24.47	-0.30	0.9874	1.417	1.336
0.6996	25.22	25.79	-0.57	0.9892	1.287	1.601
0.7996	26.30	26.67	-0.37	0.9906	1.166	2.163
0.8481	26.82	26.98	-0.16	0.9912	1.113	2.694
0.8985	27.36	27.28	0.08	0.9920	1.063	3.709
0.9487	27.98	27.64	0.34	0.9935	1.022	6.053
0.9832	28.15	28.03	0.12	0.9963	1.003	10.455
0.9981	28.14	28.27	-0.13	0.9994	1.000	14.710
1.0000	28.31	28.31	0.00	1.0000	1.000	15.493

Table B-12: Regressed data for 2-Butanol (1) + n-Dodecane (2) at 342.83 K using the Van Laar model

Experimental		Van Laar				
x_1	P/kPa	P_{cal}/kPa	ΔP/kPa	y_1 *cal*	γ_1	γ_2
0.0000	0.54	0.54	0.00	0.0000	2.329	1.000
0.0848	5.96	5.84	0.12	0.9138	2.206	1.003
0.1107	7.35	7.33	0.02	0.9329	2.168	1.004
0.1512	9.34	9.55	-0.21	0.9503	2.108	1.009
0.2000	11.85	12.03	-0.18	0.9623	2.035	1.016
0.2995	16.45	16.45	0.00	0.9749	1.884	1.043
0.3960	20.23	19.89	0.34	0.9811	1.736	1.090
0.5050	23.15	22.81	0.34	0.9852	1.569	1.185
0.5034	22.93	22.77	0.16	0.9852	1.571	1.184
0.6015	24.17	24.58	-0.41	0.9875	1.423	1.339
0.6996	25.22	25.70	-0.48	0.9890	1.282	1.630
0.7996	26.30	26.35	-0.05	0.9900	1.152	2.259
0.8481	26.82	26.60	0.22	0.9906	1.097	2.842
0.8985	27.36	26.93	0.43	0.9915	1.049	3.876
0.9487	27.98	27.43	0.55	0.9936	1.014	5.836
0.9832	28.15	27.97	0.18	0.9971	1.002	8.372
0.9981	28.14	28.27	-0.13	0.9996	1.000	10.024
1.0000	28.31	28.31	0.00	1.0000	1.000	10.275

Table B-13: Regressed data for 2-Butanol (1) + n-Dodecane (2) at 352.68 K using the T-K Wilson model

Experimental		T-K Wilson				
x_1	P/kPa	P_{cal}/kPa	ΔP/kPa	y_1 cal	γ_1	γ_2
0.0000	0.79	0.79	0.00	0.0000	4.223	1.000
0.2646	28.57	28.00	0.57	0.9757	2.326	1.095
0.3546	31.11	31.62	-0.51	0.9794	1.969	1.181
0.4548	33.53	34.21	-0.68	0.9819	1.667	1.323
0.5516	35.45	35.90	-0.45	0.9835	1.445	1.529
0.6521	37.33	37.25	0.08	0.9850	1.270	1.859
0.7517	39.31	38.54	0.77	0.9867	1.143	2.388
0.8054	40.22	39.35	0.87	0.9879	1.090	2.816
0.8530	41.42	40.19	1.23	0.9894	1.053	3.330
0.9054	42.41	41.32	1.09	0.9918	1.023	4.117
0.9471	43.37	42.43	0.94	0.9945	1.008	4.996
0.9803	43.92	43.48	0.44	0.9976	1.001	5.939
1.0000	44.19	44.19	0.00	1.0000	1.000	6.637

Table B-14: Regressed data for 2-Butanol (1) + n-Dodecane (2) at 352.68 K using the Van Laar model

Experimental		Van Laar				
x_1	P/kPa	P_{cal}/kPa	ΔP/kPa	y_1 cal	γ_1	γ_2
0.0000	0.79	0.79	0.00	0.0000	3.819	1.000
0.2646	28.57	27.83	0.74	0.9758	2.312	1.083
0.3546	31.11	31.68	-0.57	0.9798	1.974	1.163
0.4548	33.53	34.35	-0.82	0.9823	1.674	1.301
0.5516	35.45	35.95	-0.50	0.9838	1.447	1.509
0.6521	37.33	37.17	0.16	0.9851	1.268	1.844
0.7517	39.31	38.37	0.94	0.9866	1.138	2.382
0.8054	40.22	39.18	1.04	0.9879	1.086	2.809
0.8530	41.42	40.04	1.38	0.9894	1.050	3.309
0.9054	42.41	41.23	1.18	0.9919	1.021	4.047
0.9471	43.37	42.39	0.98	0.9947	1.007	4.831
0.9803	43.92	43.47	0.45	0.9978	1.001	5.630
1.0000	44.19	44.19	0.00	1.0000	1.000	6.195

Table B-15: Regressed data for Water (1) + o-Cresol (2) at 342.83 K using the Van Laar model

Experimental		Van Laar				
x_1	P/kPa	P_{cal}/kPa	ΔP/kPa	y_1 cal	γ_1	γ_2
0.0000	0.83	0.83	0.00	0.0000	5.499	1.000
0.0536	5.81	5.86	-0.05	0.8633	3.068	1.015
0.0724	7.11	6.71	0.40	0.8817	2.655	1.025
0.1080	7.38	7.88	-0.50	0.9009	2.137	1.047
0.1556	9.12	9.07	0.05	0.9158	1.736	1.080
0.2112	10.51	10.30	0.21	0.9280	1.471	1.121
0.3049	12.41	12.34	0.07	0.9437	1.242	1.187
0.4045	15.16	14.62	0.54	0.9570	1.126	1.252
0.5446	17.50	18.08	-0.58	0.9716	1.050	1.331
1.0000	30.65	30.65	0.00	1.0000	1.000	1.513

APPENDIX C

Presented in this appendix are x-y graphs for all the systems measured in this project

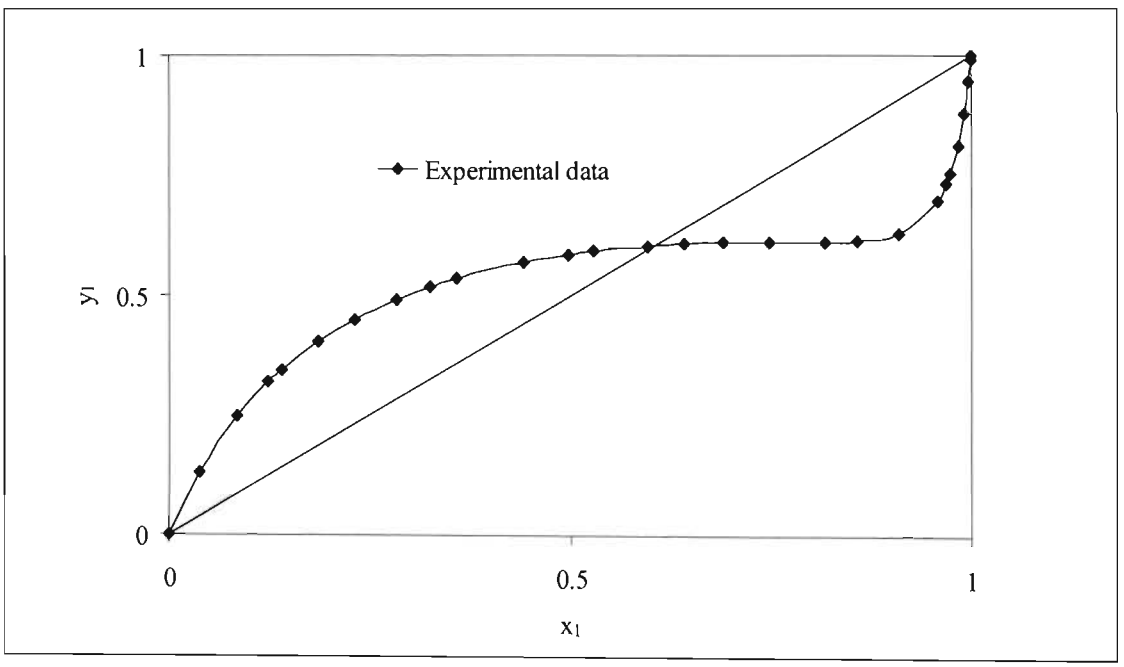

Figure C-1: The x-y diagram for Water (1) + 1-Propanol (2) system at 313.17 K

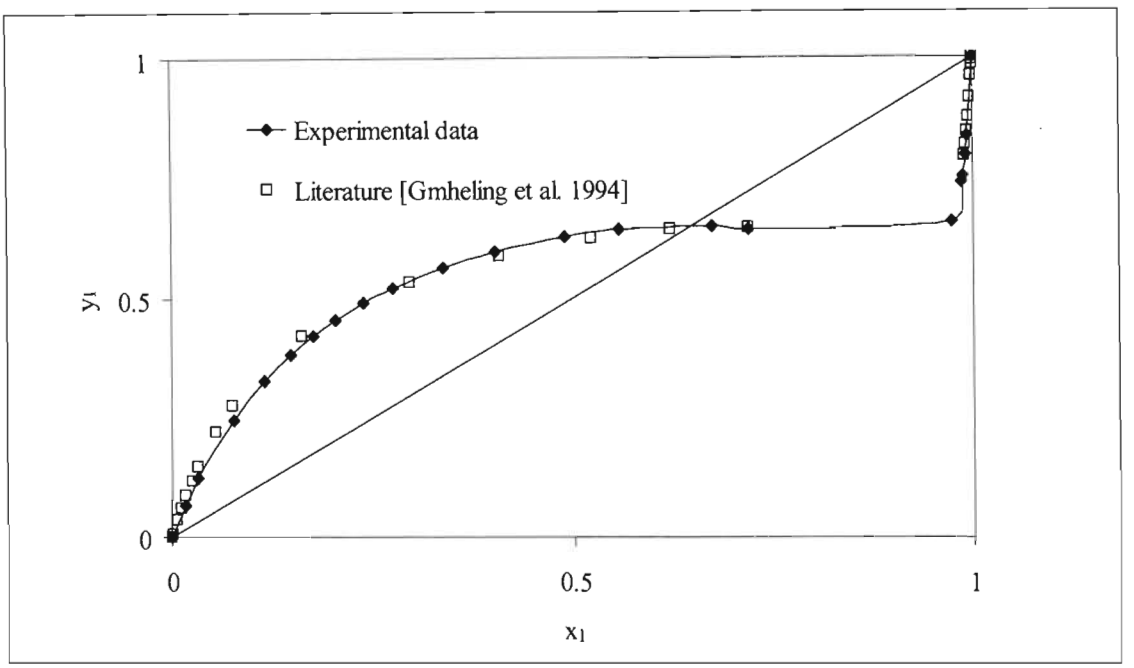

Figure C-2: The x-y diagram for Water (1) + 2-Butanol (2) system at 323.18 K

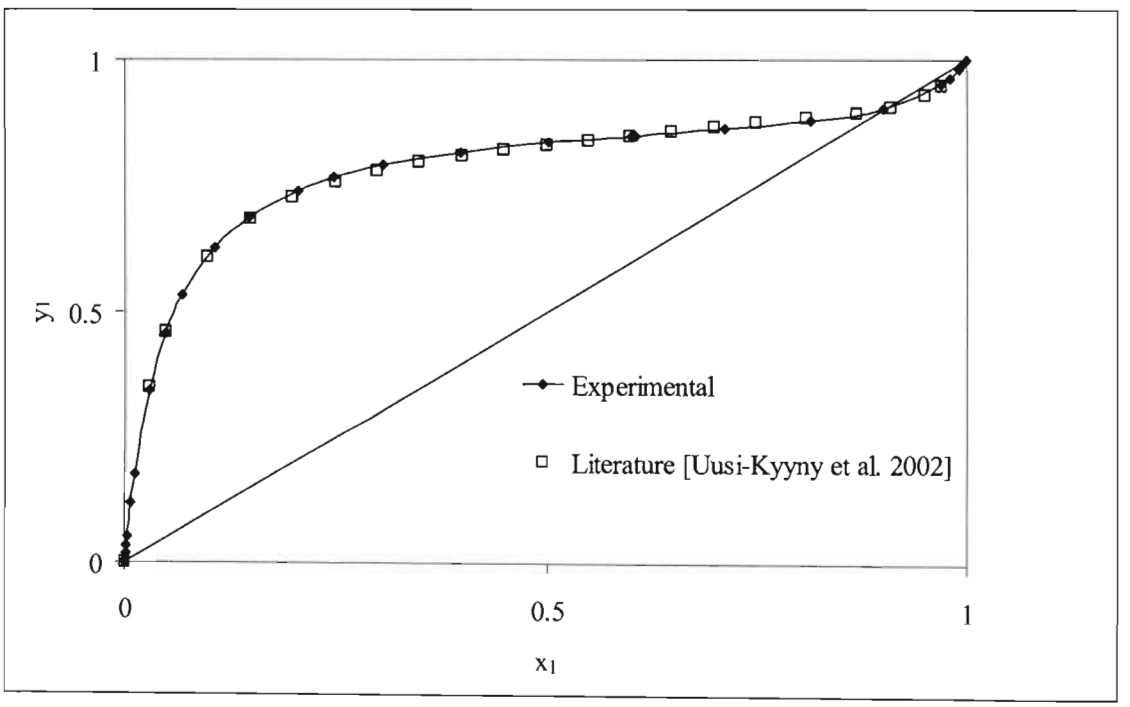

Figure C-3: The x-y diagram for n-Hexane (1) + 2-Butanol (2) at 329.22 K

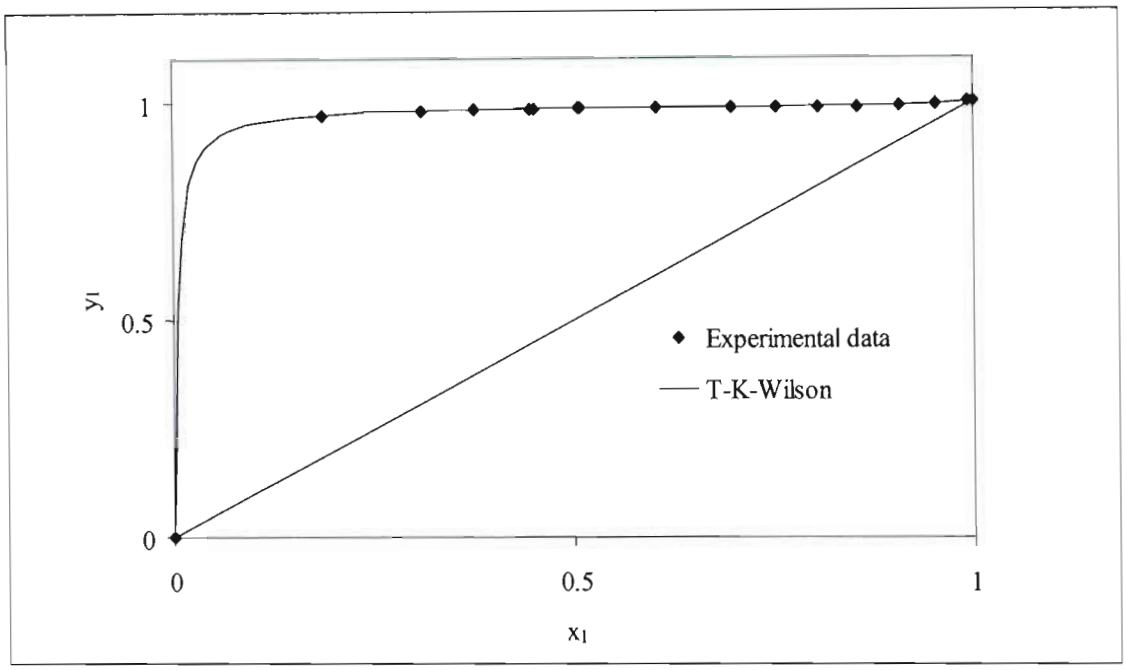

Figure C-4: The x-y diagram for 1-Propanol (1) + n-Dodecane at 342.83 K

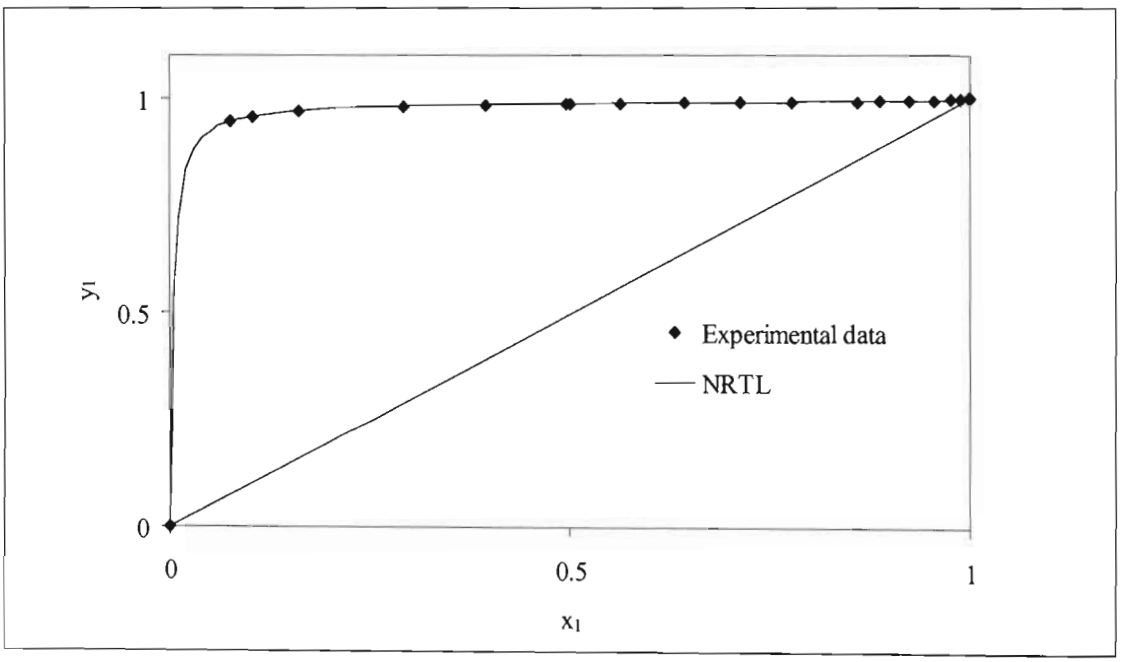

Figure C-5: The x-y diagram for 1-Propanol (1) + n-Dodecane at 352.68 K

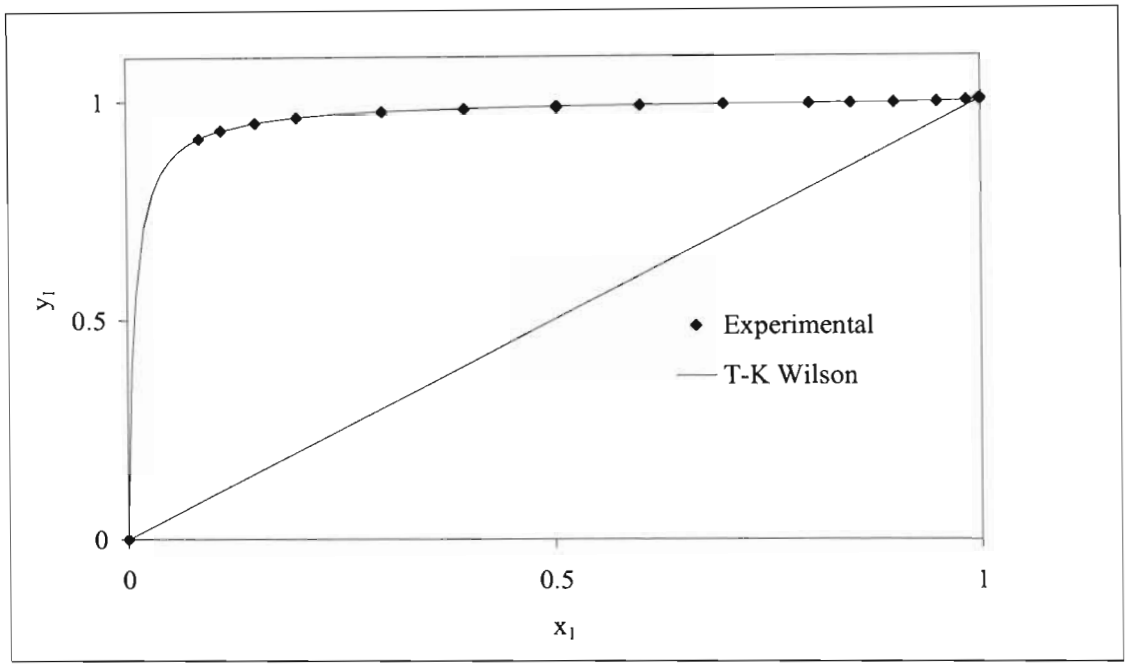

Figure C-6: The x-y diagram for 2-Butanol (1) + n-Dodecane at 342.83 K

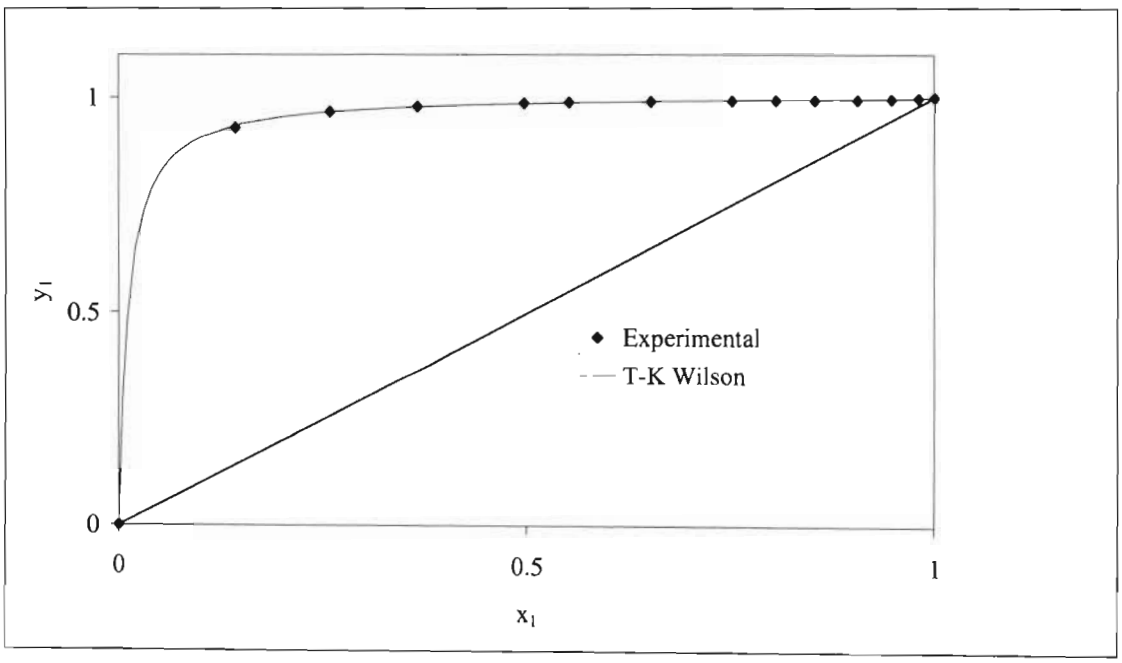

Figure C-7: The x-y diagram for 2-Butanol (1) + n-Dodecane at 352.68 K